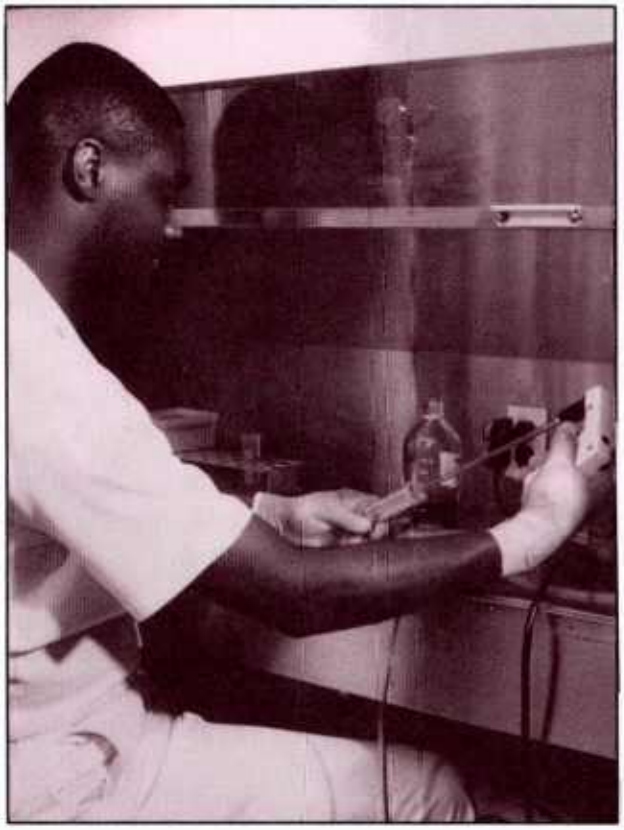

Third Quarter
1994

AFRRI Reports

Armed Forces Radiobiology Research Institute

8901 Wisconsin Avenue • Bethesda, Maryland 20889-5603

On the cover: *Air Force MSgt Kyle Sample, an AFRRI research laboratory technician, performs titration, which allows him to determine cell count, a means of measuring the effects of ionizing radiation. The effort is part of a project to develop treatments for radiation-induced gastrointestinal injury.*

REPORT DOCUMENTATION PAGE

Form Approved
OMB No. 0704-0188

1. AGENCY USE ONLY *(Leave blank)*	2. REPORT DATE	3. REPORT TYPE AND DATES COVERED
	October 1994	Reprints

4. TITLE AND SUBTITLE

AFRRI Reports, Third Quarter 1994

5. FUNDING NUMBERS

PE: NWED QAXM

6. AUTHOR(S)

7. PERFORMING ORGANIZATION NAME(S) AND ADDRESS(ES)

Armed Forces Radiobiology Research Institute
8901 Wisconsin Avenue
Bethesda, MD 20889-5603

8. PERFORMING ORGANIZATION REPORT NUMBER

SR94-15 - SR94-21

9. SPONSORING/MONITORING AGENCY NAME(S) AND ADDRESS(ES)

Uniformed Services University of the Health Sciences
4301 Jones Bridge Road
Bethesda, MD 20814-4799

10. SPONSORING/MONITORING AGENCY REPORT NUMBER

11. SUPPLEMENTARY NOTES

12a. DISTRIBUTION/AVAILABILITY STATEMENT

Approved for public release; distribution unlimited.

12b. DISTRIBUTION CODE

13. ABSTRACT *(Maximum 200 words)*

This volume contains AFRRI Scientific Reports SR94-15 through SR94-21 for July-September 1994.

14. SUBJECT TERMS

15. NUMBER OF PAGES

62

16. PRICE CODE

17. SECURITY CLASSIFICATION OF REPORT	18. SECURITY CLASSIFICATION OF THIS PAGE	19. SECURITY CLASSIFICATION OF ABSTRACT	20. LIMITATION OF ABSTRACT
UNCLASSIFIED	UNCLASSIFIED	UNCLASSIFIED	UL

CONTENTS

Scientific Reports

SR94-15: Forrest VJ, Kang Y-H, McClain DE, Robinson DH, Ramakrishnan N. Oxidative stress-induced apoptosis prevented by trolox.

SR94-16: Kalinich JF, McClain DE. Rapid isolation of nuclear transport-competent *Xenopus* nucleoplasmin produced in *Escherichia coli* strain BL21 (DE3).

SR94-17: Kandasamy SB, Rabin BM, Hunt WA, Dalton TK, Joseph JA, Harris AH. Exposure to heavy charged particles affects thermoregulation in rats.

SR94-18: Neta R, Oppenheim JJ, Wang J-M, Snapper CM, Moorman MA, Dubois CM. Synergy of IL-1 and stem cell factor in radioprotection of mice is associated with IL-1 up-regulation of mRNA and protein expression for *c-kit* on bone marrow cells.

SR94-19: Peterson VM, Adamovicz JJ, Elliott TB, Moore MM, Madonna GS, Jackson WE III, Ledney GD, Gause WC. Gene expression of hematoregulatory cytokines is elevated endogenously after sublethal gamma irradiation and is differentially enhanced by therapeutic administration of biologic response modifiers.

SR94-20: Powell EL, Newsome AL, Allen SD, Knudson GB. Identification of antigens of pathogenic free-living amoebae by protein immunoblotting with rabbit immune and human sera.

SR94-21: Winsauer PJ, Verrees JF, O'Halloran KP, Bixler MA, Mele PC. Effects of chlordiazepoxide, 8-OH-DPAT and ondansetron on radiation-induced decreases in food intake in rats.

Pergamon

Free Radical Biology & Medicine, Vol. 16, No. 6, pp. 675–684, 1994

0891-5849/94 $6.00 + .00

0891-5849(93)E0001-L

Original Contribution

OXIDATIVE STRESS-INDUCED APOPTOSIS PREVENTED BY TROLOX

VIRGINIA J. FORREST,* YUAN-HSU KANG,* DAVID E. MCCLAIN,†
DOUGLAS H. ROBINSON,* and NARAYANI RAMAKRISHNAN†

*Naval Medical Research Institute; and †Armed Forces Radiobiology Research Institute, Bethesda, MD, USA

(*Received* 23 *February* 1993; *Revised* 14 *July* 1993; *Re-revised* 24 *September* 1993; *Accepted* 5 *October* 1993)

Abstract—The ability of oxidative stress to induce apoptosis (programmed cell death), and the effect of Trolox, a water soluble vitamin E analog, on this induction were studied in vitro in mouse thymocytes. Cells were exposed to oxidative stress by treating them with 0.5–10 μM hydrogen peroxide (H_2O_2) for 10 min, in phosphate-buffered saline supplemented with 0.1 mM ferrous sulfate. Cells were resuspended in RPMI 1640 medium with 10% serum and incubated at 37°C under 5% CO_2 in air. Electron microscopic studies revealed morphological changes characteristic of apoptosis in H_2O_2-treated cells. H_2O_2 treatment fragmented the DNA in a manner typical of apoptotic cells, producing a ladder pattern of 200 base pair increments upon agarose gel electrophoresis. The percentage of DNA fragmentation (determined fluorometrically) increased with increasing doses of H_2O_2 and postexposure incubation times. Pre- or posttreatment of cells with Trolox reduced H_2O_2-induced DNA fragmentation to control levels and below. The results indicate that oxidative stress induces apoptosis in thymocytes, and this induction can be prevented by Trolox, a powerful inhibitor of membrane damage.

Keywords—Apoptosis, Oxidative stress, DNA fragmentation, Trolox, Vitamin E, Hydrogen peroxide, Thymocytes, Membrane damage, Oxygen free radicals

INTRODUCTION

Cell death can occur by either apoptosis or necrosis. Cell death by necrosis occurs due to severe injurious changes in the cell environment. Necrotic death is characterized by a generalized breakdown of cellular structure and function followed by cell lysis and tissue inflammation. Apoptosis, on the other hand, appears to be an active process of cellular self-destruction involving a series of cellular events that require active cell participation (e.g., macromolecular synthesis and enzyme activation). Apoptotic death is characterized by cell shrinkage, membrane blebbing, formation of apoptotic bodies, and fragmentation of nuclear DNA into oligonucleosomal subunits.[1–3] Apoptotic bodies are taken up and degraded by adjacent cells, which results in cell deletion without inflammation of surrounding tissue.

Cell death via apoptosis occurs under a variety of physiological conditions, including embryogenesis, metamorphosis,[4] cytotoxic T-cell mediated killing of target cells,[5] and death of autoreactive thymocytes.[6] It can be induced in normal or malignant cells of lymphatic origin by ionizing radiation,[7–9] glucocorticoids,[10–12] and by calcium ionophores.[12–14] Hydrogen peroxide (H_2O_2) has recently been implicated as an active ingredient in blastocoele fluid-induced programmed cell death in situ in the murine blastocyst.[15]

The fact that a nonspecific cytotoxic agent like H_2O_2 may induce apoptosis suggests that other agents or conditions that cause oxidative stress may also be suspect. Oxygen free radicals appear to be involved in cellular injury caused by hyperoxygenation, ischemia/reperfusion, inflammation, ionizing radiation exposure, and aging.[16] Severe oxidative injury produces necrosis in target cells. However, it is possible that lower levels of oxidative stress may induce death by apoptosis.

In this study, we investigated whether oxidative stress produced by treatment with H_2O_2 can induce apoptotic death in mouse thymocytes. We also studied the protective effects of Trolox in thymocytes exposed to H_2O_2. Trolox is a water-soluble analog of vitamin E and is a powerful antioxidant.[17] It has been shown to protect mammalian cells from oxidative damage both in vivo[18,19] and in vitro.[19,20]

Address correspondence to: Narayani Ramakrishnan, Armed Forces Radiobiology Research Institute, 8901 Wisconsin Ave., Bethesda, MD 20889-5603, USA.

MATERIALS AND METHODS

Tissue culture medium (TCM)

RPMI 1640 medium was supplemented with 25 mM HEPES buffer, 2 mM L-glutamine, 55 μM 2-mercaptoethanol, 100 U/ml penicillin, 100 μg/ml streptomycin, 0.25 μg/ml amphotericin B, and 10% heat-inactivated fetal calf serum.

Thymocyte isolation

CD2F1 male mice, 6 to 7 weeks old, were euthanized with CO_2. The thymuses were removed aseptically and rinsed in TCM. Single-cell suspensions were prepared by pressing the thymuses through wire mesh screens followed by passage through a 25-gauge needle. The cell suspensions were washed once with TCM and resuspended in TCM. These concentrated cell suspensions were counted with a coulter counter and placed on ice until exposed to H_2O_2, 30 to 60 min later.

Hydrogen peroxide exposure

Cells were resuspended in phosphate-buffered saline (PBS) supplemented with 0.1 mM ferrous sulfate at a concentration of 2×10^6 cells/ml. The cells were treated with 0.5–10 μM H_2O_2 and incubated for 10 min at 37°C under an atmosphere of 5% CO_2 in air. The control cells were incubated under the same conditions without H_2O_2. Following 10 min of incubation, catalase (100 U/ml) was added to all the samples, and the cells were immediately centrifuged at 200 $\times$ g for 10 min. The cells were resuspended in fresh TCM and returned to the incubator. All exposures and incubations were performed with 2 ml cell suspensions in 15 ml sterile disposable tubes.

Hydrogen peroxide is known to produce hydroxyl ions and hydroxyl radicals by the Fenton reaction in the presence of iron. The medium was supplemented with ferrous sulfate so that the concentration of iron would not be a limiting factor in the oxidative exposures. Unpublished results from our laboratory indicate that the addition of ferrous sulfate to PBS does not induce DNA fragmentation. Likewise, the addition of ferrous sulfate to the hydrogen peroxide exposures had no additive effect on fragmentation.

Trolox treatment

Trolox (6-hydroxyl-2,5,7,8-tetramethylchroman-2-carboxylic acid) (Hoffman-LaRoche, Nutley, NJ) is a water-soluble analog of α-tocopherol (vitamin E). Stock solutions of Trolox (100 mM) were prepared in 1 M sodium bicarbonate, due to its poor solubility in water above 1.8 mM. The pH of the stock was adjusted to 7.0 with 1 N HCl, and the stock was diluted to working concentrations with medium. Thymocytes were treated with Trolox (10 mM) before, during, or after 10 min exposure to 10 μM H_2O_2. Trolox incubations that were conducted before or after H_2O_2 exposures were performed in TCM. Trolox treatments that were administered concurrently with H_2O_2 were performed in PBS with ferrous sulfate.

DNA fragmentation assay

Cells were harvested at various times postexposure by centrifugation at 200 $\times$ g for 10 min. The cells were lysed with 0.2 ml ice-cold hypotonic lysing buffer (10 mM tris-HCl, pH 7.5, 1 mM ethylenediaminetetraacetic acid [EDTA], 0.2% Triton X-100) and centrifuged at 13,000 $\times$ g for 20 min to separate intact from fragmented DNA. The supernatant was transferred to a separate tube and 0.2 ml lysing buffer was added to the pellet and sonicated for 10 s. The amount of DNA in the supernatant and pellet fractions was determined by an automated fluorometric method using Hoechst 33258 fluorochrome as described by Ramakrishnan and Catravas.[21] The percentage of DNA fragmentation refers to the ratio of DNA in the supernatant to the total DNA in the pellet and supernatant.

DNA fragmentation pattern

Agarose gel electrophoresis was performed to determine the pattern of fragmentation produced by H_2O_2. Thymocytes were lysed in lysing buffer and incubated with proteinase K (50 μg/ml) at 37°C for 30–45 min. The DNA was sequentially extracted with equal volumes of phenol/chloroform/isoamyl alcohol (25:24:1). The DNA in the aqueous phase was precipitated by adding an equal volume of 100% ethanol and maintained at −20°C overnight. DNA was collected by centrifugation at 13,000 $\times$ g for 20 min, air-dried, and resuspended in TBE buffer (90 mM Tris, 90 mM boric acid, and 2 mM EDTA, pH 8.0). Horizontal electrophoresis was performed for 2 h at 100 volts in a 0.75% agarose gel with TBE buffer. Equal quantities of DNA (determined by Hoechst 33258 fluorescence) were loaded in each lane. The gels were stained with ethidium bromide and photographed by UV transillumination. Photographic negatives of the stained gels were scanned and quantified using a scanning laser densitometer and associated software (Molecular Dynamics Model 300B).

Table 1A. Effect of Trolox Pretreatment on DNA Fragmentation Induced by 10 μM H_2O_2

Pretreatment	Treatment	DNA Fragmentation	
		Duration of Pretreatment	
		1 h	2 h
Medium	H_2O_2	32.22% (± 1.65)	31.58% (± 2.60)
Trolox	H_2O_2	21.41% (± 1.62)	20.12% (± 1.38)
Medium	PBS	21.23% (± 0.63)	18.03% (± 1.08)
Trolox	PBS	22.50% (± 1.28)	21.43% (± 0.98)

Row 1: cells were preincubated in TCM without Trolox 1 or 2 h before H_2O_2 exposure (n = 12). Row 2: cells were preincubated in TCM plus Trolox for 1 or 2 h before H_2O_2 exposure (n = 12). Row 3: cells were preincubated in TCM without Trolox for 1 or 2 h before PBS exposure (n = 8). Row 4: cells were preincubated in TCM plus Trolox for 1 or 2 h before PBS exposure (n = 8). After the exposure regimens, cells were resuspended and incubated in TCM without Trolox. Fragmentation analyses were performed 6 h later. Data are pooled from three experiments (mean ± SEM).

Table 1B. Effect of Trolox Concurrent Treatment on DNA Fragmentation Induced by 10 μM H_2O_2

Concurrent Treatment	DNA Fragmentation
H_2O_2 without Trolox	38.11% (± 0.83)
H_2O_2 with Trolox	35.41% (± 1.51)
PBS without Trolox	23.77% (± 0.77)

Row 1: cells received H_2O_2 without Trolox. Row 2: cells received Trolox simultaneously with H_2O_2. Row 3: cells received PBS without Trolox. Following the exposure scenarios, cells were resuspended and incubated in TCM without Trolox. Fragmentation analyses were performed 6 h later. Data are pooled from three experiments (mean ± SEM, n = 12).

Electron microscopy

Five h after a 10-min exposure to 10 μM H_2O_2, the cells were fixed in 2% glutaraldehyde and 1% paraformaldehyde in 0.1 M sodium cacodylate buffer (pH 7.2) for 1 h on ice. The fixed cells were centrifuged at 200 × g for 12 min, and the cell pellet was gently washed three times with 0.1 M sodium cacodylate buffer and placed in a refrigerator overnight. Cells were postfixed in 1% osmium tetroxide in 0.1 M sodium cacodylate buffer at room temperature for 1 h. Cells were dehydrated in a series of graded ethanol solutions and embedded in Epon (Poly/Bed; Polysciences). Pale gold ultra-thin sections, prepared with a diamond knife, were stained with uranyl acetate and lead citrate. Cells were examined in a JEOL 100 CX II transmission electron microscope.

Statistics

DNA fragmentation data was analyzed for statistical significance using either an unpaired Student's t-test (Table 1, $p < .05$) or an F-test for equal means followed by Duncan's method (Figs. 3, 4, 5A and 6; $p < .05$).

Materials

RPMI 1640 medium, 2-mercaptoethanol, and the antibiotic mixture were purchased from GIBCO, Grand Island, NY; FCS was obtained from Hyclone Laboratories, Logan, UT; Hoechst 33258 fluorochrome was purchased from Calbiochem-Behring, La Jolla, CA; Trolox was a gift from Hoffman-LaRoche, Nutley, NJ.

RESULTS

The nature of cell death in thymocytes following H_2O_2 exposure was characterized by electron microscopy and agarose gel electrophoresis of DNA. Typical electron micrographs of H_2O_2-treated thymocytes, fixed 5 h after exposure, appear in Figure 1. In each of the frames in Figure 1, the cytoplasm and nuclear chromatin have become condensed, a typical apoptotic phenomenon.[1] During apoptosis, the chromatin forms dense aggregates along the nuclear membrane.[1] If the cell has been sliced through the nucleus, the aggregates may appear crescent-shaped against the membrane as in Figure 1A and 1B. However, if the cell is sliced near the edge of the nucleus, the entire nucleus may have the appearance of dense chromatin as in Figure 1C and 1D. The chromatin aggregation that occurs during apoptosis is unlike the flocculation of chromatin exhibited during necrosis.[3] Invaginations in the nuclear membrane occur as in Figure 1A and 1B, which will ultimately break the nucleus into smaller pieces as seen in Figure 1B and 1D. The plasma membrane becomes convoluted (Fig. 1B), an event preceding the formation of apoptotic bodies. The electron micrograph in Figure 1C illustrates the extrusion of an apoptotic body. The morphological changes seen here (chromatin aggregation, condensation of the nucleus and cytoplasm, convolution of the nuclear and plasma membrane) are indicative of apoptosis.

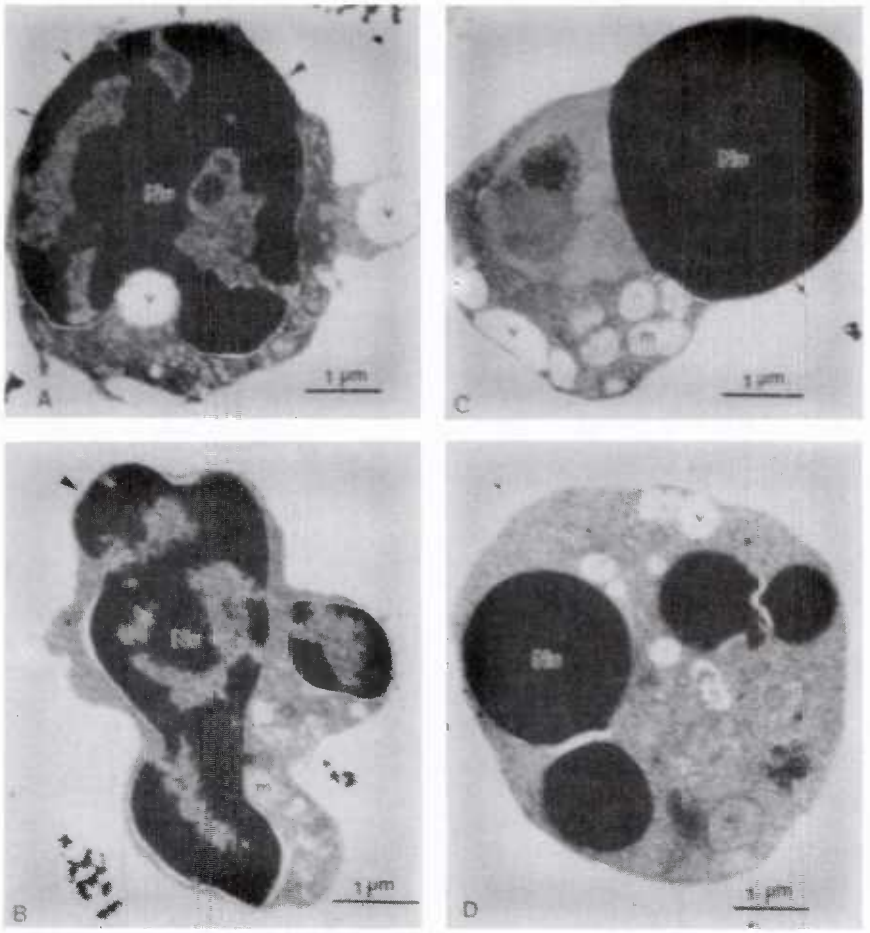

Fig. 1. Morphological features of apoptosis in thymocytes induced by 10 μM H_2O_2. Thymocytes exposed to 10 μM H_2O_2 for 10 min were resuspended in fresh TCM and incubated for 5 h at 37°C under an atmosphere of 5% CO_2 in air. The cells were fixed and analyzed by electron microscopy as described in the Materials and Methods section. Frame A: Cell in early stage of apoptosis shows condensation of chromatin and nucleoplasm (Nu), condensation of cytoplasm, and cytoplasmic vacuolization (v). The condensed chromatin forms aggregates along the nuclear membrane. Small arrows indicate close apposition of plasma membrane to nuclear membrane. Arrowhead points to the area where cytoplasm is lost. Frame B: Condensation of chromatin and nucleoplasm (Nu) is demonstrated in an apoptotic cell. Chromatin has aggregated against the nuclear membrane. Mitochondria (m) appear normal. Arrowhead indicates the close association of the plasma membrane with nuclear membrane. The plasma membrane becomes convoluted during the formation of apoptotic bodies. Frame C: This late apoptotic cell with condensed chromatin (Nu) appears to be extruding an apoptotic body. Frame D: A late apoptotic cell contains several pieces of the nucleus that will be extruded into apoptotic bodies.

Apoptosis was verified by agarose gel electrophoresis of DNA (Fig. 2A and 2B). The DNA isolated from H_2O_2-treated thymocytes exhibited a ladder pattern of DNA fragments with size multiples of 200 base pair units, as illustrated in lane C of Figure 2A. This type of DNA fragmentation into oligonucleosomal subunits is typical of apoptotic death[2,22] and differs from the random DNA breakdown that occurs during necrosis.[1] Figure 2B shows densitometric profiles of the distribution of DNA in samples from untreated and H_2O_2-treated cells derived from the photographic negatives of the gel in Figure 2A. The inset table compares selected regions of the profiles. There is apparent a general shift in density from regions of high to low molecular weight in the treated cell lane. The treated cells also demonstrate an increase in the DNA contained in internucleosomal bands. The four peaks indicated in the profile of H_2O_2-treated cells are each nearly twice as large as the analogous peaks in the untreated cell lane (expressed as a percentage of the total density area of the respective profile). Even though equal amounts of sample DNA were loaded in each lane, the total density areas differ. This is probably a reflection of the general difficulty in obtaining good quantitation from photographic negatives.

Quantitative measurements of DNA fragmentation were performed using a fluorometric method, as described in the Materials and Methods section. The ki-

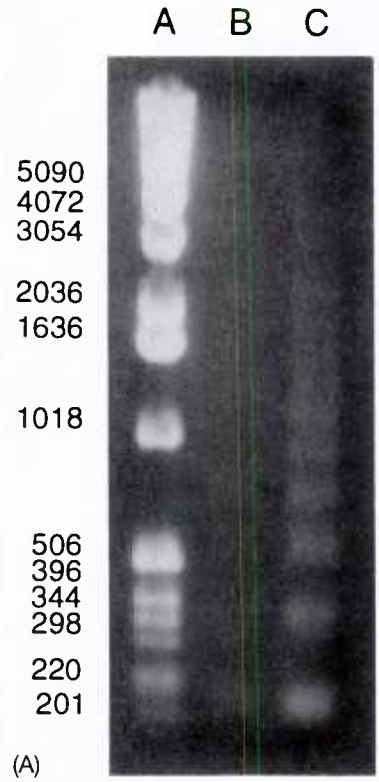

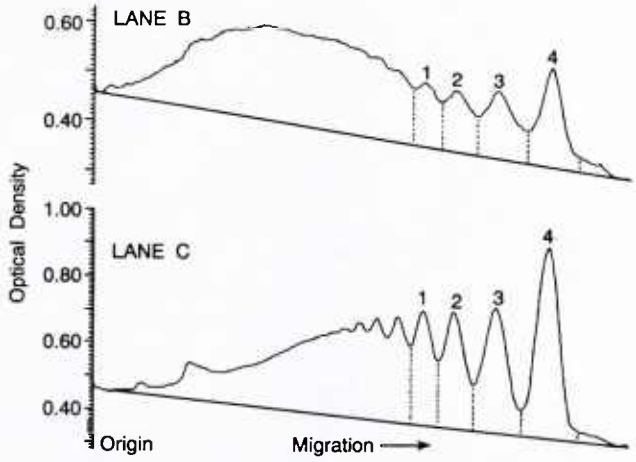

	LANE B		LANE C	
PEAK NO.	AREA	% TOTAL	AREA	% TOTAL
1	3.7	5.5	8.5	8.5
2	4.0	6.0	9.9	10.0
3	5.3	8.0	12.2	12.3
4	6.2	9.3	17.3	17.5
TOTAL AREA	66.0		98.8	

Fig. 2. (A) Agarose gel electrophoresis of DNA. Thymocytes exposed to either PBS (control) or 10 μM H_2O_2 for 10 min were resuspended in fresh TCM and incubated at 37°C under an atmosphere of 5% CO_2 in air. DNA was isolated from thymocytes after 5 h of incubation and analyzed by agarose gel electrophoresis. Lane A: 1-kb DNA marker, Lane B: PBS Control, Lane C: H_2O_2. (B) Densitometric profiles of Lanes B and C. Photographic negatives were scanned and quantified with a scanning laser densitometer and associated software.

netics of DNA fragmentation in thymocytes exposed to 0, 5, and 10 μM H_2O_2 for 10 min is shown in Figure 3. The DNA fragmentation was negligible immediately after H_2O_2 exposure (8% at 0 h). The extent of DNA fragmentation significantly increased with postexposure incubation time for each of the treatment groups. By 8 h postexposure, 42% of the DNA in 10 μM H_2O_2-exposed thymocytes had become fragmented. This was significantly greater than the DNA fragmentation exhibited by thymocytes exposed to 0 or 5 μM H_2O_2. The results indicate that H_2O_2-induced DNA fragmentation is a delayed response.

The effect of H_2O_2 concentration on DNA fragmentation was examined by treating thymocytes with 0–10 μM H_2O_2 for 10 min and comparing the percentages of fragmented DNA 8 h later (see Fig. 4). Thymocytes exposed to 0 μM H_2O_2 (PBS controls) exhibited 26% fragmentation 8 h postexposure. The three lowest concentrations of H_2O_2 did not produce fragmentation significantly greater than the PBS control. The data in Figure 4 indicate that exposure to higher concentrations, for the same duration, progressively increased the percentage of DNA fragmentation in the thymocytes. The 5 μM H_2O_2 group contained 35% DNA fragmentation that was significantly different from the 0, 0.5, 1, and 10 μM H_2O_2 treatment groups. Treatment with 10 μM H_2O_2 produced 42% fragmentation, which was significantly different from all other groups (Duncan's method, $p < .05$). These results in Figure 4 demonstrate that H_2O_2-induced DNA fragmentation is dose-dependent. The time-course display of various doses in the previous figure (Fig. 3) also suggests that H_2O_2-induced DNA fragmentation is dose-dependent.

The effect of Trolox (10 mM) on H_2O_2-induced DNA fragmentation is shown in Figure 5A. Thymocytes were exposed to either 10 μM H_2O_2 or PBS alone (controls) for 10 min, and then incubated in TCM with or without Trolox under the conditions described in the Materials and Methods section. At selected times, DNA fragmentation was determined and statistical analyses were conducted using Duncan's method ($p < .05$). The results indicate that Trolox reduced the DNA fragmentation caused by H_2O_2 to less than control levels. At the 2-, 4-, and 8-h time points, the H_2O_2 group was significantly greater than the PBS controls, and both the H_2O_2 and PBS groups were greater than

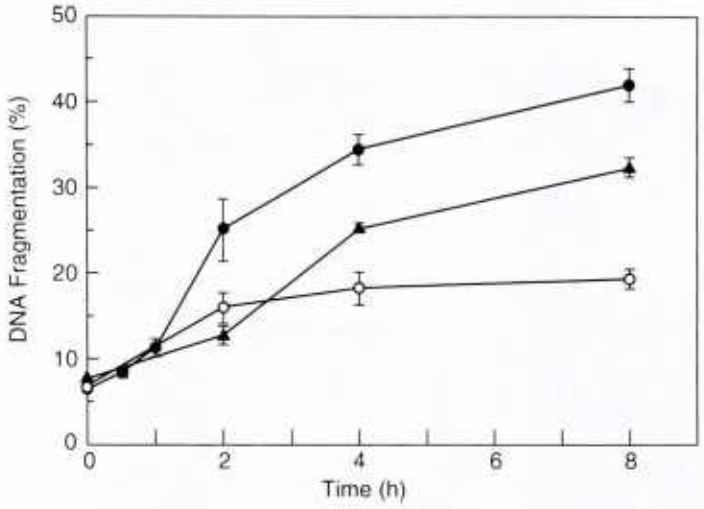

Fig. 3. DNA fragmentation increases with postexposure incubation time. Thymocytes exposed to 0, 5, and 10 μM H_2O_2 for 10 min were incubated in fresh TCM under the conditions described in Figure 1. The percentage of DNA fragmentation in the thymocytes was determined at various times postexposure, as described in the Materials and Methods sect. (●) 10 μM H_2O_2. Data are pooled from four experiments (Mean ± SEM, n = 6 to 8). (▲) 5 μM H_2O_2, (○) PBS Control, (n = 3).

the H_2O_2/Trolox group. The effect of Trolox was most evident at the 8-h time point, where H_2O_2-treated thymocytes incubated without Trolox contained 45% fragmented DNA, whereas those incubated with Trolox contained only 15%. The PBS control groups incubated with or without Trolox were not significantly different from each other at the 4- or 8-h time points.

Trolox inhibition of DNA fragmentation was further illustrated using agarose gel electrophoresis (see Fig. 5B). DNA isolated from H_2O_2-exposed thymocytes exhibited fragmentation patterns indicative of apoptosis (lane D). The DNA isolated from PBS control thymocytes contained a small amount of fragmented DNA (lane B). However, DNA isolated from H_2O_2 or PBS-exposed thymocytes that received Trolox posttreatment was unfragmented (lanes E and C, respectively).

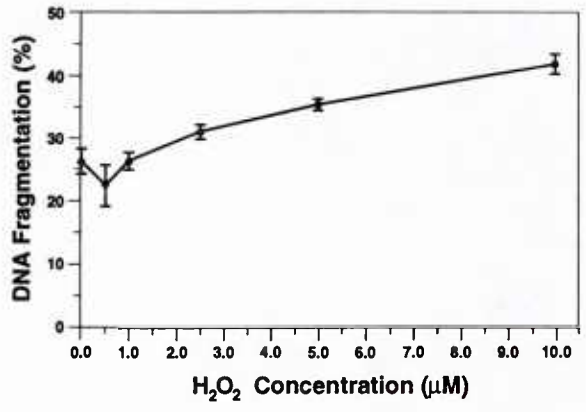

Fig. 4. DNA fragmentation increases with concentration of H_2O_2. Thymocytes were exposed to H_2O_2 for 10 min, at concentrations ranging from 0 to 10 μM. Thymocytes were incubated in TCM for 8 h and analyzed for DNA fragmentation. Data are pooled from four experiments (Mean ± SEM, n = 6 to 8).

Additional studies were carried out to determine the effect of duration of Trolox (postexposure) on inhibition of DNA fragmentation. In these studies, Trolox was removed from H_2O_2-treated thymocytes at specified times, and the cells were incubated in medium without Trolox for the remainder of the 8-h period. The results presented in Figure 6 indicate that inhibition of H_2O_2-induced DNA fragmentation is dependent upon the exposure duration of Trolox. Thirty min of Trolox treatment was not sufficient to inhibit the effects of H_2O_2. However, Trolox treatments of 1 h or more resulted in significant inhibition of H_2O_2-induced DNA fragmentation. Maximum inhibition was produced by Trolox treatment regimens of 2 or more h. Increasing the duration of Trolox treatment beyond 2 h did not significantly increase the effectiveness of Trolox (Duncan's method, $p < .05$).

The ability of Trolox to protect against oxidative-induced DNA fragmentation, when administered prior to an oxidative insult, was tested by pretreating thymocytes for 1 or 2 h with Trolox before H_2O_2 exposure. Thymocytes that did not receive Trolox during the pretreatment period exhibited 32% DNA fragmentation 6 h after H_2O_2 exposure (row 1, Table 1A). This was significantly greater than the 21 and 20% DNA fragmentation found in thymocytes that were pretreated with Trolox for 1 and 2 h, respectively, before H_2O_2 (row 2, Table 1A) (Student's t-test, $p < .05$). The percentage of DNA fragmentation present in thymocytes that were pretreated with Trolox, then ex-

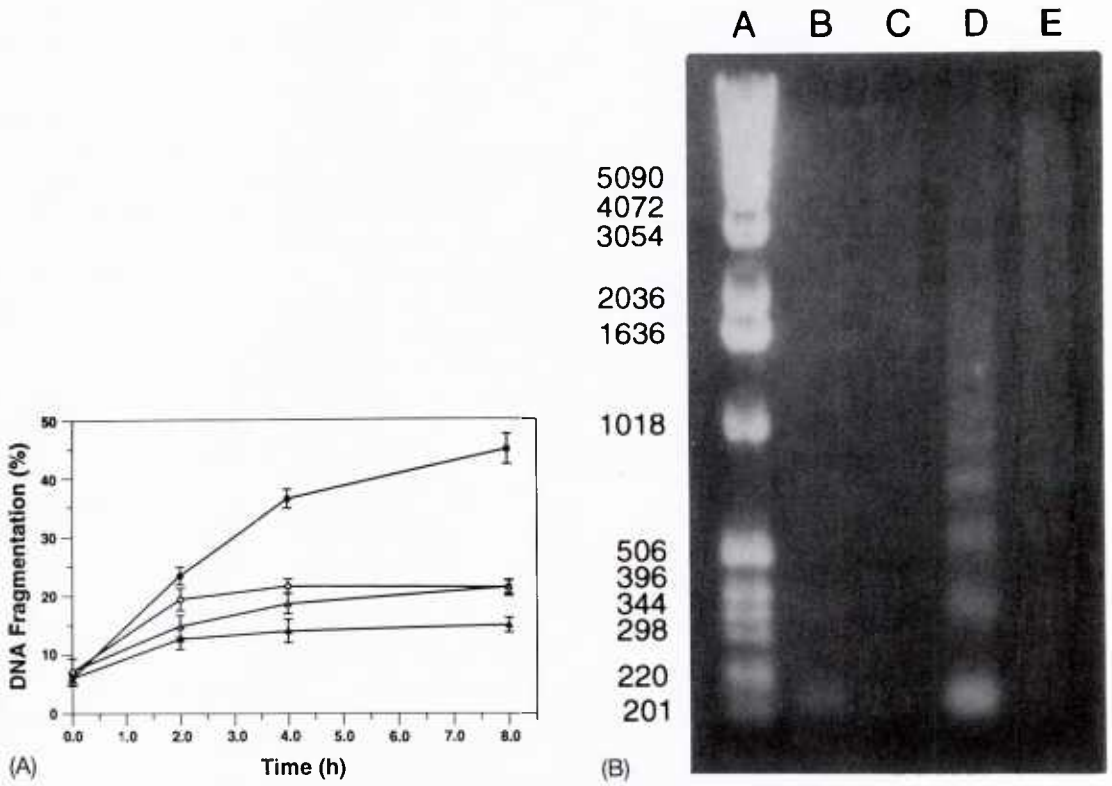

Fig. 5. (A) Postexposure treatment with Trolox inhibits H_2O_2-induced DNA fragmentation. Thymocytes were exposed to either 10 μM H_2O_2 or PBS (controls) for 10 min, then resuspended in TCM with or without Trolox (10 mM) and incubated under the conditions mentioned in Figure 1. DNA fragmentation was measured at indicated times. (●) H_2O_2, (○) PBS, (▲) H_2O_2 then Trolox, (△) PBS then Trolox. Results are pooled from three experiments (Mean ± SEM, $n = 5$). (B) Agarose gel electrophoresis. Lane A: 1-kb marker DNA, Lane B: PBS Control, Lane C: PBS Control followed by Trolox, Lane D: H_2O_2, Lane E: H_2O_2 followed by Trolox.

posed to H_2O_2, was similar to that found in the Media/PBS control and the Trolox/PBS control groups (compare row 2 with rows 3 and 4). This indicates that pretreatment of thymocytes with Trolox 1 or 2 h prior to H_2O_2 exposure does have a protective effect against DNA fragmentation.

The ability of Trolox to protect against oxidative-induced DNA fragmentation, when administered concurrently with an oxidative insult, was tested by exposing thymocytes to Trolox and H_2O_2 simultaneously for 10 min. As illustrated in Table 1B, exposure to H_2O_2 without Trolox produced 38% fragmentation 6 h later (row 1, Table 1B). Exposure to H_2O_2 and Trolox at the same time produced 35% fragmentation after 6 h (row 2). These levels of fragmentation were not significantly different from each other, but both of these were significantly different from the 24% fragmentation found in the control group that was treated with PBS without Trolox (row 3) (Student's t-test, $p < .05$). The results in Table 1B indicate that Trolox provided no protection when administered concurrently with H_2O_2.

DISCUSSION

Morphological and biochemical evidence indicate that apoptosis is induced by oxidative stress produced by H_2O_2 treatment. Electron microscopy revealed cellular morphological changes characteristic of apoptosis (Fig. 1). These changes were accompanied by internucleosomal fragmentation of DNA, qualitatively demonstrated by a DNA ladder pattern produced by agarose gel electrophoresis (Fig. 2A and 2B). Quantitative fluorometric DNA analyses demonstrated an increase in percent DNA fragmentation in H_2O_2-treated groups, which was both concentration-dependent (Figs. 3 and 4) and time-dependent (Figs. 3 and 5A). The percent DNA fragmentation in the H_2O_2 groups was significantly greater than PBS controls at the 4- and 8-h time points. These results clearly establish apoptosis as determined by the criteria set forth by Collins et al.,[2] which emphasizes the need for both morphological and biochemical indices.

It is not known whether the H_2O_2 treatment is accelerating a preexisting condition leading to spontaneous

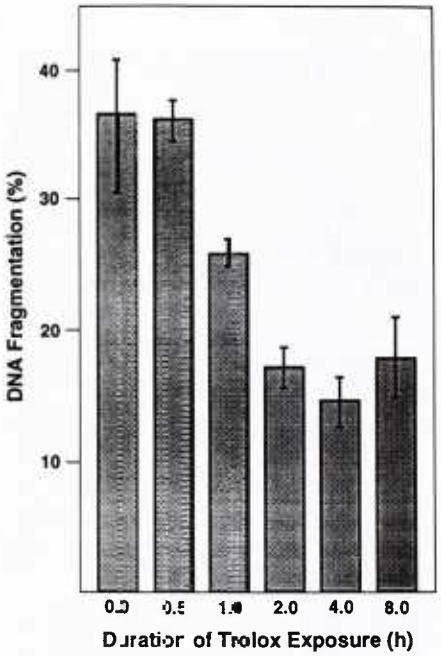

Fig. 6. Trolox inhibition of DNA fragmentation depends upon exposure duration. Thymocytes were treated with 10 μM H_2O_2 for 10 min, then resuspended in TCM with 10 mM Trolox and incubated under the conditions mentioned in Figure 1. At the times indicated, Trolox was removed by centrifugation and the cells were resuspended in Trolox-free TCM. The percentage of DNA fragmentation was determined in all of the treatment groups 8 h after the H_2O_2 exposure. Data are pooled from two experiments (Mean ± SEM, n = 8).

apoptosis, or if the H_2O_2 is inducing an apoptotic event that is distinctly different. DNA fragmentation in the controls was negligible at 0 h, but increased to 19–26% by 8 h, as illustrated in Figures 3, 4, and 5A. These levels are consistent with in vitro experiments reported by others.[8] It has been suggested by Sellins and Cohen[8] that background levels of 20–25% fragmentation are probably related to suboptimal culture conditions and preexisting (in vivo) influences, e.g., exposure to glucocorticoids. Our results suggest an alternative theory that DNA fragmentation in the controls may be due to oxidative stress received by the cells after they are removed from the animals. Cells maintained at 20–21% oxygen in vitro are exposed to much higher pO_2 levels than found in the body. This theory could be investigated by isolating and treating the thymocytes at 3% oxygen.

The time delay of DNA fragmentation (Fig. 3) following oxidative insult suggests that the DNA fragmentation is not due to a direct interaction of oxygen free radicals with DNA. It is more consistent with the process of apoptosis, which is thought to include a series of "programmed" events leading up to DNA fragmentation and suicide death.[22] We conclude that the low doses of H_2O_2 utilized here cause DNA fragmentation indirectly by initiating the series of events of apoptosis.

Activation of a calcium- and magnesium-dependent endonuclease is thought to be responsible for the DNA fragmentation that occurs during apoptosis.[11] Elevation of intracellular calcium may be involved in this activation. Cytosolic calcium has been shown to increase during apoptosis in thymocytes,[12] and it is known that calcium ionophores induce apoptosis,[12–14] whereas calcium chelators inhibit it.[23]

A review of the literature indicates that the mechanism by which calcium is elevated in apoptotic cells has not been determined. It is possible that oxidative stress interferes with calcium homeostasis by causing damage to biological membranes. Oxygen free radicals react with polyunsaturated fatty acids (PUFA) of membrane lipids, initiating self-propagating lipid peroxidation reactions.[24] Lipid–lipid covalent bonds that are formed during chain termination reactions affect the fine structure of the membranes that can result in permeability changes.[24] Free radicals derived from PUFA can inactivate membrane proteins by causing disulfide bridges, protein–lipid, and protein–protein covalent bonds.[24] Alteration of membrane permeability or inactivation of calcium pumps within the membrane could interfere with calcium homeostasis within cells.

The possibility that biological membranes are critical targets in oxidative stress-induced apoptosis is supported by the work performed with Trolox, a water-soluble vitamin E analog. Trolox is a powerful inhibitor of membrane damage and has been shown to protect mammalian cells from oxidative damage both in vivo[18,19] and in vitro.[19,20] Trolox has been shown to be eight times more efficient than vitamin E in trapping peroxyl radicals in sodium dodecyl sulfate (SDS) micelles[25] and has been demonstrated to reduce the level of phospholipid conjugated dienes in hepatocytes exposed to oxyradicals.[20]

The results presented here demonstrate that treatment with Trolox either before or after exposure to oxidative stress blocks the DNA fragmentation that accompanies apoptosis in thymocytes. We did not find it necessary for Trolox to be present continuously for it to produce its effect. For example, thymocytes incubated with Trolox for 2 h after H_2O_2 treatment were protected as much as thymocytes treated for 8 h (Fig. 6). Trolox, by protecting the biological membranes and presumably calcium homeostasis, may be precluding an initiating event in apoptosis. These results are consistent with our theory that the H_2O_2-induced DNA fragmentation is not due to a direct interaction of oxygen free radicals with DNA, but is instead a delayed effect in a series of programmed events of apoptosis.

It appears that oxidative induction of early event(s) in apoptosis is reflected in the characteristic DNA fragmentation several hours later. Similarly, protection against the initiating event(s) of apoptosis by Trolox is reflected in a decreased amount of DNA fragmentation several hours later. This rationale may also explain why Trolox pretreatment has a protective effect that is evidenced 6 h later, even though this water soluble compound would have diffused out of the cells during the 6 h posttreatment period. The protective action of Trolox may actually be occurring during or shortly after hydrogen peroxide exposure, but a suitable lag time must be given (e.g., 4–8 h) to enable differences in DNA fragmentation to become apparent.

Trolox administered concurrently with H_2O_2 was not protective against DNA fragmentation. However, this lack of protection may have been due to an inadequate exposure duration. The concurrent treatment, which lasted only 10 min, may not have allowed sufficient diffusion of Trolox into the thymocytes. This suggests that the effectiveness of Trolox in this study was due to its ability to terminate self-propagating lipid peroxidation reactions within the membranes, rather than the quenching of free radicals within the exposure medium.

Oxidative induction of apoptosis has implications for a variety of medical conditions. Oxygen free radicals have been reported to be associated with aging, hyperoxygenation, ischemia/reperfusion injury, inflammatory disorders, ionizing radiation exposure, and circulatory shock.[16] We have demonstrated here that oxidative stress produced by hydrogen peroxide treatment induces apoptosis in mouse thymocytes in vitro and that Trolox protects against this. Hydrogen peroxide also has been reported to induce apoptosis in the murine blastocyst[15] and the human promyelocytic leukemia HL-60 cell line.[26] Apoptosis occurring in vivo in response to various other stimuli, has been demonstrated in a variety of tissues, including muscle,[27] prostate,[28] liver,[29] intestinal crypt cells,[30] and brain.[31] Further investigations are needed to examine the mechanisms by which oxidative stress induces apoptosis and to identify the types of tissues affected.

Acknowledgements—This work was supported by the Naval Medical Research and Development Command Work Unit No. 61153N MR04101.001-1055. The opinions and assertions contained herein are the private ones of the authors and are not to be construed as official or reflecting the views of the naval service at large. We thank William W. Wolfe, Linda Y. Tiller, and Robert Williams for their excellent technical assistance, and Dr. George N. Catravas for his support and encouragement. We also thank Susan Cecire and Janet Gaines for preparation of this manuscript and Regina Hunt for her assistance with the illustrations. Trolox was kindly provided by Hoffman-La Roche, Nutley, NJ. Research was conducted according to the principles enunciated in the Guide for the Care and Use of Laboratory Animals prepared by the Institute of Laboratory Animal Resources, National Research Council, DDH, Pub. No. (NIH) 85-23.

REFERENCES

1. Kerr, J. F. R.; Harmon, B. V. Definition and incidence of apoptosis: An historical perspective. In Tomei, L. D., Cope, F. O. eds.: *Apoptosis: The molecular basis of cell death.* New York: Cold Spring Harbor Laboratory Press; 1991:5–29.
2. Collins, R. J.; Harmon, B. V.; Gobe, G. C.; Kerr, J. F. R. Internucleosomal DNA cleavage should not be the sole criterion for identifying apoptosis. *Int. J. Radiat. Biol.* **61**:451–453; 1992.
3. Duvall, E.; Wyllie, A. H. Death and the cell. *Immunology Today* **7**:115–119; 1986.
4. Kerr, J. F. R.; Wyllie, A. H.; Currie, A. R. Apoptosis: A basic biological phenomenon with wide ranging implications in tissue kinetics. *Br. J. Cancer* **26**:239–257; 1972.
5. Duke, R. C.; Chervenak, R.; Cohen, J. J. Endogenous endonuclease-induced DNA fragmentation: An early event in cell-mediated cytolysis. *Proc. Natl. Acad. Sci.* **80**:6361–6365; 1983.
6. MacDonald, H. R.; Lees, R. K. Programmed death of autoreactive thymocytes. *Nature* **343**:642–644; 1990.
7. Yamada, T.; Ohyama, H. Radiation-induced interphase death of rat thymocytes is internally programmed (apoptosis). *Int. J. Radiat. Biol.* **53**:65–75; 1988.
8. Sellins, K. S.; Cohen, J. J. Gene induction by γ-irradiation leads to DNA fragmentation in lymphocytes. *J. Immunol.* **139**:3199–3206; 1987.
9. Ashwell, J. D.; Schwartz, R. H.; Mitchell, J. B.; Russo, A. Effect of gamma radiation on resting B lymphocytes. *J. Immunol.* **136**:3649–3656; 1986.
10. Wyllie, A. H. Glucocorticoid-induced thymocyte apoptosis is associated with endogenous endonuclease activation. *Nature* **284**:555–556; 1980.
11. Cohen, J. J.; Duke, R. C. Glucocorticoid activation of calcium-dependent endonuclease in thymocyte nuclei leads to cell death. *J. Immunol.* **132**:38–42; 1984.
12. McConkey, D. J.; Hartzell, P.; Nicotera, P.; Orrenius, S. Calcium-activated DNA fragmentation kills immature thymocytes. *FASEB J.* **3**:1843–1849; 1989.
13. Wyllie, A. H.; Morris, R. G.; Smith, A. L.; Dunlop, D. Chromatin cleavage in apoptosis: Association with condensed chromatin morphology and dependence on macromolecular synthesis. *J. Pathol.* **142**:67–77; 1984.
14. Smith, C. A.; Williams, G. T.; Kingston, R.; Jenkinson, E. J.; Owen, J. J. T. Antibodies to CD3/T-cell receptor complex induce death by apoptosis in immature T cell in thymic cultures. *Nature* **337**:181–184; 1989.
15. Parchment, R. E. Programmed cell death (apoptosis) in murine blastocysts: Extracellular free-radicals, polyamines, and other cytotoxic agents. *In Vivo* **5**:493–500; 1991.
16. Bulkley, G. B. The role of oxygen free radicals in human disease processes. *Surgery* **94**:407–411; 1983.
17. Barclay, L. R. C.; Locke, S. J.; MacNeil, J. M.; VanKessel, J. Autoxidation of micelles and model membranes. Quantitative kinetic measurements can be made by using either water-soluble or lipid-soluble initiators with water-soluble or lipid-soluble chain-breaking antioxidants. *J. Am. Chem. Soc.* **106**:2479–2481; 1984.
18. Casini, A. F.; Pompella, A.; Comporti, M. Liver glutathione depletion induced by bromobenzene, iodobenzene, and diethylmaleate poisoning and its relation to lipid peroxidation and necrosis. *Am. J. Path.* **118**:225–237; 1985.
19. Mickle, D. A. G.; Li, R.-K.; Weisel, R. D.; Birnbaum, P. L.; Wu, T.-W.; Jackowski, G.; Madonik, M. M.; Burton, G. W.; Ingold, K. U. Myocardial salvage with Trolox and ascorbic acid for an evolving infarction. *Ann. Thorac. Surg.* **47**:553–557; 1989.
20. Wu, T.-W.; Hashimoto, N.; Wu, J.; Carey, D.; Li, R.-K.; Mickle, D. A. G.; Weisel, R. D. The cytoprotective effect of Trolox

demonstrated with three types of human cells. *Biochem. Cell Biol.* **68:**1189–1194; 1990.

21. Ramakrishnan, N.; Catravas, G. N. *N*-(2-mercaptoethyl)-1,3-propanediamine (WR-1065) protects thymocytes from programmed cell death. *J. Immunol.* **148:**1817–1821; 1992.
22. Arends, M. J.; Morris, R. G.; Wyllie, A. H. Apoptosis. The role of the endonuclease. *Am. J. Pathol.* **136:**593–608; 1990.
23. Story, M. D.; Stephens, L. C.; Tomasovic, S. P.; Meyn, R. E. A role for calcium in regulating apoptosis in rat thymocytes irradiated in vitro. *Int. J. Radiat. Biol.* **61:**243–251; 1992.
24. Horton, A. A.; Fairhurst, S. Lipid peroxidation and mechanisms of toxicity. *CRC Crit. Rev. Toxicol.* **18:**27–79; 1987.
25. Castle, L.; Perkins, M. J. Inhibition kinetics of chain-breaking phenolic antioxidants in SDS micelles. Evidence that intermicellar diffusion rates may be rate-limiting for hydrophobic inhibitors such as α-tocopherol. *J. Am. Chem. Soc.* **108:**6381–6382; 1986.
26. Lennon, S. V.; Martin, S. J.; Cotter, T. G. Dose-dependent induction of apoptosis in human tumour cell lines by widely diverging stimuli. *Cell Prolif.* **24:**203–214; 1991.
27. Darby, I.; Skalli, O.; Gabbiani, G. α-Smooth muscle actin is transiently expressed by myofibroblasts during experimental wound healing. *Lab. Invest.* **63:**21–29; 1990.
28. Kyprianou, N.; Isaacs, J. T. Activation of programmed cell death in the rat ventral prostate after castration. *Endrocrinol.* **122:**552–562; 1988.
29. Pritchard, D. J.; Butler, W. H. Apoptosis—The mechanism of cell death in dimethylnitrosamine-induced hepatotoxicity. *J. Path.* **158:**253–260; 1989.
30. Potten, C. S. Extreme sensitivity of some intestinal crypt cells to X and γ-irradiation. *Nature* **269:**518–521; 1977.
31. Inouye, M.; Tamaru, M.; Kameyama, Y. Effects of cycloheximide and actinomycin D on radiation-induced apoptotic cell death in the developing mouse cerebellum. *Int. J. Radiat. Biol.* **61:**669–674; 1992.

PROTEIN EXPRESSION AND PURIFICATION 5, 324–330 (1994)

Rapid Isolation of Nuclear Transport-Competent *Xenopus* Nucleoplasmin Produced in *Escherichia coli* Strain BL21(DE3)

John F. Kalinich and David E. McClain
Radiation Biochemistry Department, Armed Forces Radiobiology Research Institute, 8901 Wisconsin Avenue, Bethesda, Maryland 20889-5603

Received October 19, 1993, and in revised form January 12, 1994

Nucleoplasmin is a thermostable karyophilic protein widely used in nuclear transport studies. An expression vector was constructed that contains a string of 10 histidine residues ligated, in frame, to the amino terminal end of the *Xenopus* nucleoplasmin gene. The vector was then transformed into *Escherichia coli* strain BL21(DE3). This strain possesses the gene for T7 RNA polymerase under control of the lacUV5 promoter. The induction of the RNA polymerase and subsequent production of nucleoplasmin occurs after exposure to isopropyl-β-D-thiogalactopyranoside. The nucleoplasmin, produced in milligram quantities per liter of culture, is then isolated by a rapid purification method that includes metal chelation chromatography to purify the oligohistidine-linked nucleoplasmin. Nuclear transport studies indicate that fluorescently labeled nucleoplasmin is translocated to the nuclear interior of permeabilized V79A03 cells, while nucleoplasmin that lacks a nuclear localization signal (core nucleoplasmin) is not imported. The use of this method to produce nuclear transport-competent nucleoplasmin avoids the lengthy purification procedure used to isolate nucleoplasmin from *Xenopus laevis* oocytes as well as the cost of purchasing and maintaining a toad colony.

The process of protein translocation into the cell nucleus is currently an area of great interest. One of the most widely used probes for nuclear transport studies is nucleoplasmin, a thermostable acidic pentameric protein involved in histone binding and nucleosome formation (1–4). A procedure to produce small amounts of radiolabeled nucleoplasmin via a coupled *in vitro* transcription/translation protocol has been reported (5). However, isolation of milligram quantities of nucleoplasmin requires the use of *Xenopus laevis* oocytes, where nucleoplasmin constitutes up to 10% of the nuclear protein (6,7). To avoid the high cost of purchasing and maintaining toads, we have devised a method to produce and isolate milligram quantities of nuclear transport-competent nucleoplasmin from *Escherichia coli*.

The expression vector pET-16b contains the lac operator and repressor downstream of the T7 promoter (8). This allows transcription of the cloned gene to be almost completely eliminated until induction is initiated. In addition, pET-16b codes for a stretch of 10 histidine residues after the initiator methionine, followed by a Factor Xa protease cleavage site (9). A small cloning region allows for the introduction of the gene of interest in frame with the oligohistidine and protease cleavage regions. The oligohistidine region permits the rapid purification of the expressed protein by metal chelation chromatography (10,11).

E. coli strain BL21(DE3) contains a single copy of the T7 RNA polymerase gene under control of the lacUV5 promoter (12,13). This allows for the overexpression of a T7 plasmid-containing gene following induction with isopropyl-β-D-thiogalactopyranoside (IPTG). This system, along with the expression vector pET-16b, was used to produce nucleoplasmin in *E. coli*. Rapid purification of the nucleoplasmin was then accomplished by a heating step and metal chelation chromatography. Experiments indicated that purified *E. coli*-produced nucleoplasmin can substitute for nucleoplasmin isolated from *X. laevis* oocytes in nuclear transport studies. This method circumvents the time-consuming procedure of isolating and purifying nucleoplasmin from *X. laevis* oocytes as well as the costs involved with purchasing and maintaining a toad colony.

EXPERIMENTAL

Construction of pET16b-NED

Plasmid pET-16b was purchased from Novagen (Madison, WI). Plasmid pET16b-NED was constructed

1046-5928/94 $6.00

by ligation of a 0.68-kb *NdeI/Bam*HI fragment, containing the *X. laevis* nucleoplasmin gene, from pT7-NED (5) into *NdeI/Bam*HI-cut pET-16b. The nucleoplasmin cDNA (23) used to construct pT7-NED was kindly provided by Dr. Thomas Burglin (Massachusetts General Hospital, Boston, MA). *E. coli* strain DH1 was transformed with the ligation mixture using $CaCl_2$, and transformants possessing the pET16b-NED plasmid were selected by plating on LB medium supplemented with 50 μg/ml carbenicillin. Restriction digestions, agarose gel electrophoresis, ligation reactions, and transformations were as described (14). The linkage region between the pET-16b oligohistidine leader sequence and the nucleoplasmin gene was confirmed by DNA sequencing using the dideoxy method (15).

Preparation of Transformed BL21(DE3)

E. coli strain BL21(DE3) (F^- *hsd*S *gal omp*T $r_B^- m_B^-$) was kindly provided by Dr. Paul Herring (Indiana University, Indianapolis, IN). Preparation of plasmid pET16b-NED DNA and transformation of *E. coli* strain BL21(DE3) using $CaCl_2$ were as described (14). Stable transformants were selected by plating on M9ZYB medium (1 g/liter NH_4Cl, 3 g/liter KH_2PO_4, 6 g/liter Na_2HPO_4, 4 g/liter glucose, 2 mM $MgSO_4$, 0.1 mM $CaCl_2$, 10 g/liter tryptone, 5 g/liter NaCl, 5 g/liter yeast extract) supplemented with 50 μg/ml carbenicillin and 1.0 mM IPTG (12).

Expression and Isolation of Nucleoplasmin

A 25-ml culture of *E. coli* strain BL21(DE3) containing pET16b-NED was grown overnight at 37°C and 200 rpm in M9ZYB medium supplemented with 50 μg/ml carbenicillin. The overnight culture was used to inoculate 500 ml of M9ZYB–carbenicillin. After reaching an OD_{600} of 1.0, the culture was induced by the addition of IPTG to 1.0 mM. After 3 h the cells were harvested by centrifugation at 3000*g* and 4°C for 10 min, pooled, and washed once with water. The pellet was resuspended in 20 mM Tris–HCl, pH 7.9, containing 0.5 M NaCl, 5 mM imidazole, 1 mM phenylmethylsulfonyl fluoride (PMSF), and 1 μg/ml each of pepstatin, leupeptin, and aprotinin (10 ml/liter of culture) and disrupted by sonication (4 × 30 s, setting 7; Heat Systems Cell Disruptor with microtip). The mixture was centrifuged at 12,000*g* for 15 min at 4°C. The supernatant, containing the nucleoplasmin, was heated at 80°C for 10 min and centrifuged at 12,000*g* for 30 min at 4°C. To purify the nucleoplasmin further, the supernatant was loaded onto a Ni^{2+}-metal chelation resin column (20 mg protein/2.5 ml column volume) (Novagen). Column preparation and chromatography were conducted as described in the manufacturer's instructions. Briefly, the column was washed with 10 column vol of binding buffer (20 mM Tris–HCl, pH 7.9, 0.5 M NaCl, 5 mM imidazole) and 6 column vol of wash buffer (20 mM Tris–HCl, pH 7.9, 0.5 M NaCl, 60 mM imidazole). The oligohistidine-linked nucleoplasmin was eluted from the column with 6 column vol of elution buffer (20 mM Tris–HCl, pH 7.9, 0.5 M NaCl, 1 M imidazole). The eluted protein was concentrated in a Centricon C-10 microconcentrator (W. R. Grace Co., Beverly, MA) and desalted by passage through a Sephadex G-25 column. The oligohistidine region could be removed from the nucleoplasmin by treating with Factor Xa (16), but since this region had no apparent effect on the ability of the protein to localize to the nucleus of permeabilized cells, it was not routinely removed.

Miscellaneous Methods

Nucleoplasmin lacking a nuclear localization signal (core nucleoplasmin) was prepared as described (17). Electrophoresis of nucleoplasmin purification fractions using SDS–polyacrylamide gels was performed by the method of Laemmli (18). Antiserum to nucleoplasmin was kindly provided by Dr. Carl Feldherr (University of Florida, Gainsville, FL). Western blot analysis was performed as described (19). Purified nucleoplasmin and core nucleoplasmin were fluorescently labeled with tetramethylrhodamine isothiocyanate (TRITC) by the method of Newmeyer *et al.* (20). Polyacrylamide gels and Western blots were scanned by a Molecular Dynamics Laser Densitometer (Sunnyvale, CA) and the density volumes calculated using the associated ImageQuant software.

Cell Culture Conditions

Alpha minimal essential medium, fetal calf serum, penicillin, streptomycin, L-glutamine, and *N*-2-hydroxyethylpiperizine-*N*″-2-ethane sulfonic acid (Hepes) were purchased from Gibco/BRL (Gaithersburg, MD). Chinese hamster lung fibroblasts (clone V79A03) were maintained as monolayer cultures at 37°C in an atmosphere of 5% CO_2 in air in alpha minimal essential medium supplemented with 10% fetal calf serum, 100 U/ml penicillin, 100 μg/ml streptomycin, 2 mM L-glutamine, and 25 mM Hepes. For nuclear transport experiments, cells were plated onto glass coverslips (9 × 35 mm). Cells were used when they were 70–80% confluent. To prepare for permeabilization the cells were placed on ice, washed with cold Buffer A* (20 mM Hepes, pH 7.3, 110 mM potassium acetate, 2 mM magnesium acetate, 1 mM EGTA, 2 mM dithiothreitol, 1 μg/ml each of aprotinin, leupeptin, and pepstatin) (21,22) and then incubated 5 min on ice with 35 μg/ml digitonin in Buffer A*. The cells were washed once again after permeabilization with cold Buffer A* and left in cold Buffer A* until needed.

Preparation of Cytosolic Fraction

V79A03 cells were harvested by scraping from the tissue culture plates with a rubber policeman. The cells were washed with cold Hanks' balanced salt solution and resuspended in hypotonic buffer (10 mM Hepes, pH 7.4, 5 mM $MgCl_2$, 1 mM PMSF, and 1 μg/ml each of aprotinin, leupeptin, and pepstatin) at 10 ml/10^8 cells. The cell suspension was left on ice for 15 min and then disrupted with 15 strokes of a Dounce homogenizer (pestle A). The mixture was centrifuged at 1000*g* and 4°C for 10 min, producing a supernatant that was then centrifuged at 10,000*g* and 4°C for 20 min. The supernatant resulting from this step was centrifuged at 150,000*g* and 4°C for 2 h. The resulting supernatant from this high-speed centrifugation step was dialyzed overnight at 4°C against multiple changes of Buffer A*, concentrated in a Centricon C-10 microconcentrator, and brought to a protein concentration of 40 mg/ml with Buffer A*.

In Vitro Nuclear Transport

A standard transport reaction contained bovine serum albumin (1 mg/ml), ATP (1 mM), creatine kinase (20 U/ml), creatine phosphate (5 mM), cytosolic fraction (10 mg protein/ml), and TRITC–nucleoplasmin (5 μg/ml), brought to a final volume of 20 μl with Buffer A* (22). Coverslips, containing the digitonin-permeabilized cells, were blotted on a paper towel to remove excess fluid and placed cell side down onto 20 μl of the transport mixture on a sheet of parafilm. Transport reactions were run in a humidified box at 30°C for 15 min. Other additions to the transport reactions are as given in the figure legends. Reactions were terminated by the addition of 250 μl of cold Buffer A*. The coverslips were washed once with cold Buffer A* and fixed on ice for 5 min with 3% paraformaldehyde in Buffer A (Buffer A* minus dithiothreitol and protease inhibitors). The coverslips were washed with cold Buffer A, blotted on a paper towel, and mounted on a glass slide on one drop of 1 mg/ml phenylenediamine in 90% glycerol/10% phosphate-buffered saline. Nail polish was used to seal the edges of the coverslip. Slides were examined with an Olympus AH-3 fluorescence microscope and photomicrographs taken with Polaroid Type-57 film.

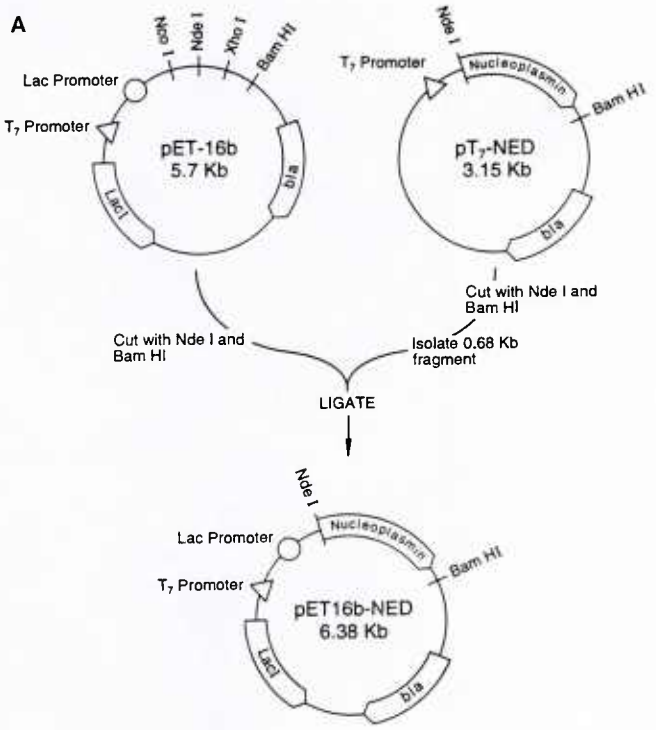

FIG. 1. Construction of pET16b-NED. (A) Plasmid maps of pET-16b and pT7-NED and the construction of pET16b-NED. Details are given in the text. The lac repressor gene is represented by lacI, while the gene conferring carbenicillin (ampicillin) resistance is denoted by bla (β-lactamase). (B) DNA sequence of the expressed linker region between pET-16b and the nucleoplasmin gene. The first 62 base pairs (uppercase) are derived from pET-16b. The next 20 base pairs (lowercase) are a result of the cloning procedure used to subclone the nucleoplasmin cDNA into pT7-7 (5). The bold letters represent the first base pairs of the nucleoplasmin cDNA (23). (C) The amino acid sequence of the linker region described in B. The underlined region indicates the Factor Xa protease cleavage site.

RESULTS AND DISCUSSION

The construction of pET16b-NED is shown in Fig. 1A. A 0.68-kb *Nde*I/*Bam*HI fragment from pT7-NED containing the coding region for the *X. laevis* nucleoplasmin gene was ligated into *Nde*I/*Bam*HI-digested pET-16b. The resulting plasmid, pET16b-NED, contained the nucleoplasmin gene plus an additional 21 amino acids attached to the amino terminal end of the protein. This stretch of amino acids contains 10 histidine residues that allow for protein purification by metal chelation chromatography and a Factor Xa protease site that allows for removal of the "leader sequence" from the nucleoplasmin. The base and amino acid sequences of the linker region are shown in Figs. 1B and 1C. The presence of the leader sequence did not affect

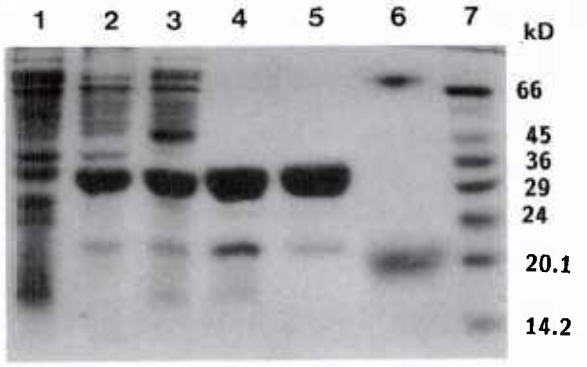

FIG. 2. SDS–polyacrylamide gel of nucleoplasmin isolation fractions. The uninduced (lane 1), induced (lane 2), homogenate (lane 3), heat (lane 4), and column (lane 5) fractions from a typical nucleoplasmin isolation, as well as core nucleoplasmin (lane 6), were electrophoresed on a 12.5% SDS–polyacrylamide gel (50 μg protein per lane). The gel was stained with Coomassie blue and destained in 10% acetic acid/methanol solution. Lane 7 contains the molecular mass markers (Sigma): bovine serum albumin, 66 kDa; egg albumin, 45 kDa; glyceraldehyde-3-phosphate dehydrogenase, 36 kDa; carbonic anhydrase, 29 kDa; trypsinogen, 24 kDa; trypsin inhibitor, 20.1 kDa; and α-lactalbumin, 14.2 kDa.

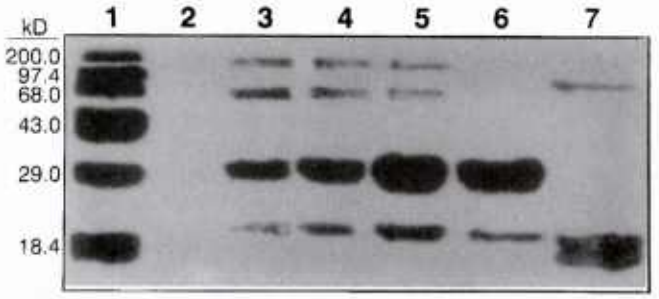

FIG. 3. Western blot of nucleoplasmin isolation fractions. Nucleoplasmin isolation fractions were electrophoresed on 12.5% SDS–polyacrylamide gels as described and transferred to nitrocellulose. The blot was probed with antisera (1:500 dilution) developed in rabbit against *X. laevis* nucleoplasmin. After incubation with horseradish peroxidase–goat anti-rabbit IgG (Sigma), color development was achieved using 4-chloro-1-naphthol. The following samples are represented: molecular mass markers (lane 1), uninduced fraction (lane 2), induced fraction (lane 3), homogenate fraction (lane 4), heat fraction (lane 5), column fraction (lane 6), and core nucleoplasmin (lane 7). Prestained molecular mass markers (Gibco/BRL, Gaithersburg, MD) are myosin H-chain, 200 kDa; phosphorylase b, 97.4 kDa; bovine serum albumin, 68 kDa; ovalbumin, 43 kDa; carbonic anhydrase, 29 kDa; β-lactoglobulin, 18.4 kDa.

the ability of the nucleoplasmin to be imported to the nuclear interior, so it was not routinely removed (data not shown).

A representative Coomassie blue-stained SDS–polyacrylamide gel of the fractions obtained during the purification of nucleoplasmin is shown in Fig. 2. Lane 1 is an uninduced culture of BL21(DE3) containing pET16b-NED. The protein profile in lane 2 was obtained following a 3-h induction of nucleoplasmin by IPTG. As seen, an intense nucleoplasmin band migrating at a molecular weight of approximately 32 kDa constitutes much of the protein in this fraction. Lane 3 is the supernatant resulting from the sonication and centrifugation of the bacteria. After heat treatment (10 min/80°C) and centrifugation, the profile in lane 4 was obtained. This step eliminated the majority of the bacterial proteins. However, along with the nucleoplasmin, two additional bands, migrating at approximately 21 and 26 kDa, are apparent. To purify the nucleoplasmin further, metal chelation chromatography was used. The nucleoplasmin-containing fraction was chromatographed on a Ni^{2+} column, which bound the oligohistidine leader sequence ligated to the nucleoplasmin. The contaminating proteins were then washed from the column and the nucleoplasmin was eluted as described. The column-purified nucleoplasmin is shown in lane 5. The 21- and 26-kDa bands were still present in this fraction, albeit as only a very small percentage of the total protein (0.9 and 0.3%, respectively). Lane 6 is core nucleoplasmin (nucleoplasmin lacking a nuclear localization signal) and was prepared by treating intact nucleoplasmin with trypsin (17). The 20-kDa band is the monomeric form of the core nucleoplasmin, while the higher-molecular-weight band represents the pentameric form. A Western blot of the nucleoplasmin isolation fractions is shown in Fig. 3. Lane 2 (uninduced culture) shows no reaction. A 32-kDa band was recognized by antisera produced against *X. laevis* nucleoplasmin in each of the isolation fractions (lanes 3–6). Lane 7 (core nucleoplasmin) shows a reaction at 20 kDa.

In addition to the 32-kDa band, the nucleoplasmin antisera also recognized the 21- and 26-kDa bands seen in the Coomassie-stained gel, indicating that these

TABLE 1

Purification of Nucleoplasmin

Fraction	Protein (mg)	Percentage nucleoplasmin	Percentage yield	Fold purification
Induced	2131.0	32.1	100	—
Homogenate	870.6	37.8	48	1
Heat	96.0	76.7	11	2
Column	78.6	98.8	11	3

Note. Protein concentrations were determined using the method of Bradford (25) and are based on a 1-liter culture. SDS–polyacrylamide gels were scanned by laser densitometry. The density volume of the nucleoplasmin band (32 kDa) was calculated and divided by the density volume obtained from scanning the entire sample lane to yield "percentage nucleoplasmin" (nucleoplasmin as a percentage of total protein).

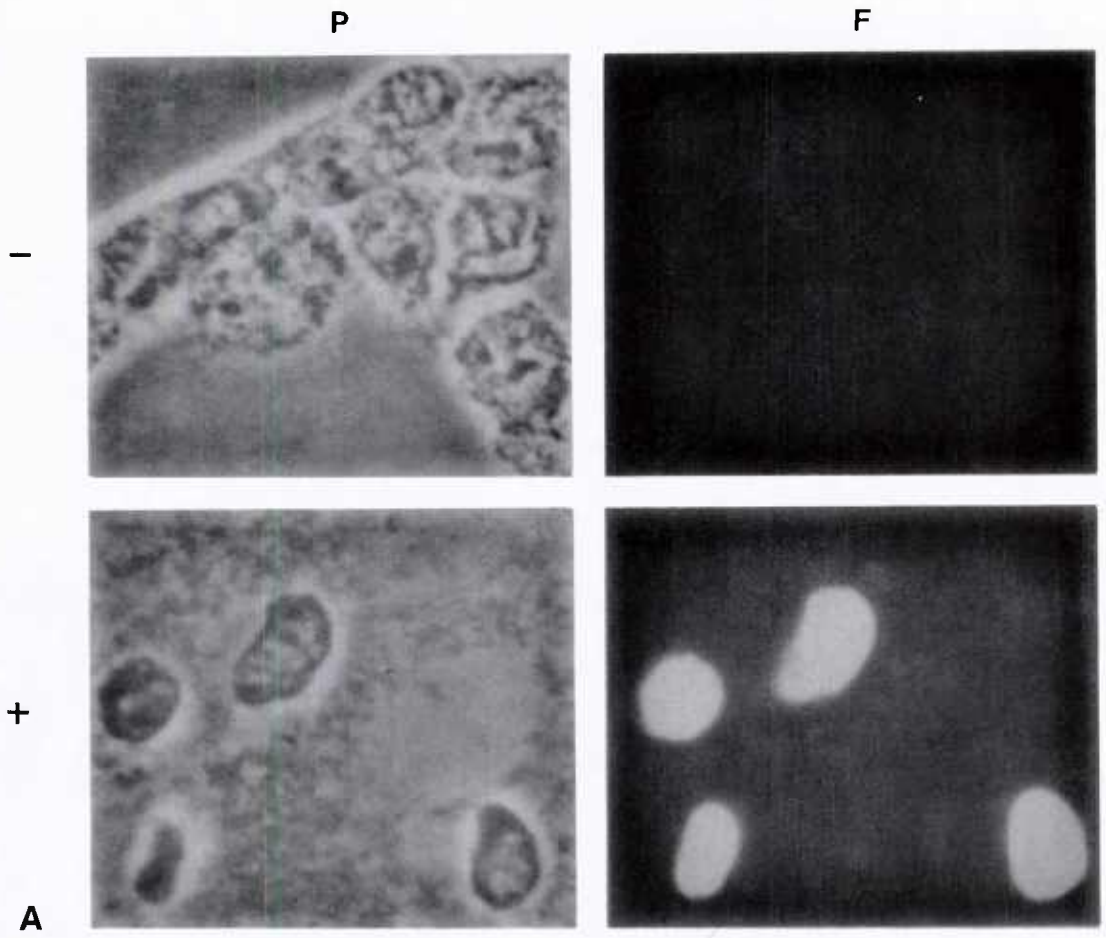

FIG. 4. Photomicrographs of nuclear transport experiments. (A) Requirement for cytosolic factors. Transport experiments (30°C/15 min) were conducted either in the presence (+) or absence (–) of cytosolic factors as described in the text. Both phase contrast (P) and fluorescence (F) photomicrographs are shown. (B) Import of core nucleoplasmin. Transport experiments (30°C/15 min) were conducted as described, except TRITC–nucleoplasmin was replaced with an equal concentration of TRITC–core nucleoplasmin. (C) ATP requirement. Transport experiments (30°C/15 min) were conducted as described in the text, except the ATP regenerating system (ATP, creatine kinase, and creatine phosphate) was omitted and replaced with an equal volume of Buffer A*.

bands represent a truncated form of nucleoplasmin. Even though these proteins had no affect on the ability of nucleoplasmin to accumulate in the nuclear interior, we sought to determine their origin. Originally it was thought these bands represented proteins produced from methionine residues 3′ to the initiator methionine. This should result in shorter forms of nucleoplasmin that might still be immunologically recognized by the nucleoplasmin antisera. However, if this were the case, the oligohistidine leader sequence would not be present, and the truncated nucleoplasmin species would not bind to the Ni^{2+} column. As shown in both Figs. 2 and 3, the truncated forms of nucleoplasmin bound to the Ni^{2+} column. The shortened nucleoplasmin species may have resulted from proteolysis during the isolation procedure. However, the presence of the protease inhibitors PMSF, pepstatin, leupeptin, and aprotinin during isolation would tend to argue against that possibility. Furthermore, *E. coli* strain BL21(DE3) is deficient in both the *lon* and the *omp*T proteases that would contribute to sample proteolysis (13). We attempted to eliminate these truncated nucleoplasmin bands by treating the bacterial culture with rifampicin (30 min after IPTG induction) to inhibit transcription by the bacterial RNA polymerases and production of any bacterial proteases. However, no differences were observed between the gel patterns of nucleoplasmin obtained from rifampicin-treated and -untreated cultures. Changing the incubation temperature (30, 35, 37°C), the culture medium (M9ZYB, LB), and the harvest time (30 min to 3 h post-IPTG induction) also had no effect on the distribution of the intact and truncated forms of the nucleoplasmin (data not shown). The origin of these bands remains to be determined.

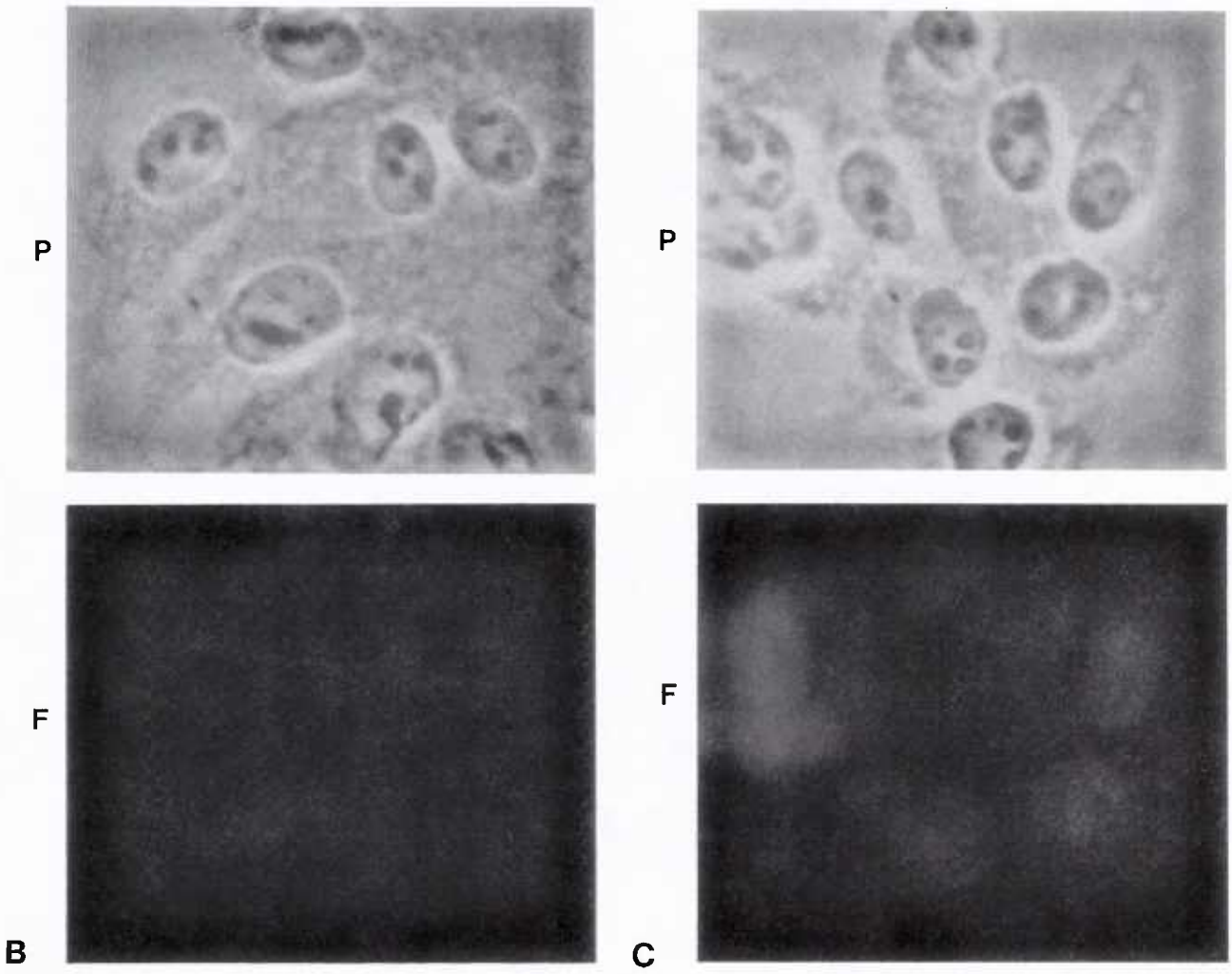

FIG. 4—*Continued*

Table 1 is a summary of the purification of nucleoplasmin. After induction with IPTG, almost $\frac{1}{3}$ of the protein present in the "induced fraction" was nucleoplasmin. Sonication and centrifugation of the bacteria yielded the "homogenate fraction." Nucleoplasmin accounted for greater than $\frac{1}{3}$ of the protein content of this fraction. The "heat fraction" was obtained after heat treatment and centrifugation. Nucleoplasmin made up well over 75% of the protein found in this fraction, with the truncated nucleoplasmin forms and small-molecular-weight contaminants accounting for the remainder. After metal chelation chromatography, greater than 98% of the protein in the "column fraction" was nucleoplasmin (32 kDa) with the remaining protein being mostly 21- and 26-kDa truncated forms of nucleoplasmin (approximately 1 and 0.5%, respectively).

After isolation, the nucleoplasmin was fluorescently labeled with rhodamine and tested in an *in vitro* nuclear transport system using permeabilized mammalian cells (21,22). Shown in Fig. 4A are the phase contrast and fluorescent photomicrographs of a 30°C/15 min transport experiment run with and without the cytosolic fraction. When incubated in the presence of the cytosolic fraction and an ATP regenerating system, nucleoplasmin is imported to the nuclear interior of digitonin-permeabilized V79A03 cells. When the cytosolic fraction is omitted, the nucleoplasmin does not localize to the nucleus. This confirms the results of other investigators using nucleoplasmin isolated from *X. laevis* oocytes in similar nuclear transport systems (21,22,24). Figure 4B demonstrates that nucleoplasmin lacking a nuclear localization signal (core nucleoplasmin) does not translocate to the nuclear interior. The requirement for ATP is represented in Fig. 4C, which shows that only a small amount of nucleoplasmin is localized to the nucleus if an ATP regenerat-

ing system is omitted from the reaction mixture. The small amount of import observed can be attributed to endogenous ATP in the cytosolic preparation. As demonstrated in Fig. 4, nucleoplasmin produced in *E. coli* and purified by this procedure performs in a manner analogous to the protein isolated from *X. laevis* oocytes.

We have developed a procedure for isolating milligram quantities of nucleoplasmin produced in *E. coli* strain BL21(DE3). The isolation procedure is rapid and routinely yields 70–80 mg of nucleoplasmin per liter of bacterial culture. The nucleoplasmin produced by this procedure migrates at the same apparent molecular mass on SDS–polyacrylamide gels as nucleoplasmin isolated from *X. laevis* oocytes and is recognized by antisera produced against the *Xenopus* nucleoplasmin. The *E. coli*-produced nucleoplasmin is also transport-competent. It is imported to the nuclear interior of digitonin-permeabilized V79A03 cells. Nucleoplasmin lacking a nuclear localization signal (core nucleoplasmin) does not associate with the cell nucleus. As with other systems, nuclear import is dependent upon not only an intact nuclear localization signal but also the presence of cytosolic factors and ATP. This procedure provides an easy method for producing and purifying nucleoplasmin for nuclear transport studies.

ACKNOWLEDGMENTS

This work was supported by the Armed Forces Radiobiology Research Institute under Work Unit 00150. We thank Dr. Thomas Burglin for providing the nucleoplasmin cDNA, Dr. Paul Herring for providing *E. coli* strain BL21(DE3), and Dr. Carl Feldherr for his gift of antiserum to nucleoplasmin.

REFERENCES

1. Laskey, R. A., Honda, B. M., Mills, A. D., and Finch, J. T. (1978) Nucleosomes are assembled by an acidic protein which binds histones and transfers them to DNA. *Nature* **275,** 416–420.
2. Earnshaw, W. C., Honda, B. M., and Laskey, R. A. (1980) Assembly of nucleosomes: The reaction involving *X. laevis* nucleoplasmin. *Cell* **21,** 373–383.
3. Dingwall, C., Sharnick, S. V., and Laskey, R. A. (1982) A polypeptide domain that specifies migration of nucleoplasmin into the nucleus. *Cell* **30,** 449–458.
4. Sealy, L., Burgess, R. R., Cotten, M., and Chalkley, R. (1989) Purification of *Xenopus* egg nucleoplasmin and its use in chromatin assembly *in vitro*. *Methods Enzymol.* **170,** 612–631.
5. Kalinich, J. F., and Douglas, M. G. (1989) *In vitro* translocation through the yeast nuclear envelope. *J. Biol. Chem.* **264,** 17979–17989.
6. Mills, A. D., Laskey, R. A., Black, P., and DeRobertis, E. M. (1980) An acidic protein which assembles nucleosomes *in vitro* is the most abundant protein in *Xenopus* oocyte nuclei. *J. Mol. Biol.* **139,** 561–568.
7. Krohne, G., and Franke, W. W. (1980) Immunological identification and localization of the predominant nuclear protein of the amphibian oocyte nucleus. *Proc. Natl. Acad. Sci. USA* **77,** 1034–1038.
8. Dubendorff, J. W., and Studier, F. W. (1991) Controlling basal expression in an inducible T7 expression system by blocking the target T7 promoter with lac repressor. *J. Mol. Biol.* **219,** 45–59.
9. Hoffmann, A., and Roeder, R. G. (1991) Purification of his-tagged proteins in non-denaturing conditions suggests a convenient method for protein interaction studies. *Nucleic Acids Res.* **19,** 6337–6338.
10. Smith, M. C., Furman, T. C., Ingolia, T. D., and Pidgeon, C. (1988) Chelating peptide-immobilized metal affinity chromatography—A new concept in affinity chromatography for recombinant proteins. *J. Biol. Chem.* **263,** 7211–7215.
11. Ljungquist, C., Breitholtz, A., Brinj-Nilsson, H., Moks, T., Uhlen, M., and Nilsson, B. (1989) Immobilization and affinity purification of recombinant proteins using histidine peptide fusions. *Eur. J. Biochem.* **186,** 563–569.
12. Studier, F. W., and Moffatt, B. A. (1986) Use of bacteriophage T7 RNA polymerase to direct selective high-level expression of cloned genes. *J. Mol. Biol.* **189,** 113–130.
13. Studier, F. W., Rosenberg, A. H., Dunn, J. J., and Dubendorff, J. W. (1990) Use of T7 RNA polymerase to direct expression of cloned genes. *Methods Enzymol.* **185,** 60–89.
14. Sambrook, J., Fritsch, E. F., and Maniatis, T. (1989) "Molecular Cloning: A Laboratory Manual," 2nd ed., Cold Spring Harbor Laboratory, Cold Spring Harbor, NY.
15. Sanger, F., Coulson, A. R., Hong, G. F., Hill, D. F., and Peterson, G. B. (1982) DNA sequencing with chain-termination inhibitors. *Proc. Natl. Acad. Sci. USA* **79,** 729–733.
16. Nagai, K., and Thogersen, H. C. (1984) Generation of β-globin by sequence-specific proteolysis of a hybrid protein produced in *Escherichia coli*. *Nature* **309,** 810–812.
17. Feldherr, C. M., Kallenbach, E., and Schultz, N. (1984) Movement of a karyophilic protein through the nuclear pores of oocytes. *J. Cell Biol.* **99,** 2216–2222.
18. Laemmli, U. (1970) Cleavage of structural proteins during the assembly of the head of bacteriophage T4. *Nature* **227,** 680–685.
19. Towbin, H., Staehelin, T., and Gordon, J. (1979) Electrophoretic transfer of proteins from polyacrylamide gels to nitrocellulose sheets: Procedure and some applications. *Proc. Natl. Acad. Sci. USA* **76,** 4350–4354.
20. Newmeyer, D. D., Finlay, D. R., and Forbes, D. J. (1986) *In vitro* transport of a fluorescent protein and exclusion of non-nuclear proteins. *J. Cell. Biol.* **103,** 2091–2102.
21. Adam, S. A., Sterne-Marr, R. E., and Gerace, L. (1990) Nuclear protein import in permeabilized mammalian cells requires soluble cytoplasmic factors. *J. Cell Biol.* **111,** 807–816.
22. Moore, M. S., and Blobel, G. (1992) The two steps of nuclear import, targeting to the nuclear envelope and translocation through the nuclear pore, require different cytosolic factors. *Cell* **69,** 939–950.
23. Burglin, T. R., Mattaj, I. W., Newmeyer, D. D., Zeller, R., and DeRobertis, E. M. (1987) Cloning of nucleoplasmin from *Xenopus laevis* oocytes and analysis of its developmental expression. *Genes Dev.* **1,** 97–107.
24. Newmeyer, D. D., and Forbes, D. J. (1990) An *N*-ethyl maleimide-sensitive cytosolic factor necessary for nuclear protein import: Requirement in signal-mediated binding to the nuclear pore. *J. Cell Biol.* **110,** 547–557.
25. Bradford, M. M. (1976) A rapid and sensitive method for the quantitation of microgram quantities of protein utilizing the principle of protein dye binding. *Anal. Biochem.* **72,** 248–254.

RADIATION RESEARCH 139, 352–356 (1994)

Exposure to Heavy Charged Particles Affects Thermoregulation in Rats

Sathasiva B. Kandasamy,* Bernard M. Rabin,*,† Walter A. Hunt,*,[1] Thomas K. Dalton,*
James A. Joseph*,[2] and Alan H. Harris*

*Behavioral Sciences Department, Armed Forces Radiobiology Research Institute, Bethesda, Maryland 20889-5603; and
†Department of Psychology, University of Maryland Baltimore County, Baltimore, Maryland 21228-5398

Kandasamy, S. B., Rabin, B. M., Hunt, W. A., Dalton, T. K., Joseph, J. A. and Harris, A. H. Exposure to Heavy Charged Particles Affects Thermoregulation in Rats. *Radiat. Res.* **139**, 352–356 (1994).

Rats exposed to 0.1–5 Gy of heavy particles (^{56}Fe, ^{40}Ar, ^{20}Ne or ^{4}He) showed dose-dependent changes in body temperature. Lower doses of all particles produced hyperthermia, and higher doses of ^{20}Ne and ^{56}Fe produced hypothermia. Of the four HZE particles, ^{56}Fe particles were the most potent and ^{4}He particles were the least potent in producing changes in thermoregulation. The ^{20}Ne and ^{40}Ar particles produced an intermediate level of change in body temperature. Significantly greater hyperthermia was produced by exposure to 1 Gy of ^{20}Ne, ^{40}Ar and ^{56}Fe particles than by exposure to 1 Gy of ^{60}Co γ rays. Pretreating rats with the cyclo-oxygenase inhibitor indomethacin attenuated the hyperthermia produced by exposure to 1 Gy of ^{56}Fe particles, indicating that prostaglandins mediate ^{56}Fe-particle-induced hyperthermia. The hypothermia produced by exposure to 5 Gy of ^{56}Fe particles is mediated by histamine and can be attenuated by treatment with the antihistamines mepyramine and cimetidine.

INTRODUCTION

When manned exploration of the solar system continues, astronauts leaving the protection of the Earth's magnetic field will be exposed to types and doses of radiation significantly different from those in low-Earth orbit, primarily cosmic rays. Cosmic rays are composed of protons, α particles and heavy particles with high charge and energy (HZE). Previous research using a variety of end points has shown that exposure to HZE particles, especially ^{56}Fe ions, can cause deficits in behavioral and neurochemical processes at doses that are significantly lower than those required for similar effects after exposure to γ rays. Protecting the organism against the deleterious effects of exposure to HZE particles requires that we determine the toxicity of these particles across a range of different physiological and behavioral end points, and that we understand the mechanisms by which such exposures can affect these end points (*1–6*).

One of the physiological effects of exposure to ionizing radiation involves alterations in the regulation of body temperature. In rats, γ irradiation produces a dual effect: lower doses (~5 Gy) produce hyperthermia, and higher doses (~50 Gy) produce hypothermia (*7, 8*). This effect results from direct irradiation of the brain because exposures that exclude the brain have no significant effects on the thermoregulatory system (*7, 8*). The dual effects on thermoregulation observed after irradiation with γ rays apparently are mediated by two separate mechanisms. Radiation-induced hyperthermia is mediated by a release of prostaglandins and can be prevented by pretreating rats with indomethacin, which acts to inhibit synthesis of prostaglandins. In contrast, the hypothermia observed after higher doses of radiation is mediated by the release of histamine and can be prevented by treatment with antihistamines (*7, 8*).

Thermoregulation is one of a group of homeostatic processes that mediate the adjustment of an organism to its environment by functioning to maintain a relatively constant internal environment. The observation that exposure to ionizing radiation can disrupt the functioning of this system may be indicative of the potential disruption of a variety of other homeostatic systems. As such, it would be important to establish the sensitivity of homeostatic processes, such as thermoregulation, and the mechanisms that mediate the responses of these systems to HZE particles, to assess the possible effects of such exposures on the performance of astronauts on long-term missions outside the magnetosphere. This is particularly important because, as indicated above, previous research has shown that exposure to heavy particles can disrupt behavioral and physiological functioning at significantly lower doses than exposure to γ rays (*1–6*).

Our experiments were designed to evaluate the effects of exposure to different HZE particles on thermoregulation

[1]Present address: Division of Basic Research, National Institutes of Health, Rockville, MD 20857.

[2]Present address: USDA-ARS at Tufts University, Room 919, 711 Washington Street, Boston, MA 02111.

0033-7587/94 $5.00

by establishing the dose–response relationships between exposure to iron, argon, neon and helium ions and changes in body temperature. In addition, the roles of prostaglandins and histamine in changes in thermoregulation induced by HZE particles were investigated to determine whether mechanisms that are similar to those that mediate these responses after exposure to γ rays (*7, 8*) also mediate these changes after exposure to heavy particles.

MATERIALS AND METHODS

Experimental animals. Male Sprague-Dawley Crl:CD(SD)BRD rats weighing 200–300 g (Charles River) were used in these experiments. The rats were maintained at Lawrence Berkeley Laboratory (LBL) in AAALAC-accredited facilities. Commercial rodent chow and water were available *ad libitum*. Animal holding rooms were maintained at 21 ± 1°C with a 12-h light:dark cycle.

Radiation and dosimetry. Exposure to heavy particles was performed using the BEVALAC at LBL. Rats were exposed unilaterally to doses of 0.1–5 Gy at dose rates from 0.2 Gy/min to 2 Gy/min. All exposures were in the plateau region of the Bragg curve. Sham-irradiated rats were held in restraining cages for the same of length of time and in the same environment as their irradiated counterparts. Groups of rats were exposed to the following particles (8 rats/particle/dose): iron [^{56}Fe, 600 MeV/*u*, linear energy transfer (LET) = ~190.0 keV/μm]; neon (^{20}Ne, 522 MeV/*u*, LET = ~28.0 keV/μm); argon (^{40}Ar, 670 MeV/*u*, LET = ~85.0 keV/μm); and helium (^{4}He, 165 MeV/*u*, LET = ~2.0 keV/μm).

Dosimetry was provided by the staff of the BEVALAC facility. These procedures have been detailed in previous reports (*5, 9–11*).

Drugs and administration. The drugs tested for effects on changes in thermoregulation induced by HZE particles were indomethacin (Sigma Chemical Co., St. Louis, MO) dissolved in a mixture of 1% sodium hydroxide and sterile nonpyrogenic saline, mepyramine maleate (Mallinckrodt Inc., St. Louis, MO) dissolved in saline, and cimetidine (Smith Kline and French Laboratories, Philadelphia, PA) dissolved in 0.1 ml of 1*N* HCl and diluted to the final volume with sterile nonpyrogenic saline. Indomethacin is a cyclo-oxygenase inhibitor which acts to inhibit prostaglandin synthesis. Mepyramine and cimetidine are antihistamines, which are H1 and H2 antagonists, respectively.

Indomethacin was administered by intraperitoneal (ip) injection. Mepyramine and cimetidine were administered using intracerebro-ventricular injection with chronic cannulas placed in the lateral ventricle. Cannulas were implanted stereotaxically in rats anesthetized with an intramuscular injection of 1 ml/kg of a mixture of ketamine (50 mg/kg), xylazine (5 mg/kg) and acepromazine (1 ml/kg). A single cannula was inserted aseptically into the lateral ventricle at 0.8 mm posterior and 2.5 mm lateral to bregma, using coordinates derived from the atlas of Pelligrino *et al.* (*12*). The cannula was lowered until cerebrospinal fluid rose in the cannula. Dental acrylic was used to secure the cannula. The rats were allowed to recover for 2 days before being used for experiments. After the experiment, the rats were sacrificed with CO_2 inhalation, and the injection site was verified histologically.

Procedure. All experiments were performed at an environmental temperature of 21 ± 1°C. The measurement of body temperature was performed as described previously (*7, 8*). Briefly, the animals were placed in acrylic restraining cages 30 min before irradiation, and body temperatures were measured with thermistor probes (YSI series 700, Yellow Springs Instrument Co., Inc., Yellow Springs, OH) inserted approximately 6 cm into the rectum and connected to a datalogger (Minitrend 205). The probes were removed from the animals for irradiation. After exposure, the probes were reinserted, and body temperatures were observed for an additional 30 min. Immediately after radiation exposure, rats developed hyperthermia or hypothermia, depending on the dose, reaching maximum temperature responses in 10 min which lasted for 1 h and then gradually declined.

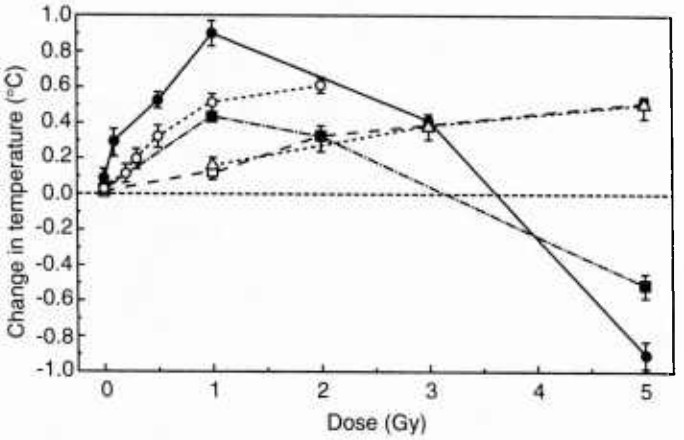

FIG. 1. Average change in rectal temperatures of rats 10 min after exposure to varying doses of (●) ^{56}Fe, (○) ^{40}Ar, (■) ^{20}Ne, (□) ^{4}He and (△) ^{60}Co. Data for ^{60}Co have been regraphed from ref. (*8*). Error bars indicate the standard error of the mean.

For the experiments on the mechanisms of radiation-induced changes in thermoregulation, the appropriate drugs were administered to independent groups of rats (8 rats/group) 30 min before exposure to ^{56}Fe particles. The role of prostaglandins in ^{56}Fe-particle-induced hyperthermia was determined in rats given ip injections of indomethacin and exposed to 1 Gy. The role of histamine in ^{56}Fe-particle-induced hypothermia was determined in rats given either cimetidine or mepyramine injections (intracerebro-ventricular) and exposed to 5 Gy. After exposure, body temperatures were monitored for an additional 30 min. Control animals were administered only the vehicle prior to irradiation. Previous research (*7, 8*) has shown that administration of these drugs alone produces no significant changes in body temperature.

Statistics. Statistical evaluations of the data were performed using analyses of variance. *Post hoc* comparisons between groups were performed using Tukey's *t* test.

RESULTS

The effects of exposure to heavy particles on body temperature are summarized in Fig. 1. Exposing rats to 0.1–5 Gy of ^{56}Fe, ^{40}Ar, ^{20}Ne or ^{4}He particles produced significant dose-dependent changes in body temperature (independent one-way analyses of variance, all $P < 0.001$). Lower doses of all particles produced significant increases in body temperature, while higher doses of ^{56}Fe and ^{20}Ne particles (>3 Gy) caused significant hypothermia.

Figure 1 also shows that the doses needed to produce hyperthermia after exposure were different for the heavy particles. The lowest effective dose for a significant increase in body temperature was observed after exposure to ^{56}Fe particles (~0.1 Gy), while the highest effective dose was observed after exposure to ^{4}He particles (~0.5 Gy). The intermediate effective dose for a significant increase in temperature was observed after exposure to 0.3 Gy of ^{20}Ne or 0.2

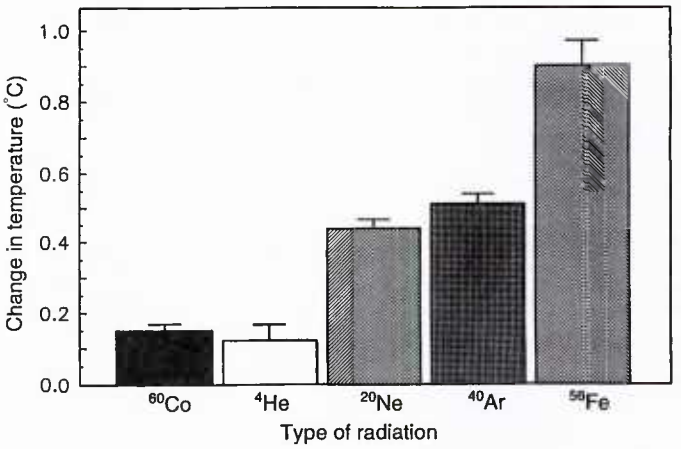

FIG. 2. Comparison of the hyperthermia produced by exposure to 1 Gy of ^{60}Co γ rays with that produced by exposure to 1 Gy of heavy particles. Data for ^{60}Co have been regraphed from ref. (*8*). Error bars indicate the standard error.

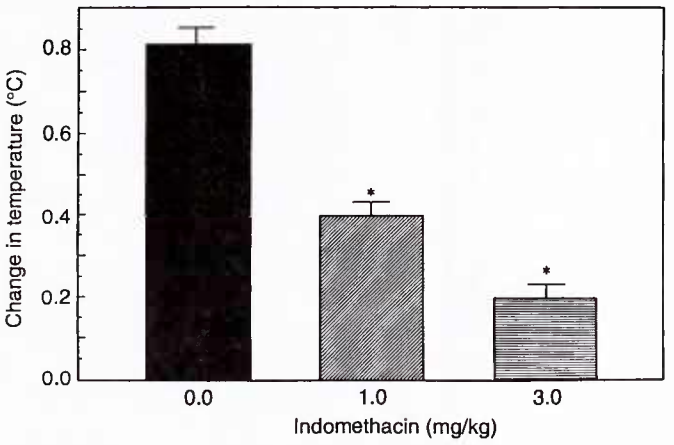

FIG. 3. Effect of indomethacin (1.0 or 3.0 mg/kg) on hyperthermia induced by exposure to 1 Gy of ^{56}Fe particles. *Significantly different from ^{56}Fe-particle-induced hypothermia, $P < 0.05$. Error bars indicate the standard error.

Gy of ^{40}Ar particles. Differences were also observed in the hypothermia induced by exposure to different particles. Compared to nonirradiated controls, rats exposed to either ^{56}Fe or ^{20}Ne particles showed a significant reduction in body temperature [$t(14) = 12.52$, $P < 0.01$; $t(14) = 10.67$, $P < 0.01$, respectively] at the highest dose (5 Gy). In contrast, the rats exposed to 5 Gy of ^{4}He particles continued to show a significant increase in body temperature [$t(14) = 8.16$, $P < 0.01$].

The amount of change in body temperature produced by exposure to 1 Gy of heavy particles or to 1 Gy of ^{60}Co γ rays is shown in Fig. 2. This dose was selected because it was common to all of the types of radiation tested. Compared to 1 Gy ^{60}Co γ rays (*7*, *8*), exposure to ^{4}He particles produced an equivalent increase in body temperature [$t(14) = 0.42$, $P > 0.05$]. In contrast, exposure to ^{20}Ne, ^{40}Ar or ^{56}Fe particles produced a significantly greater rise in body temperature than did exposure to ^{60}Co or ^{4}He (all $P < 0.01$). In addition, the hyperthermia produced by ^{56}Fe was significantly greater than that produced by exposure to either ^{20}Ne [$t(14) = 7.72$, $P < 0.01$] or ^{40}Ar [$t(14) = 6.47$, $P < 0.01$], which did not differ significantly from each other [$t(14) = 1.25$, $P > 0.05$].

The dose rate for HZE varied by a factor of 10. For ^{60}Co, the dose rate is 10–20 Gy/min. Because the data for ^{60}Co have been regraphed from ref. (*8*), the dose rates were not included in this paper. Research using low-LET radiation in the Armed Forces Radiobiology Research Institute has indicated that there is no significant change in temperature responses with dose rates between 10–20 Gy per minute.

The effect of pretreatment with indomethacin on ^{56}Fe-particle-induced hyperthermia is shown in Fig. 3. Compared to irradiated rats given only the vehicle, both doses of indomethacin (1 or 3 mg/kg, ip) produced a significant attenuation of the hyperthermia induced by a 1-Gy dose of ^{56}Fe particles [$t(14) = 7.90$, $P < 0.01$; $t(14) = 11.74$, $P < 0.01$, respectively]. Similarly, the 3-mg/kg dose of indomethacin produced a significantly greater attenuation of ^{56}Fe-particle-induced hyperthermia than did the 1-mg/kg dose [$t(14) = 3.83$, $P < 0.01$].

Compared to the vehicle-treated rats (Fig. 4), both mepyramine and cimetidine (100 and 300 ng) produced significant dose-dependent attenuations of the hypothermia produced by exposure to 5 Gy ^{56}Fe particles (all $P < 0.01$). The degree of attenuation of the ^{56}Fe-particle-induced hypothermia was greater for the higher doses of both the mepyramine-treated [$t(14) = 4.80$, $P < 0.01$] and the cimetidine-treated [$t(14) = 4.60$, $P < 0.01$] rats. The differences between the effectiveness of ^{56}Fe-particle-induced hypothermia attenuated by mepyramine and cimetidine were not statistically significant (all $P > 0.05$).

DISCUSSION

The present results show that exposure to heavy particles produces significant dose-dependent changes in body temperature in rats. As observed after exposure to γ rays (*7*, *8*), lower doses of HZE particles induce hyperthermia, whereas higher doses of ^{20}Ne and ^{56}Fe particles induce hypothermia.

The ^{56}Fe particles were the most effective in producing changes in thermoregulation. Exposure to ^{56}Fe particles produced significant hyperthermia at the lowest dose and also produced the greatest amount of change in body temperature at any given dose. Exposing rats to ^{60}Co γ rays produces a significant increase in body temperature at a dose of 5 Gy, whereas a dose of 50 Gy is needed to produce

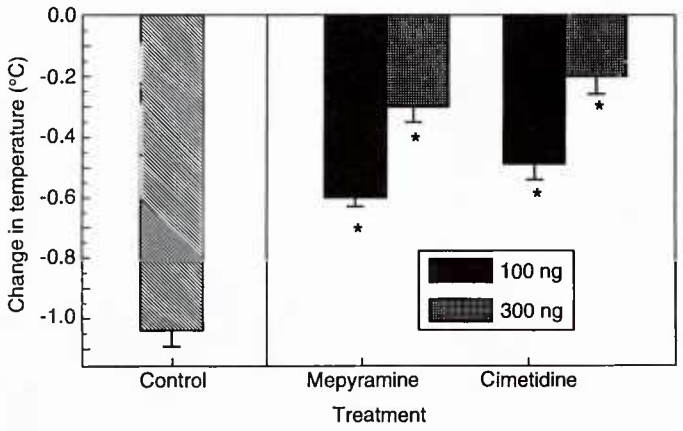

FIG. 4. Effect of mepyramine and cimetidine (100 and 300 ng, intracerebro-ventricular injection) on hypothermia induced by exposure to 5 Gy of ^{56}Fe particles. Control animals received vehicle only. *Significantly different from ^{56}Fe-particle-induced hypothermia, $P < 0.05$. Error bars indicate the standard error.

a significant decrease in body temperature (*7*, *8*). In contrast, significant increases in body temperature are obtained after exposure to 0.1 Gy of ^{56}Fe particles and significant decreases are obtained with 5 Gy.

This observation extends the results of previous studies using a variety of different neurochemical and behavioral end points to the maintenance of physiological homeostasis. In agreement with the results of previous research that used conditioned taste aversion (*2*, *4*) and striatal dopamine release (*1*, *3*, *5*) in rats and emesis in ferrets (*6*), the present results show that ^{56}Fe particles produce changes in thermoregulation at significantly lower doses than the other particles tested.

Although exposure to ^{56}Fe particles is significantly more effective in producing changes in thermoregulation than exposure to ^{20}Ne or ^{40}Ar particles, these latter particles are nevertheless significantly more effective than ^{4}He particles or ^{60}Co. These results indicate that, for this particular end point, the effectiveness of exposure to these particles in producing changes in thermoregulation generally parallels the LET of the particles. The most effective particle, ^{56}Fe, was the one with the highest LET (~190 keV/μm), while the particle with the lowest LET, ^{4}He (~2 keV/μm), did not differ from ^{60}Co γ rays (LET, 0.3 keV/μm) in effectiveness. The two particles with intermediate LETs, ^{20}Ne (~28 keV/μm) and ^{40}Ar (~85 keV/μm), showed an intermediate level of effectiveness in eliciting changes in thermoregulation compared to ^{60}Co and ^{56}Fe. However, there were no differences in the changes in thermoregulation produced by ^{20}Ne and ^{40}Ar in rats exposed to the common dose of 1 Gy, despite the differences in particle LET.

In terms of the relationship between LET and the amount of change behavior and neurochemistry produced by exposure to different types of radiation, the present results differ from those obtained using the conditioned taste aversion (*2*, *4*) or striatal dopamine release (Joseph, Rabin, Hunt and Kandasamy, unpublished observations) as experimental end points. In those experiments, ^{60}Co γ rays and ^{4}He, ^{20}Ne and ^{40}Ar ions were equally effective in producing changes in behavior and neurochemistry. With these end points, only ^{56}Fe particles were significantly more effective than γ rays. These results therefore emphasize the importance of the specific end point in determining the effectiveness of heavy particles (*1*, *2*, *4*, *9*, *13–15*).

As observed previously after exposure to ^{60}Co γ rays (*7*, *8*), separate mechanisms mediate hyperthermia and hypothermia after exposure to ^{56}Fe particles. Hyperthermia produced by exposure to 1 Gy of ^{56}Fe particles is mediated by α particle-induced release of prostaglandins because pretreatment with the cyclo-oxygenase inhibitor indomethacin, which inhibits prostaglandin synthesis, causes a significant reduction in the ^{56}Fe-particle-induced increase in body temperature. Hypothermia produced by exposure to 5 Gy of ^{56}Fe particles is mediated by the release of histamine and can be prevented by pretreatment with either H1 (mepyramine) or H2 (cimetidine) antagonists. Because these compounds have identical effects on changes in thermoregulation produced by exposure to γ rays and HZE particles, similar mechanisms must mediate the thermoregulatory responses after exposure to these different types of radiation. This observation, that similar mechanisms mediate the response of the organism both to γ rays and to ^{56}Fe particles, is in agreement with the report that lesions of the area postrema are equally effective in disrupting the acquisition of a conditioned taste aversion produced by exposure to both types of radiation (*2*). Thus the present results would be consistent with the hypothesis that the differences between ^{60}Co γ rays and ^{56}Fe particles seem to be differences in the potency with which these types of radiation effect changes, either directly or indirectly, in the functioning of the nervous system.

In summary, the present results show that exposure to HZE particles produces changes in the regulation of body temperature at doses that are significantly lower than those needed after exposure to γ rays. These results therefore extend previous research which used a variety of other neurochemical and behavioral end points (*1–6*) to the maintenance of physiological homeostasis. Homeostatic mechanisms, including regulation of body temperature, salt balance, glucose metabolism, etc., function to maintain a relatively constant internal environment despite wide variations in the external environment. The observation that exposure to relatively low doses of heavy charged particles (specifically, ^{20}Ne, ^{40}Ar and ^{56}Fe) can disrupt the homeostatic regulation of body temperature suggests that other homeostatic systems may be sensitive to low doses of HZE particles.

Because changes in thermoregulation produced by ionizing radiation are mediated by the brain (*7*), these results suggest the possibility that the cumulative effects of exposure to HZE particles on long-term space missions beyond the Earth's magnetosphere could result in a disturbance of homeostatic processes that could in turn affect the performance capabilities of astronauts. However, because the fluences of HZE particles are low and because the sensitivity of humans to these particles is unknown, additional research will be necessary, at some point, to evaluate this possibility.

ACKNOWLEDGMENTS

The authors wish to acknowledge the assistance of Drs. E. John Ainsworth, Patricia Durbin and Bernhard Ludewigt and the staff at the Lawrence Berkeley Laboratory, without whose help these studies could not have been undertaken. This research was supported by the Armed Forces Radiobiology Research Institute, Defense Nuclear Agency, under work unit 00157. This research was conducted according to the principles described in the Guide for the Care and Use of Laboratory Animals prepared by the Institute of Laboratory Animal Research, National Research Council.

Received: August 5, 1993; accepted: April 26, 1994

REFERENCES

1. W. A. Hunt, J. A. Joseph and B. M. Rabin, Behavioral and neurochemical abnormalities after exposure to low doses of high-energy iron particles. *Adv. Space Res.* **9**, 333–336 (1989).

2. B. M. Rabin, W. A. Hunt and J. A. Joseph, An assessment of the behavioral toxicity of high-energy iron particles compared to other qualities of radiation. *Radiat. Res.* **119**, 113–122 (1989).

3. W. A. Hunt, T. K. Dalton, J. A. Joseph and B. M. Rabin, Reduction of 3-methoxytyramine concentrations in the caudate nucleus of rats after exposure to high-energy iron particles: Evidence for deficits in dopaminergic neurons. *Radiat. Res.* **121**, 169–174 (1990).

4. B. M. Rabin, W. A. Hunt, J. A. Joseph, T. K. Dalton and S. B. Kandasamy, Relationship between linear energy transfer and behavioral toxicity in rats following exposure to protons and heavy particles. *Radiat. Res.* **128**, 216–221 (1991).

5. J. A. Joseph, W. A. Hunt, B. M. Rabin and T. K. Dalton, Possible "accelerated aging" induced by ^{56}Fe heavy-particle irradiation: Implications for manned space flights. *Radiat. Res.* **130**, 88–93 (1992).

6. B. M. Rabin, W. A. Hunt, M. E. Wilson and J. A. Joseph, Emesis in ferrets following exposure to different types of radiation: A dose–response study. *Aviat. Space Environ. Med.* **63**, 702–705 (1992).

7. S. B. Kandasamy, W. A. Hunt and G. A. Mickley, Implication of prostaglandins and histamine H1 and H2 receptors in radiation-induced temperature responses of rats. *Radiat. Res.* **114**, 42–53 (1988).

8. S. B. Kandasamy and W. A. Hunt, Involvement of prostaglandins and histamine H1 and H2 in radiation-induced temperature responses in rats. *Radiat. Res.* **121**, 84–90 (1990).

9. B. M. Rabin, J. A. Joseph, W. A. Hunt, S. B. Kandasamy, A. H. Harris and B. Ludewigt, Behavioral end points for radiation injury. *Adv. Space Res.* **14**, 457–466 (1994).

10. J. T. Lyman and J. Howard, Dosimetry and instrumentation for helium and heavy ions. *Int. J. Radiat. Oncol. Biol. Phys.* **3**, 81–85 (1977).

11. A. R. Smith, L. D. Stephens and R. H. Thomas, Dosimetry for radiobiological experiments using energetic heavy ions. *Health Phys.* **34**, 387 (1978).

12. L. S. Pelligrino, A. S. Pelligrino and A. J. Cushman, *A Stereotaxic Atlas of the Rat Brain*. Plenum, New York, 1979.

13. E. J. Ainsworth, Early and late mammalian responses to heavy charged particles. *Adv. Space Res.* **6**, 153–165 (1986).

14. J. T. Leith, E. J. Ainsworth and E. L. Alpen, Heavy ion radiobiology: Normal tissue studies. In *Advances in Radiation Biology* (J. T. Lett, Ed.), Vol. 10, pp. 191–236. Academic Press, New York, 1983.

15. G. Kraft, W. Kraft-Weyrather, S. Ritter, M. Scholz and J. Stanton, Cellular and subcellular effect of heavy ions: A comparison of the induction of strand breaks and chromosomal aberrations with the incidence of inactivation and mutation. *Adv. Space Res.* **9**, 59–72 (1989).

Synergy of IL-1 and Stem Cell Factor in Radioprotection of Mice Is Associated with IL-1 Up-Regulation of mRNA and Protein Expression for c-*kit* on Bone Marrow Cells[1]

Ruth Neta,[2]* Joost J. Oppenheim,† Ji-Ming Wang,† Clifford M. Snapper,‡ Mark A. Moorman,‡ and Claire M. Dubois§

*Department of Experimental Hematology, Armed Forces Radiobiology Research Institute, Bethesda, MD 20889; †Laboratory of Molecular Immunoregulation, National Cancer Institute, Frederick, MD 21702; ‡Department of Pathology, Uniformed Services University for Health Sciences, Bethesda, MD 20889; and §University of Sherbrooke, Sherbrooke, Quebec, Canada.

Administration of IL-1 and stem cell factor (SCF) to mice 18 h before lethal ^{60}Co whole-body irradiation resulted in synergistic radioprotection, as evidenced by increased numbers of mice surviving 1,200 to 1,300 cGy doses of radiation and the recovery of increased numbers of c-*kit*$^+$ bone marrow cells at 1 and 4 days after the lethal dose of 950 cGy. Anti-SCF Ab inhibited IL-1-induced radioprotection, indicating that endogenous production of SCF is necessary for radioprotection by IL-1. Conversely, radioprotection induced by SCF was reduced by anti-IL-1R Ab, indicating that endogenous IL-1 contributes to SCF radioprotection. SCF, unlike IL-1, does not induce hemopoietic CSFs and IL-6 or gene expression of a scavenging mitochondrial enzyme manganese superoxide dismutase in the bone marrow, suggesting that SCF and IL-1 radioprotect by distinct pathways. The mRNA expression for c-*kit* (by Northern blot analysis) and ^{125}I-SCF binding on bone marrow cells was elevated within 2 and 4 h of IL-1 administration respectively. Four days after LD 100/30 radiation the recovery of c-*kit*$^+$ bone marrow cells was increased sixfold in IL-1-treated mice, almost 20-fold in SCF-treated mice, and 40-fold in mice treated with the combination of the two cytokines. Thus, endogenous production of both IL-1 and SCF is required for resistance to lethal irradiation and the synergistic radioprotective effect of the two cytokines may, in part, depend on IL-1 and SCF-induced increases in numbers of c-*kit*$^+$ hemopoietic stem and progenitors cells that survive lethal irradiation. *The Journal of Immunology*, 1994, 153: 1536.

Death from LD 100/30 of ionizing radiation can be prevented by a supply of undamaged bone marrow cells and has therefore been attributed to a lethal hemopoietic syndrome (1). The death of animals receiving LD 100/30 doses of radiation can also be prevented by administration of immunomodulatory agents or proinflammatory cytokines before irradiation, with subsequent recovery of the hemopoietic system (2–5). We have demonstrated that, in the case of immunomodulatory LPS, the radioprotective effect is mediated by endogenously produced proinflammatory cytokines, IL-1 and TNF, because Abs to these cytokines block LPS-induced radioprotection (6). Radioprotection with IL-1 and TNF in turn could also be blocked by anti-IL-6 Ab as well as by anti-TNF and anti-IL-1R Abs (6, 7), providing evidence that obligatory interaction of these three endogenously produced cytokines is required for protection by IL-1 or TNF from lethal hemopoietic syndrome.

Recently, a receptor for hemopoietic cytokine (c-*kit*) and its ligand (SCF)[3] have been identified and cloned (8, 9). Numerous studies determined that SCF synergizes with

Received for publication January 25, 1994. Accepted for publication May 16, 1994.

The costs of publication of this article were defrayed in part by the payment of page charges. This article must therefore be hereby marked *advertisement* in accordance with 18 U.S.C. Section 1734 solely to indicate this fact.

[1] This work was supported by the Armed Forces Radiobiology Research Institute, Defence Nuclear Agency, under work unit 00129. Views presented in this paper are those of the authors; no endorsement by the Defence Nuclear Agency has been given or should be inferred. Research was conducted according to the principles enunciated in the Guide for the Care and Use of Laboratory Animals, prepared by the Institute of Laboratory Animal Resources, National Research Council.

[2] Address correspondence and reprint requests to Dr. Ruth Neta, Department of Experimental Hematology, Armed Forces Radiobiology Research Institute, Bethesda, Maryland 20889-5603.

[3] Abbreviations used in this paper: SCF, *kit* ligand; BMC, bone marrow cells; G-CSF, granulocyte CSF; GM-CSF, granulocyte-macrophage CSF; MnSOD, manganese superoxide dismutase; PE, phycoerythrin.

0022-1767/94/$02.00

hemopoietic cytokines (IL-1, IL-3, GM-CSF, G-CSF, and IL-6) to stimulate the growth of hemopoietic progenitor cells in vitro and stimulates hemopoiesis in vivo (10–14). The SCF receptor (c-*kit*) is expressed on hemopoietic stem cells and progenitor cells in the bone marrow (estimated as 0.05% and 5% of the total bone marrow population, respectively), but not on mature neutrophils or nucleated erythroid cells (14–16). Thus, c-*kit* provides a marker for monitoring changes in progenitor populations. Mice treated with Ab to c-*kit* displayed a loss of hemopoietic progenitor cells (13).

We recently demonstrated that Ab to SCF blocks IL-1 and LPS-induced radioprotection and also reduces the resistance of untreated mice to radiation lethality (17). This result suggested that endogenous SCF may be the penultimate mediator required for radioprotection. To test this hypothesis, we further investigated the interaction of IL-1 with SCF in radioprotection. In this report we present results that show that IL-1 contributes to SCF radioprotection, that IL-1 and SCF synergize in radioprotection, and that this synergy may be based in part on IL-1-induced increases in numbers of bone marrow cells (BMC) expressing c-*kit*, which suggests that IL-1 generates more progenitor cells with the capacity to respond more effectively to SCF.

Materials and Methods

Mice

B6D2F1 female mice, 8 to 10 wks old, were purchased from The Jackson Laboratory (Bar Harbor, ME). Mice were handled as described previously (6). Adrenalectomized mice were purchased from Charles River Laboratories. The experiments were performed within 2 wk after adrenalectomy.

Abs

Rat monoclonal IgG1, anti-IL-1R Ab (35F5), and anti-IL-6 (20F3) were generous gifts from Dr. Richard Chizzonite (Hoffmann-La Roche, Nutley, NJ) and Dr. John Abrams (DNAX, Palo Alto, CA), respectively. A rat mAb to β-galactosidase (GL113) was used as a control. The polyclonal anti-murine SCF Ab was generously provided by Dr. Douglas Williams (Immunex, Seattle, WA). Chromatographically purified rat IgG (Sigma Chemical Co., St. Louis, MO) was used as an additional control. R-phycoerythrin (R-PE)-conjugated rat anti-mouse c-*kit* mAb 3 CI (IgG2b), and PE-conjugated rat IgG2b (control) were purchased from PharMingen (San Diego, CA).

Treatment

Human rIL-1 (rHu IL-1α 117–271 Ro 24–5008 lot IL 1 2/88, activity 3×10^8 U/mg) was kindly provided by Dr. Peter Lomedico (Hoffmann-La Roche).

Rat PEG-SCF was prepared and coupled with polyethylene glycol and was kindly provided by Dr. Ian McNiece, (Amgen, Thousand Oaks, Ca). PEG was used as a control for its nonspecific effect as a radioprotector. G-CSF was provided by Amgen, and IL-6 (SDZ 280–969, Batch PPG 9001; SA 5.2×10^7 U/mg) was a generous gift from Dr. E. Liehl (Sandoz, Vienna, Austria). The Abs and recombinant cytokines were diluted in pyrogen-free saline on the day of injection. Abs or control Ig were given i.p. 6 to 20 h before i.p. injection of 5 μg/mouse of SCF. Mice were also treated with 1 μg/mouse of IL-1, 3 μg/mouse of SCF, or the combination thereof, before or after irradiation.

Irradiation

Mice were randomized, placed in ventilated Plexiglass containers, and bilaterally irradiated using the AFRRI ^{60}Co whole body irradiator. Before irradiating the mice, the midline tissue (MLT) dose rate was measured by placing a 0.5-cc tissue equivalent in the ionization chamber (calibration factor traceable to the National Institute of Standards and Technology) at the center of 2.5-cm diameter, cylindrical acrylic mouse phantom. The tissue-to-air ratio (TAR), dose ratio was 0.96, and the field was uniform to within ± 5%. Exposure time was adjusted so that each animal received the specified dose at a fixed MLT dose rate of 0.4 Gy/min. Dosimetric measurements were made in accordance with the American Association of Physics in Medicine protocol for the determination of absorbed dose from high-energy photon and electron beams. The number of surviving mice was recorded daily for 30 days.

FACS Analysis

BMC were obtained by flushing femurs into RPMI media containing 5% FCS. After washing, cells were counted and resuspended in Dulbecco's PBS with 2% FCS at the concentration of 2×10^6/ml. Cells were stained for 30 min with 10 μg/ml of either PE-conjugated anti-murine c-*kit* Ab (3C1) or PE-conjugated, control IgG2b. The cells were washed twice and resuspended in 1 ml of 2% FCS-Dulbecco PBS. The percentage of c-*kit*$^+$ cells were calculated by subtracting the percentage of cells stained with control Ab from percentage of cells stained with c-*kit* Ab. In experiments in which bone marrow cells from irradiated mice were evaluated, each group consisted of a pool from eight femurs at 1 day (D+1) and 14 femurs at 4 days (D+4) after irradiation. Normal, nonirradiated mice were examined individually, with pools of cells from both femurs.

Immunofluorescence analysis was performed with an EPICS ELITE flow cytometer (Coulter Cytometry, Miami, FL) using logarithmic amplification. RBCs, platelets, and debris were excluded from the analysis on the basis of light scatter criteria. Twenty-five thousand cells were counted for each histogram.

SCF binding to BMC

Mouse rSCF was iodinated by the chloramine T method, which yielded ^{125}I-SCF preparations with sp. act. of approximately 20 μCi/μg protein. BMC (5×10^6) were distributed in duplicate Eppendorf tubes containing 200 μl binding medium (RPMI 1640, 25 mM HEPES, 1% BSA, 0.05% sodium azide) and 0.5 ng ^{125}I-SCF corresponding to approximately 10^5 cpm. Parallel duplicate tubes contained the 400-fold excess of unlabeled SCF. The cells were incubated at 4°C overnight, under rotation, and centrifuged through a 10% sucrose-PBS cushion. The tips of the tubes with cell pellets were removed, and the radioactivity was measured in a gamma counter (Gamma 400, Beckman Instruments, Fullerton, CA). Nonspecific binding determined in the presence of unlabeled SCF was subtracted from total binding to obtain specific binding.

For steady-state binding, cells were incubated in duplicate with different concentrations of ^{125}I-murine SCF. Matching replicates also contained a 100-fold excess of unlabeled ligand. The radioactivity associated with cell pellets was measured as in standard binding assays. To estimate the binding sites per cell and the K_d values, a nonlinear regression calculation was used (18). In all cases, complete sets of data generated in the assays were used in the analysis. Scatchard plots were reformatted presentations of nonlinear regression.

RNA extraction and Northern blot analysis

BMC collected from six femurs/group were pelleted and total cellular RNA was isolated by acid guanidine thiocyanate-phenol-chloroform extraction according to Chomczynski and Sacchi (19). RNA was separated by electrophoresis on 1% agarose and transferred onto a Hybond-N (Amersham, Oakville, Canada) membrane for Northern blot analysis. Membranes were prehydrated for 4 h in a mixture containing 120 mM Tris, 8 mM EDTA, 0.1% NaPP, 0.2% SDS, and 100 μg/ml heparin. Hybridization was conducted overnight at 68°C in prehybridization buffer containing 625 μg/ml heparin and 10% dextran sulfate. The murine c-*kit* probe was a 3710-bp *Eco*R1-Hind31 insert of the c-*kit* cDNA clone pGEM3 (c-*kit*3) and the human superoxide dismutase probe was a 0.1-Kb *Pst*I insert of the SODI cDNA clone, pSP 64 cSOD. The c-*kit* probe was further fragmented with *Dra*1-*Acc*1 and the fragments were labeled using

Table I. *Effect of anti-IL-1R Ab on SCF-induced radioprotection*[a]

Treatment	Dead/Tested	% Survival
Saline	30/30	0
Saline + SCF	11/30	63
Rat Ig + SCF	12/33	64
Anti-IL-1R + SCF	24/32	25*

[a] B6D2F1 mice received 100 μg/mouse anti-IL-1R Ab or rat IgG 6 h before administration of 3 μg/mouse of SCF. Twenty-four hours later, mice were irradiated with 1050 cGy ^{60}Co source. The 30-day survival of mice receiving anti-IL-1R Ab and SCF was signficantly lower (* indicates $p < 0.001$) than that of control saline and rat Ig-pretreated SCF-radioprotected mice.

a multiprime DNA labeling system (Amersham), with [α-^{32}P]dCTP (sp. act. >3000 Ci/mM. Amersham). The membranes were then washed once at room temperature for 20 min in 2X SSC, 0.1% SDS at 68°C for 60 min, and then rinsed at room temperature with 0.1X SSC. The membranes were exposed to Kodak XAR-5 film (Eastman Kodak, Rochester, NY) with intensifying screens at −80°C. Signal intensity was quantified by densitometry using a Pharmacia LKB Ultrascan XL (Pharmacia, Canada). As a control for RNA integrity, blots were rehybridized with a 1-kb *Pst*1 cDNA probe (American Tissue Culture Collection, Rockville, MD) of the housekeeping gene glyceraldehyde phosphate dehydrogenase (GAPDH).

CSF, IL-6, and fibrinogen assays

Circulating CSF and IL-6 were determined in the sera of mice bled 2 to 3 h after treatment with IL-1 or SCF, as previously described (20). Fibrinogen was determined in the citrated plasma of such mice bled 18 h after treatment, by the rate of conversion of fibrinogen to fibrin in the presence of excess thrombin, using a Sigma Chemical Company Diagnostic Kit.

Statistical analysis

Statistical evaluation of the results was conducted using χ^2 analysis, probit analysis, and analysis of variance followed by a Bonferroni corrected *t*-test.

Results

Effect of anti-IL-1R Ab on SCF radioprotection

To examine whether endogenously produced IL-1 contributes to SCF-induced radioprotection, mice were treated with 100 μg/mouse of anti-IL-1R Ab, rat IgG at an equivalent dose or saline, and 6 h later with a single dose of 3 μg/mouse PEG-SCF. Whereas at a dose of 1,050 cGy of radiation, 63% of saline pretreated and 64% of IgG pretreated mice were protected from death by SCF, only 25% of mice receiving anti-IL-1R Ab and SCF survived irradiation (Table I). Thus, although anti-IL-1R Ab did not entirely abolish the survival-enhancing effect of SCF, it reversed the protective effect by 40%, indicating that IL-1 contributes to radioprotection of SCF-treated mice.

Effect of anti-IL-1 and anti-IL-6 Abs on survival of anti-SCF Ab-treated mice

Our previous work showed reduced incidence of survival after LD 50/30 (875 cGy) irradiation of mice treated with anti-SCF, anti-IL-1R, or anti-IL-6 Abs (6, 7). To evaluate the contribution of endogenous IL-1 and IL-6 in addition to SCF, mice were given the Abs in combination. The results in Figure 1 indicate that addition of anti-IL-1R and anti-IL-6 Abs further reduced survival significantly, at nonlethal 750 cGy irradiation of anti-SCF Ab-treated mice suggesting that IL-1, IL-6, and SCF are mutually interdependent in protecting mice from lethal irradiation.

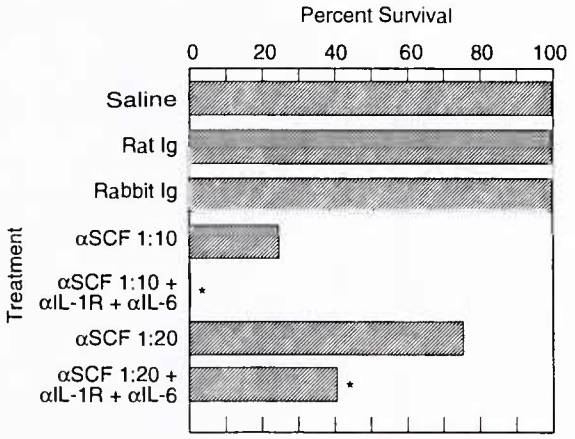

FIGURE 1. Abs to IL-1R and IL-6 further reduce survival of anti-SCF Ab-treated, irradiated mice. Groups of B6D2F1 mice (16 to 26 per group in two to three separate experiments) received rat IgG, 1:10 dilution of rabbit preimmune serum, 1:10 and 1:20 dilution of rabbit anti-SCF Ab, or the combination of anti-SCF Ab with 100 μg/mouse of anti-IL-1R Ab and 600 μg/mouse of anti-IL-6 Ab (as indicated). The mice were exposed a day later to a sublethal 750 cGy dose ^{60}Co irradiation (LD50/30 = 866 cGy). The survival of mice that received the combination of Abs was significantly lower ($p < 0.01$) than that of mice treated with anti-SCF alone.

Effect of combinations of IL-1 and SCF in protection from lethal irradiation

The observed codependence of SCF- and IL-1-induced radioprotection led us to examine the effect of their combined administration on survival of irradiated mice. We chose the doses of 3 μg/mouse of SCF and 1 μg/mouse of IL-1, because 5 μg of SCF and 3 μg of IL-1 conferred identical protection. Results in Figure 2 document that a single injection of both cytokines 18 h before irradiation resulted in synergistic radioprotection at 1200 to 1300 cGy doses of radiation. Whereas the control saline-treated mice had an LD50/30 of 866 cGy (95% confidence limits: 828 to 888), IL-1-treated LD50/30 of 1009 cGy (991 to 1034), and SCF-treated mice LD50/30 of 1106 cGy (1048 to 1194), and the combination of the two cytokines resulted in an LD50/30 of 1273 (1248 to 1317) cGy. Administration of both cytokines 48 or 4 h before or 1 h after irradiation (Table II) had either a greatly reduced effect (at 4 h before) or no effect (at 48 h before or 1 h after). As was the case with IL-1, SCF given alone 48 h before or 1 h after irradiation did not afford significant protection.

The radioprotective effect of SCF was not associated with the induction of early or late acute serum proteins

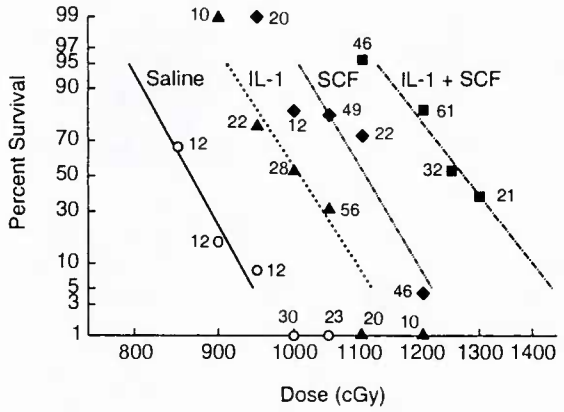

FIGURE 2. Effect of treatment with IL-1, SCF, or their combination on survival of B6D2F1 lethally irradiated mice. Mice received i.p. 1 μg IL-1, 3 μg SCF, their combinations, or saline; and 18 h later received ^{60}Co radiation in doses indicated. Survival was recorded daily for 30 days and plotted using probit analysis. The numbers indicate the number of mice per given treatment.

Table II. *Survival percentage of mice receiving IL-1 and SCF treatment before and after irradiation*[a]

	48 h Before	4 h Before		1 h After
Treatment	1000 cGy	1000 cGy	1050 cGy	1000 cGy
Saline	0	0	0	0
IL-1	0	25*	10	0
SCF	0	19*	0	0
SCF + IL-1	0	75*	0	0

[a] B6D2F1 mice (10 to 16 mice per group) were administered i.p. 1 μg of IL-1, 3 μg of SCF, or their combination, before or after irradiation. Survival of mice was recorded daily for 30 days.

* Significantly lower ($p < 0.01$) than survival obtained with 8-h pretreatment (see Fig. 2).

Table III. *Comparison of IL-1 and SCF for induction of CSF, IL-6, and fibrinogen*[a]

Treatment	Fibrinogen (mg/dcl)	CSF (U/ml)	IL-6 (pg/ml)
Saline	203.6 ± 4	<20	<50
IL-1	384.0 ± 16*	2513 ± 388*	1600
SCF	188.0 ± 3	<20	<20

[a] Mice received i.p. 1 μg/mouse of IL-1, S μg/mouse SCF, or saline (control) and were bled 2 to 3 h later to determine CSF and IL-6 or 18 h later, for fibrinogen determination.

* $p < 0.01$ compared to control.

such as IL-6, CSF, or fibrinogen, all of which are induced with IL-1 (Table III). Similarly, SCF treatment, in contrast with IL-1, did not up-regulate the mRNA for MnSOD (Fig. 3).

Determination of changes in c-kit expression by BMC

Both IL-1 and SCF were reported to induce BMC cycling and increases in progenitor compartment (21, 22). Such changes should be reflected in increased numbers of c-*kit*$^+$

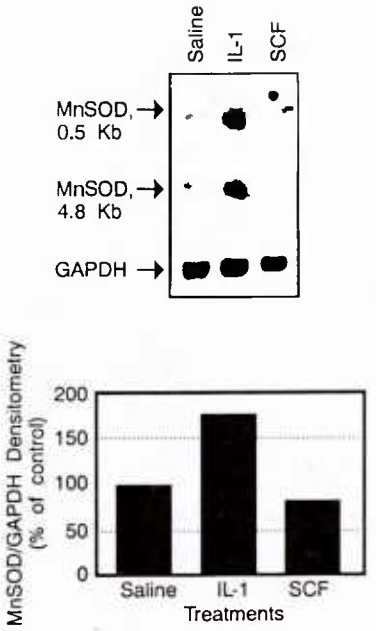

FIGURE 3. IL-1, but not SCF, induces MnSOD gene expression. Groups of mice (4 mice/group) received i.p. 1 μg IL-1, 3 μg SCF, or saline. BMC were obtained 4 h after injections (see *Materials and Methods* for details of procedures).

Table IV. *The effect of treatment of mice with cytokines on the recovery of c-kit*$^+$ *BMC after 950 cGy irradiation*[a]

	Day 0	Day +1	Day +4
Treatment	c-*kit*$^+$ cells/femur (×10^5)	c-*kit*$^+$ cells/femur (×10^4)	c-*kit*$^+$ cells/femur (×10^4)
Saline	2.6 ± 1.4	2.0 ± 0.1	0.3 ± 0.1
IL-1	3.6 ± 1.8	6.0 ± 1.4*	1.9 ± 0.9[b]
SCF	2.0 ± 0.2	2.5	5.7 ± 3.5*
IL-1 + SCF	2.3 ± 1.3	9.4 ± 0.8**	12.0 ± 2.0**

[a] Mice received i.p. 1 μg/mouse of IL-1, 3 μg/mouse of SCF, alone or in combination, or saline and 18 h later, 950 cGy ^{60}Co irradiation. BMC were obtained from unirradiated mice (D 0) and at 1 day and 4 days after irradiation. Each group of mice consisted of a pool of eight femurs (D 0, D + 1) and 14 femurs (D + 4). The results are the mean ± SD of two experiments. The numbers of c-*kit*$^+$ cells were significantly higher than in control, saline-treated mice.

[b] $p = 0.063$; *$p < 0.05$; ** $p < 0.01$.

BMC, as c-*kit* is expressed on stem cells and all immature progenitors, but not on mature neutrophils, nucleated erythrocytes, or macrophages (13, 14). To determine whether treatment with cytokines before radiation results in an improved survival of progenitor and stem cells, FACS analysis was used to compare the numbers of c-*kit*$^+$ BMC from cytokine and saline control-treated lethally irradiated mice. As shown in Table IV, BMC obtained from IL-1-, SCF- or IL-1 + SCF-treated mice 1 day after lethal (LD 100/30) irradiation (950 cGy) had increased numbers of surviving c-*kit*$^+$ cells compared with control saline-treated mice. At 4 days after irradiation, with progressive loss of total nucleated BMC, these differences became more striking, with IL-1-treated mice showing a sixfold increase, SCF-treated mice,

Table V. *Effect of treatment of mice with IL-1, SCF alone, or the two in combination on specific binding of ^{125}I-SCF on BMC*[a]

Treatment	4 h	10 h	24 h	48 h
IL-1	47%	65%	26.5 ± 0.5%	62 ± 2%
SCF	ND	ND	32.5 ± 4.5%	63 ± 18%
IL-1 + SCF	ND	ND	67 ± 11%*	105 ± 30%*

[a] Mice received cytokines as specified in Table IV. BMC were treated as specified in *Materials and Methods*. The results are expressed as percentage of specific binding above that of specific binding of control BMC. Each experimental group consisted of four mice. The results for 24 and 48 h are the mean ± SD of two separate experiments.

* Statistical comparisons at 24 and 48 h for each of the sum of specific binding for IL-1 and SCF with that for the combination treatment do not reject ($p > 0.1$) the hypothesis that the treatment effects are additive.

Table VI. *The effect of adrenalectomy on specific binding of ^{125}I-SCF on BMC of IL-1- vs saline-treated mice*[a]

	Saline	IL-1 (0.1 μg)	% Increase
ADX. I	1030*	2867	178
ADX. II	879	1472	70
Sham ADX	1092	1455	33

[a] Adrenalectomized (ADX I and ADX II) or sham-adrenalectomized mice (four mice per group) received i.p. saline or IL-1 injections and BMC were obtained 4 h later for the binding assay.

* Specific binding (cpm) calculated as indicated in *Materials and Methods*. For comparison, see Table 5.

an approximately 20-fold increase and IL-1- and SCF-treated mice, a 40-fold increase in c-*kit*$^+$ BMC per femur, relative to saline control. Because the nadir in the BMC number occurs at 3 days after irradiation, these results suggest that a substantially greater number of c-*kit*$^+$ BMC survive lethal doses of radiation in mice pretreated with IL-1, SCF, or their combinations.

Repeated attempts to establish that, in normal unirradiated mice, treatment with IL-1, SCF, and their combination results in increased numbers of c-*kit*$^+$ BMC within 24 h, were not successful. This may be a result of an increase in only a small cohort of BMC, i.e., selected populations of early progenitor cells.

Effect of IL-1 on SCF binding by BMC

Therefore, we have examined the changes in c-*kit*$^+$ BMC by evaluating SCF binding to such cells. A binding assay of radiolabeled ligand provides a sensitive means of assessing changes in the numbers and affinity of receptors. Administration of 1 μg/mouse of IL-1, a dose used in a combined IL-1/SCF radioprotective treatment, increased binding of radiolabeled SCF (Table V). In contrast with our previous observation that IL-1-induced up-regulation of IL-1R on BMC was mediated by corticosteroid and G-CSF (23), G-CSF in doses ranging from 0.3 to 5 μg/mouse did not up-regulate SCF binding (results not shown), and adrenalectomized mice did not differ from normal mice in up-regulation of SCF binding in response to IL-1 (Table VI). Furthermore, treatment with dexamethasone at 2 and 10 μg/mouse did not affect SCF binding on normal BMC (data not shown). SCF treatment resulted in similar increases as IL-1 in ^{125}I-SCF binding on BMC, and the combined treatment of IL-1 and SCF resulted in an approximately additive effect (Table V).

Scatchard analysis performed with normal cells and cells from mice treated for 10 and 48 h with IL-1 showed increases of 25 and 50%, respectively, in the number of receptors/cell with no change in affinity (Fig. 4). Previous reports determined two affinities (10^{-11} K_d, and 10^{-9} K_d) for human c-*kit* receptors (24, 25). However, in our study only one affinity (10^{-9} K_d) receptor can be detected on murine BMC. Although the results are expressed as numbers of receptors per cell, we actually determined an increase in total numbers of receptors on populations of BMC. Because less than 5% of BMC express c-*kit* receptors, and the number of receptors decreases with BMC lineage differentiation, we could not distinguish whether such an increase reflects greater numbers of cells with high or low receptor expression or the combination of the two.

Effect of IL-1 treatment on c-kit gene expression

To determine that the up-regulation of SCF binding on the IL-1-treated BMC was associated with increased c-*kit* gene expression, a Northern blot analysis was performed to compare mRNA for c-*kit* in saline with that of IL-1-treated BMC. Results (Fig. 5) demonstrate that IL-1 induced dose-dependent increases in c-*kit* mRNA, which could be detected within 2 h of IL-1 treatment and, which peaked at 6 h. In contrast, treatment with IL-6 did not up-regulate c-*kit* gene expression (Fig. 6).

Discussion

Our previous studies using Abs to SCF and IL-1R suggested that endogenous production of both cytokines is required to protect mice treated with LPS or IL-1 from lethal radiation (17). This study further establishes that radioprotection with SCF requires the participation of IL-1 (Table I) and that IL-1 and SCF protect synergistically at 1200 to 1300 cGy doses of radiation (Fig. 2). This synergistic protection is evidenced by an increase in the percentage of mice surviving doses of radiation over 45% greater than LD 100/30.

There is considerable evidence that administration of IL-1 induces an increase in numbers of progenitor cells. We and others previously observed that IL-1 increased cycling of hemopoietic progenitor cells and progressively increased proliferative expansion of myeloid progenitor cells in the marrow from 6 to 48 h (21, 26, 27). In a more recent study, Hestdal et al. (28) demonstrated that IL-1 treatment of mice results within 24 h in a fivefold up-regulation of HPP-CFC and twofold to threefold up-regulation of CFU-c when grown in the presence of GM-CSF or IL-3. In this study, we found a 50% increase in transcription of c-*kit*, a phenotypic marker of progenitor cells, and a 50% increase in SCF binding as early as 2 and 4 h,

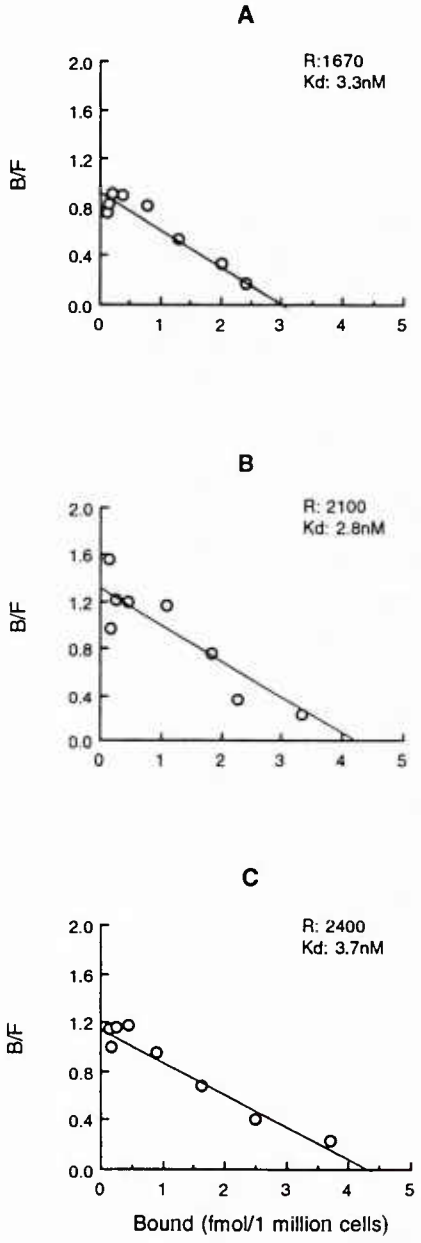

FIGURE 4. Binding of ^{125}I-SCF to murine BMC. Cells (5×10^6) in 200 μl of binding medium were incubated in duplicate with different concentrations of ^{125}I-SCF. Matching replicates also contained 100-fold of unlabeled SCF. Receptor number S(R) and K_d values were analyzed as described in *Materials and Methods*. Scatchard plots from one of two experiments with virtually similar results represent: *Panel a*) BMC obtained from untreated mice; *b*) BMC from mice treated with IL-1 (1 μg/mouse) after 10 h; c) BMC from mice treated with IL-1 after 48 h.

respectively, after IL-1 treatment. These results are strengthened by the equilibrium binding studies with ^{125}I-SCF, which show that, within 10 h after IL-1 treatment, BMC express 25% more c-*kit* receptors. Despite such increases in c-*kit* expression, a significant increase in numbers of c-*kit*$^+$ BMC was not observed by FACS analysis. Taken together, our results suggest that the observed increase in binding sites may occur on progenitor cells expressing more receptors.

The stimulating effects of IL-1 on progenitor cells and hemopoiesis may contribute to its radioprotective effects. The hemopoietic effects may depend in part on the ability of IL-1 to induce hemopoietic IL-6 and CSFs (29, 30). In addition, Il-1 induction of the scavenging mitochondrial enzyme, MnSOD in BMC (Ref. 31, and confirmed in our study), and its ability in vivo to induce BMC to enter a relatively radioresistant S phase of cell cycle (21), should contribute to radioprotection. Most recently, Zucali et al. have shown that in vitro treatment with IL-1 of male mouse BMC and irradiation results in greater survival than treatment without IL-1, of short-term and long-term repopulating stem cells transferred to female mice (32). These results clearly document, for the first time, the direct radioprotective effects of IL-1 on hemopoietic stem and progenitor cells. In our study, 1 day after lethal irradiation the total number of c-*kit*$^+$ BMC in the femurs of IL-1-treated and IL-1- and SCF-treated mice were threefold and fivefold greater, respectively, than that in control saline-treated mice. This provides evidence that in vivo IL-1 actually has the capacity to induce increases in numbers of progenitor cells surviving lethal irradiation.

As with IL-1, SCF treatment of mice given in two injections before irradiation, increased the numbers of surviving mice concomitant with hemopoietic recovery evident within 6 to 10 days after irradiation (33). Our work confirms and extends these findings by demonstrating that even a single injection of SCF is highly radioprotective. However, as shown in this report, SCF does not induce production of hemopoietic growth factors (CSF), IL-6, acute phase response, or MnSOD, all believed to contribute to radioprotection by IL-1. Despite this, multiple doses of SCF in several previous reports (22, 34, 35) and a single injection, as shown in this study, induce hemopoietic expansion. Because in multiple reports SCF was shown to require costimulatory addition of CSFs to induce in vitro proliferation of hemopoietic colonies, it is likely that these growth factors are available in sufficient supply in vivo to allow hemopoietic expansion.

In contrast with IL-1 and SCF, well-known hemopoietic cytokines, such as G-CSF and IL-6, promote in vitro expansion of hemopoietic cells, yet their in vivo hemopoietic effects as shown here and elsewhere (36) are much more limited than these of IL-1 or SCF. Possibly this is because IL-6 and G-CSF do not cause an increase in the expression of c-*kit* by BMC. In fact, hemopoietic growth factors IL-3 and GM-CSF are reported to actually down-regulate the expression of mRNA for c-*kit* on mast cells and progenitor cell lines (37), which is consistent with the role of these factors in promoting differentiation of progenitor cells. These contrasting in vivo and in vitro hemopoietic effects support the fundamental importance of IL-1 and SCF in

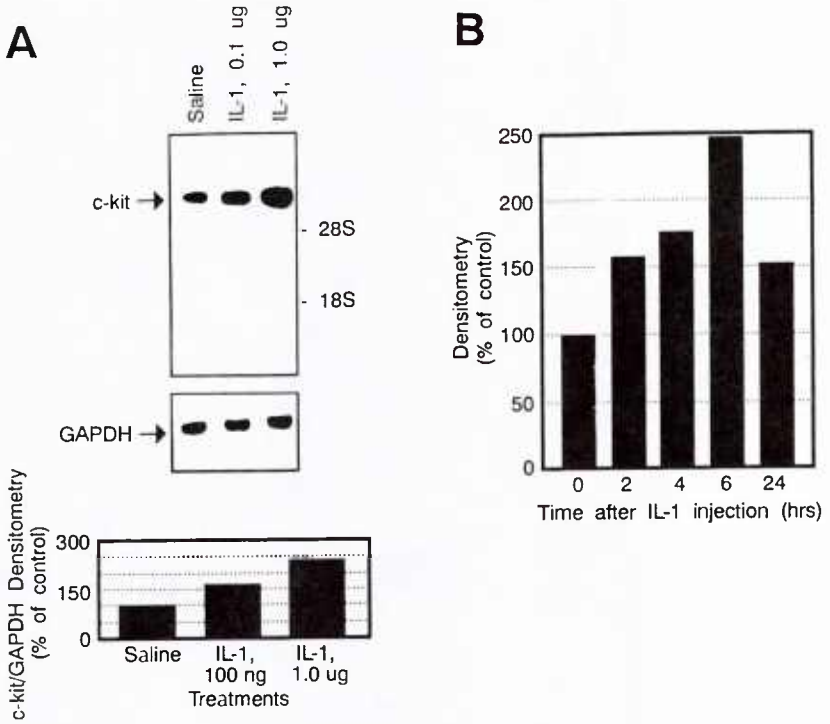

FIGURE 5. Effect of treatment with IL-1 on c-*kit* gene expression. *Panel a*) mice were treated with 0.1 and 1.0 μg/mouse of IL-1 or saline and 4 h later BMC were harvested for Northern blot analysis. *Panel b*) BMC from mice receiving 1.0 μg/mouse of IL-1 were assessed at different times for c-*kit* mRNA expression. Each group represents a pool of BMC from four mice.

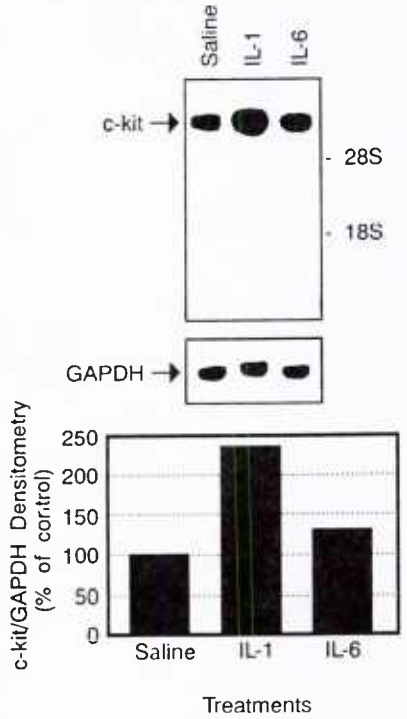

FIGURE 6. Comparison of treatment of IL-1 vs IL-6 on c-*kit* gene expression. Mice were treated with 1 μg of IL-1 or 2 μg of IL-6 or saline and BMC were recovered 4 h later for Northern blot analysis. Each group represents a pool of four mice.

increasing the numbers of c-*kit*$^+$ progenitor cells and, thus, facilitating hemopoietic recovery from radiation.

The mechanism of radioprotection with SCF remains to be established. The findings that SCF acts as a most potent comitogen on multilineage cells (10–14) and that Ab to SCF increases lethality of irradiation to mice (17) provide strong evidence that SCF is required for the regeneration of hemopoiesis. If such were the case, however, merely supplying SCF after irradiation should suffice for this effect. Yet SCF administration at 1 h after irradiation (Table II) did not result in significant radioprotection. Thus a lag period similar to that required for IL-1 is also required for radioprotection with SCF. Such results would suggest that the increase in numbers of progenitor cells in the BM before irradiation may account for the observed increase in resistance to radiation conferred by these two cytokines. However, the findings that the radioprotective effect of IL-1, SCF, or their combination cannot be demonstrated 48 h after their administration (Table II), despite a progressive increase in numbers of progenitor cells, suggest that either differentiation of these cells or, as previously suggested (21, 33), a particular phase in their cycle contribute to radioprotection.

Acknowledgments

We thank Drs. Ian McNiece and Les Redpath for stimulating disscussions, Drs. G.D. Ledney and T.J. MacVittie for critical review of the manuscript, Natalie Davis, Nasima J. Ali, and Francine Grondin for their excellent technical assistance, Modeste Greenville for editorial comments, and William Jackson for statistical analysis of the results.

References

1. Lorenz, E., D. Uphoff, T. R. Reid, and E. Shelton. 1951. Modification of irradiation injury in mice and guinea pigs by bone marrow injections. *J. Natl. Cancer Inst. 12:197.*

2. Van Bekkum, D. W. 1969. Bone marrow transplantation and partial body shielding for estimating cell survival and repopulation. In *Comparative Cellular and Species Radiosensitivity*, V. P. Bond, and T. Sugahara, eds. Igaku Shoin, Tokyo, p. 175.
3. Ainsworth, E. J., and M. H. Hatch. 1958. Decreased x-ray mortality in endotoxin-treated mice. *Radiat. Res. 9:96.*
4. Neta R., S. D. Douches, and J. J. Oppenheim. 1986. Interleukin-1 is a radioprotector. *J. Immunol. 136:2483.*
5. Neta R., J. J. Oppenheim, and S. D. Douches. 1988. Interdependence of the radioprotective effects of human recombinant IL-1, TNF, G-CSF, and murine recombinant GM-CSF. *J. Immunol. 140:108.*
6. Neta R., J. J. Oppenheim, R. D. Schreiber, R. Chizzonete, G. D. Ledney, and T. J. MacVittie. 1991. Role of cytokines (interleukin 1, tumor necrosis factor, and transforming growth factor β) in natural and lipopolysaccharide-enhanced radioresistance. *J. Exp. Med. 173: 1177.*
7. Neta, R., R. Perlstein, S. N. Vogel, G. D. Ledney, and J. Abrams. 1992. Role of IL-6 in protection from lethal irradiation and in endocrine responses to IL-1 and TNF. *J. Exp. Med. 175:689.*
8. Williams, D. E., J. Eisenman, A. Baird, C. Rauch, K. Van Ness, C. J. March, L. S. Park, U. Martin, D. Y. Mochizuki, H. S. Boswell, G. S. Burgess, D. Cosman, and S. D. Lyman. 1990. Identification of a ligand for c-*kit* proto-oncogene. *Cell 63:167.*
9. Zsebo, K. M., J. Wypych, I. K. McNiece, H. S. Lu, K. A. Smith, S. B. Karkare, R. K. Sachdev, V. N. Youshenkoff, N. C. Birkett, L. R. Williams, V. N. Sayagal, R. A. Bosselman, E. A. Mendiaz, and K. E. Langley. 1990. Identification, purification and biological characterization of hematopoietic stem cell factor from Buffalo rat-conditioned medium. *Cell 63:195.*
10. de Vries, P., K. A. Brasel, J. R. Eisenman, A. R. Alpert, and D. E. Williams. 1991. The effect of recombinant mast cell growth factor on purified murine hematopoietic stem cells. *J. Exp. Med. 173:1205.*
11. Muench, M. O., J. G. Schneider, and M. A. S. Moore. 1991. Interactions among colony-stimulating factors, IL-1β, IL-6, and *kit*-ligand in the regulation of primitive murine hematopoietic cells. *Exp. Hematol. 20:339.*
12. Broxmeyer, H. E., R. Maze, R. Miazawa, C. Carow, P. C. Hendrie, S. Cooper, G. Hangoc, S. Vadjan-Raj, and L. Lu. 1991. The *kit* receptor and its ligand, steel factor, as regulators of hemopoiesis. *Cancer Cells 3:480.*
13. Ogawa, M., Y. Matsuzaki, S. Nishikawa, S. Hayashi, T. Kunisada, T. Sudo, T. Kina, H. Nakauchi, and S. Nishikawa. 1991. Expression and function of c-*kit* in hematopoietic progenitor cells. *J. Exp. Med. 174:63.*
14. Metcalf, D., and N. A. Nicola. 1991. Direct proliferative actions of stem cell factor on murine bone marrow cells in vitro: effects of combination with colony-stimulating factors. *Proc. Natl. Acad. Sci. USA 88:6239.*
15. Okada, S., H. Nakauchi, K. Nagayoshi, S.-I. Nishikawa, Y. Miura, and T. Suda. 1992. In vivo and in vitro stem cell function of c-*kit*- and Sca-1-positive murine hematopoietic cells. *Blood 80:3044.*
16. Ikuta, K., and I. L. Weissman. 1992. Evidence that hematopoietic stem cells express mouse c-*kit* but do not depend on steel factor for their generation. *Proc. Natl. Acad. Sci. USA 89:1502.*
17. Neta, R., D. Williams, F. Selzer, and J. Abrams. 1993. Inhibition of c-*kit* ligand/steel factor by antibodies reduces survival of lethally-irradiated mice. *Blood 81:324.*
18. Bates, D. M., and D. G. Watts. 1988. *Nonlinear Regression and its Application*, Wiley, New York.
19. Chomczynski, P., and N. Sacchi. 1987. Single step method of RNA isolation by guanidium thiocyanate-phenol chloroform extraction. *Anal. Biochem. 162:156.*
20. Neta, R., S. N. Vogel, J. M. Plocinski, N. S. Tare, W. Benjamin, R. Chizzonite, and M. Pilcher. 1990. In vivo modulation with anti-IL 1 receptor antibody 35F5 of the response to interleukin 1. The relationship of radioprotection, colony-stimulating factor, and interleukin 6. *Blood 76:57.*
21. Neta, R., M. B. Sztein, J. J. Oppenheim, S. Gillis, and S. D. Douches. 1987. In vivo effects of IL-1. I. Bone marrow cells are induced to cycle after administration of IL-1. *J. Immunol. 139:1861.*
22. Fleming, W. H., E. J. Alpern, N. Uchida, K. Ikuta, and I. L. Weissman. 1993. Steel factor influences the distribution and activity of murine hematopoietic stem cells in vivo. *Proc. Natl. Acad. Sci. USA 90:3760.*
23. Dubois, C. M., F. W. Ruscetti, J. R. Keller, J. J. Oppenheim, K. Hestdal, R. Chizzonite, and R. Neta. 1991. In vivo interleukin 1 (IL-1) administration indirectly promotes type II IL-1 receptor expression on hematopoietic bone marrow cells: novel mechanism for the hematopoietic effects of IL-1. *Blood 78:2841.*
24. Broudy, V. C., F. O. Smith, N. Lin, K. M. Zsebo, J. Egrie, and I. D. Bernstein. 1992. Blasts from patients with acute myelogenous leukemia express functional receptors for stem cell factor. *Blood 80:60.*
25. Abkowitz, J. L., V. C. Broudy, L. G. Bennett, K. M. Zsebo, and F. H. Martin. 1992. Absence of abnormalities of c-*kit* or its ligand in two patients with Diamond-Blakfan anemia. *Blood 79:25.*
26. Johnson, C. S., D. J. Keckler, M. I. Topper, P. G. Braunschweiger, and P. Furmanski. 1989. In vivo hematopoietic effects of recombinant interleukin 1a in mice: Stimulation of granulocytic, monocytic, megakaryocytic and early erythroid progenitors; suppression of late stage erythropoiesis, and reversal of erythroid suppression with erythropoietin. *Blood 73:678.*
27. Schwartz, G. N., T. J. MacVittie, R. M. Vigneulle, M. L. Patchen, S. D. Douches, J. J. Oppenheim, and R. Neta. 1987. Enhanced hematopoietic recovery in irradiated mice pretreated with interleukin-1 (IL-1). *Immunopharmacol. Immunotoxicol. 9:371.*
28. Hestdal, K., S. E. W. Jacobson, F. W. Ruscetti, C. M. Dubois, D. L. Longo, R. Chizzoneti, J. J. Oppenheim, and J. R. Keller. 1992. In vivo effect of interleukin 1a on hematopoiesis: role of colony-stimulating factor receptor modulation. *Blood 80:2486.*
29. Neta, R., S. N. Vogel, J. D. Sipe, G. G. Wong, and R. P. Nordan. 1988. Comparison of in vivo effects of human recombinant IL-1 and human recombinant IL-6 in mice. *Lymphokine Res. 7:403.*
30. Vogel, S. N., S. D. Douches, E. N. Kaufman, and R. Neta. 1987. Induction of colony-stimulating factor in vivo by recombinant interleukin-1α and recombinant tumor necrosis factor-α. *J. Immunol. 138:2143.*
31. Eastgate, J., J. Moreb, and H. S. Nick. 1993. A role for manganese superoxide dismutase in radioprotection of hematopoietic stem cells with interleukin 1. *Blood 81:69.*
32. Zucali, J. R., J. Moreb, W. Gibbons, J. Alderman, A. Suresh, Y. Zhang, and B. Shelby. 1993. Radioprotection of hematopoietic stem cells by interleukin 1. *Exp. Hematol. In press.*
33. Zsebo, K. M., K. A. Smith, C. A. Hartley, M. Greenblatt, K. Cooke, W. Rich, and I. K. McNiece. 1992. Radioprotection of mice by recombinant stem cell factor. *Proc. Natl. Acad. Sci. USA 89:9464.*
34. Bodine, D., N. Seidel, K. Zsebo, and D. Orlic. 1993. In vivo administration of stem cell factor to mice increases the absolute number of pluripotent hematopoietic stem cells. *Blood 82:445.*
35. Tong, J., M. Gordon, E. Srour, R. Cooper, A. Orazi, I. McNiece, and R. Hoffman. 1993. In vivo administration of recombinant methionyl human stem cell factor expands the number of human marrow hematopoietic stem cells. *Blood 82:784.*
36. Dubois, C. M., R. Neta, J. R. Keller, S. E. W. Jacobsen, J. J. Oppenheim, and F. Ruscetti. 1993. Hematopoietic growth factors and glucocorticoids synergize to promote hematopoiesis in vivo partly through induction of IL 1 receptor expression on bone marrow cells. *Exp. Hematol. 21:303.*
37. Welham, M. J., and J. W. Schrader. 1991. Modulation of c-*kit* mRNA and protein by hematopoietic growth factors. *Mol. Cell. Biol. 11:2901.*

Gene Expression of Hematoregulatory Cytokines Is Elevated Endogenously After Sublethal Gamma Irradiation and Is Differentially Enhanced by Therapeutic Administration of Biologic Response Modifiers[1]

Verlyn M. Peterson,* Jeffrey J. Adamovicz,† Thomas B. Elliott,[2‡] Mary M. Moore,‡ Gary S. Madonna,† William E. Jackson III,§ G. David Ledney,‡ and William C. Gause†

*Burn Research Laboratory, Division of Plastic and Reconstructive Surgery, Department of Surgery, University of Colorado Health Sciences Center, Denver, CO 80262; †Department of Microbiology, Uniformed Services University of the Health Sciences, Bethesda, MD 20889; and ‡Departments of Experimental Hematology and §Computer and Electronics, Armed Forces Radiobiology Research Institute, Bethesda, MD 20889

Prompt, cytokine-mediated restoration of hematopoiesis is a prerequisite for survival after irradiation. Therapy with biologic response modifiers (BRMs), such as LPS, 3D monophosphoryl lipid A (MPL), and synthetic trehalose dicorynomycolate (S-TDCM) presumably accelerates hematopoietic recovery after irradiation by enhancing expression of cytokines. However, the kinetics of the cytokine gene response to BRMs and/or irradiation are poorly defined. One hour after sublethal (7.0 Gy) ^{60}Cobalt gamma irradiation, B6D2F1/J female mice received a single i.p. injection of LPS, MPL, S-TDCM, an extract from *Serratia marcescens* (Sm-BRM), or Tween 80 in saline (TS). Five hours later, a quantitative reverse transcription-PCR assay demonstrated marked splenic gene expression for IL-1β, IL-3, IL-6, and granulocyte-CSF (G-CSF). Enhanced gene expression for TNF-α, macrophage-CSF (M-CSF), and stem cell factor (SCF) was not detected. Injection of any BRM further enhanced cytokine gene expression and plasma levels of CSF activity within 24 h after irradiation and hastened bone marrow recovery. Mice injected with S-TDCM or Sm-BRM sustained expression of the IL-6 gene for at least 24 h after irradiation. Sm-BRM-treated mice exhibited greater gene expression for IL-1β, IL-3, TNF-α, and G-CSF at day 1 than any other BRM. When challenged with 2 $LD_{50/30}$ of *Klebsiella pneumoniae* 4 days after irradiation, 100% of Sm-BRM-treated mice and 70% of S-TDCM-treated mice survived, whereas $\leq$30% of mice treated with LPS, MPL, or TS survived. Thus, sublethal irradiation induces transient, splenic cytokine gene expression that can be differentially amplified and prolonged by BRMs. BRMs that sustained and/or enhanced irradiation-induced expression of specific cytokine genes improved survival after experimental infection. *The Journal of Immunology,* 1994, 153: 2321.

Bone marrow failure is an inevitable consequence of life-threatening radiation injuries, and the severity and duration of the resulting neutropenia influence morbidity and mortality (1, 2). Survival after irradiation requires regeneration of bone marrow from quiescent hematopoietic stem cells (3, 4). Proliferation and differentiation of these hematopoietic progenitors depends on the endogenous expression of hematoregulatory cytokines (3–5). Therapeutic administration of IL-1, TNF-α, IL-6, or SCF[3] after lethal irradiation improves survival in animals, suggesting the importance of these hematopoietic regulatory cytokines after radiation (6–10). Neta et al. (11–14) report that pretreatment of irradiated mice with Abs specific for IL-1 receptor, TNF-α, IL-6, or SCF significantly decreases survival, whereas administration of

Received for publication January 24, 1994. Accepted for publication May 30, 1994.

The costs of publication of this article were defrayed in part by the payment of page charges. This article must therefore be hereby marked *advertisement* in accordance with 18 U.S.C. Section 1734 solely to indicate this fact.

[1] This research was supported by the Armed Forces Radiobiology Research Institute, Defense Nuclear Agency under work unit 4440-00129. Views presented in this report are those of the authors; no endorsement by the Defense Nuclear Agency has been given or should be inferred. Research was approved by the Institutional Animal Care and Use Committee and was conducted according to the principles enunciated in the Guide for the Care and Use of Laboratory Animals prepared by the Institute of Laboratory Animal Resources, National Research Council. These studies were accomplished while V.M.P. was on sabbatical at the Uniformed Services University of the Health Sciences and the Armed Forces Radiobiology Research Institute, Bethesda, MD.

[2] Address correspondence and reprint requests to Dr. Thomas B. Elliott, Experimental Hematology Department, Armed Forces Radiobiology Research Institute, 8901 Wisconsin Avenue, Bethesda, MD 20889-5603.

[3] Abbreviations used in this paper: SCF, stem cell factor; AFRRI, Armed Forces Radiobiologic Research Institute; BRM, biologic response modifier; MPL, 3D monophosphosphoryl lipid A; S-TDCM, synthetic trehalose dicorynomycolate; Sm-BRM, extract from *Serratia marcescens*; TS, 2% Tween 80 in 0.9% NaCl; RT-PCR, reverse transcription-PCR; HPRT, hypoxanthine guanine phosphoribosyl transferase; CFU-GM, CFU-granulocyte macrophage (bipotential myeloid progenitor); CFU-S, CFU-spleen (multipotential progenitor); G-CSF, granulocyte-CSF; M-CSF, macrophage-CSF.

0022-1767/94/$02.00

Abs specific for IL-3, IL-4, GM-CSF, or IFN-γ does not alter survival. These data suggest that after radiation injury presence of specific cytokines are critical for restoration of bone marrow and host survival but do not address the issue of induction or elevation of these cytokines.

It is clear that the therapeutic administration of a single hematoregulatory cytokine can accelerate hematopoietic recovery in vivo after radiation injury. However, in vitro studies indicate that bone marrow must be exposed to multiple hematopoietic growth factors to achieve optimal myeloproliferation (3, 4). An alternative to the therapeutic administration of multiple cytokines in vivo after irradiation is the use of a single BRM that induces the endogenous expression of many hematoregulatory cytokines (15). For example, LPS stimulates expression of several CSFs, IL-1, TNF-α, and IL-6, and administration of LPS to mice after lethal irradiation improves survival (16–18). Unfortunately, preclinical and clinical studies indicate that LPS is prohibitively toxic (19–22). Consequently, other bacterially derived BRMs have been developed that retain radioprotective and/or radiotherapeutic properties but exhibit less toxicity. These agents include MPL, a dephosphorylated derivative of the lipid A moiety of LPS; S-TDCM, a chemical preparation similar to a native cell wall-associated glycolipid isolated from *Corynebacterium* species; and Sm-BRM, a cell membrane/ribosomal RNA-sized vesicle preparation isolated from *Serratia marcescens*.

Although therapeutic administration of BRMs appears to improve host survival by enhancing endogenous expression of cytokines that accelerate bone marrow recovery, the effects of BRMs on the kinetics of cytokine gene expression after irradiation are not well defined, largely because quantitation of cytokine gene expression in hypoplastic, irradiated tissues has been technically difficult (17, 23). Recently developed RT-PCR assay techniques, however, enable quantitation of gene expression of multiple cytokines from limited quantities of mRNA (24, 25). The purpose of this investigation was to determine in a murine model of sublethal gamma irradiation whether: 1) irradiation alone is sufficient to induce cytokine gene expression; 2) therapeutic administration of BRMs alters post-irradiation cytokine gene expression; and 3) therapeutic administration of BRMs alters hematopoietic recovery and/or improves survival after experimental bacterial infection. Our results indicate that gene expression of specific cytokines is induced within 5 h after gamma irradiation and is differentially enhanced and/or prolonged by the therapeutic administration of BRMs. Despite the observation that therapeutic administration of any one of these BRMs accelerated bone marrow recovery, only the administration of S-TDCM or Sm-BRM sustained expression of specific, irradiation-induced cytokine genes and improved survival of irradiated mice infected with *Klebsiella pneumoniae*. These data then suggest that the selection of BRMs capable of enhancing and/or prolonging gene expression of hematoregulatory cytokines is an important factor in determining survival to infection after sublethal irradiation.

Materials and Methods

Mice

B6D2F1/J female mice (The Jackson Laboratory, Bar Harbor, ME), 11 wk of age, 18 to 22 g, were held in quarantine for 2 wk. Necropsy specimens from sentinel mice were examined to ensure the absence of specific intestinal bacteria and common murine diseases by microbiology, serology, and histopathology. Up to 10 mice were housed in sanitized 46 cm × 24 cm × 15 cm polycarbonate boxes with a filter cover (MicroIsolator; Lab Products, Inc., Maywood, NJ) on sterilized hardwood chip bedding in a facility accredited by the American Association for Accreditation of Laboratory Animal Care. Mice were given feed and acidified (pH 2.5) water freely. The animal holding room was maintained with conditioned fresh air that was changed at least 10 times per hour at approximately 21°C and 50% (±10%) relative humidity and with a 12-h light/dark full spectrum lighting cycle. All research was approved by the Institutional Animal Care and Use Committee.

Irradiation

Mice were placed in ventilated Plexiglas containers and exposed bilaterally to gamma radiation from the AFRRI ^{60}Co source, as previously described (26). Exposure time was adjusted so that each animal received a 7.0-Gy midline tissue-absorbed dose at a nominal dose rate of 0.4 Gy/min at ambient temperature. Using a standardized technique, the midline tissue dose rate was measured by placing a 0.5-cc tissue equivalent ionization chamber at the center of a 2.5-cm diameter cylindrical acrylic mouse phantom before irradiation of animals (27). The tissue-to-air ratio, defined as the ratio of the dose rate in free air to the dose rate measured in the phantom, for this array was 0.96. Variation within the exposure field was less than 4% (26). The lethal dose for 50% of B6D2F1/J female mice 30 days after exposure ($LD_{50/30}$) to this source was 9.6 ± 0.30 Gy.

BRMs

All BRMs were administered i.p. 1 h after irradiation as sterile solutions at dosages indicated in the results section. S-TDCM (Ribi ImmunoChem Research, Inc., Hamilton, MT) was prepared as an aqueous suspension by a modification of the procedure of Vosika and Gray (28), as described previously (23). Briefly, 2-mg aliquots of S-TDCM were solubilized in 0.2 ml of chloroform methanol (9:1), placed in a 5-ml Potter-Elvehjem tissue homogenizer, dried under nitrogen, and suspended with homogenization in TS to contain 400 μg/ml. Synthesis of S-TDCM was previously described (23, 29). Sm-BRM (generously provided by Dr. Catherine McCall, Cell Technology, Inc., Boulder, CO) contains two distinct particle classes, i.e., natural bacterial cell membrane vesicles and ribosomes derived from *Serratia marcescens* (31). Sterile distilled water was used to dilute 1000 μg of lyophilized Sm-BRM to a final concentration of 200 μg/ml. Sm-BRM was injected within 1 h of reconstitution. MPL (400 μg/ml) derived from *Salmonella enteritidis* ser. *typhimurium* (Ribi ImmunoChem Research, Inc.) and protein-free, phenol water-extracted LPS (50 μg/ml) from *Escherichia coli* K235 (kindly provided by Dr. Stephanie N. Vogel, Uniformed Services University of the Health Sciences, Bethesda, MD) were prepared as described previously (32).

Collection of tissues

Sterile technique was used throughout. Mice were deeply anesthesized with methoxyflurane (Pitman-Moore, Washington Crossing, NJ) before exsanguination by percutaneous cardiac puncture using a syringe rinsed with sodium heparin solution. Blood was transferred into a vial that contained ethylene diamine tetraacetate then placed immediately on ice and centrifuged within 1 h at 4°C. Separated plasma was then frozen at −70°C until assayed for CSF activity. Spleens were pressed through stainless steel mesh into 5 ml RPMI 1640 medium to disperse cells. Bone marrow cells were obtained by flushing both tibia with 1 ml of RPMI 1640 per tibia. A 500-μl aliquot of both cell suspensions was monodispersed by gentle pipetting, centrifuged, resuspended in RPMI 1640 supplemented with 10% FCS, and kept on ice until cultured for CFU-GM.

Table I. *Primer sequences for amplification of cytokine cDNA during PCR and probe sequences for detection of amplified DNA product on Southern blot*

Cytokine	Antisense and Sense Primer	Bases Spanned (size)	Probe	Bases Spanned	No. of PCR Cycles	Ref.
HPRT	GTTGGATACAGGCCAGACTTTGTTG GATTCAACTTGCGCTCATCTTAGGC	514–538 652–678 (164)	GTTGTTGGATATGCCCTTGAC	562–582	12	24
G-CSF	GAGCAAGTGAGGAAGATCCAG TTAGGCACTGTGTCTGCTGC	572–592 1072–78/ 1325–37 (172)	AGTTGTGTGCCACCTACA	618–22/ 971–83	29	63
M-CSF	ATTGGGAATGGACACCTGAAG GCTGTTGTTGCAGTTCTTGG	286–306 662–681 (396)	TTCCATGAGACTCCTCTC	571–588	21	64
IL-3	ACTGATGATGAAGGACC TTAGCACTGTCTCCAGATC	1000–1016 2485–2504 (256)	TCGGAGAGTAAACCTGTCCA	2030–2049	28	65
TNF-α	TTCTGTCTACTGAACTTCGGGG ACTTGGGCAGATTGACCTCAGC	955–976 2437–2458 (514)	CCCGACTACGTGCTCCTCACC	2248–2268	23	65
IL-6	TTCCATCCAGTTGCCTTCTTGG CTTCATGTACTCCAGGTAG	73–94 414–432 (359)	ACTTCACAAGTCCGGAGA	127–144	21	24
IL-1β	GGGATGATGATGATAACCTG TTGTCGTTGCTTGGTTCTCCT	397–416 572–592 (195)	GGCTCCGAGATGAACAACAA	454–473	14	66
SCF (c-*kit* ligand)	GATAACCCTCAACTATGTCGC TACTGCTGTCATTCCTAAGG	156–176 576–595 (439)	GAGGCCAGAAACTAGATCCT	384–403	25	67

The remainder of the splenocytes were promptly centrifuged, resuspended in 200 μl HBSS, homogenized 3 to 5 s in 1.5 ml RNAzol B (Cinna/Biotecx Laboratories International, Inc., Friendswood, TX) by using a tissue homogenizer, frozen in liquid nitrogen, and stored at −70°C until RNA extraction could be performed.

Culture of granulocyte-macrophage progenitor cells

Myeloid progenitors (CFU-GM) in the bone marrow and spleen were quantitated in soft agar using modifications of a previously described technique (31). Briefly, 1×10^5 nucleated bone marrow cells or 1×10^6 splenocytes were cultured in 1 ml of 0.3% agar-McCoy's 5a medium supplemented with 15% FCS and 100 μl of an Amicon-filtered human urine concentrate that served as a source of CSF. Cells were plated in 35-mm plastic culture dishes and incubated for 7 days in 6% CO_2 at 37°C. Colonies comprised of ≥50 cells were enumerated with a dissecting microscope, and data were expressed as CFU-GM per organ.

Bioassay for CSF in plasma

The presence of CSF activity in plasma was detected with modifications of a bioassay described previously (31). Briefly, twofold dilutions of pooled plasma were added to duplicate 35-mm tissue culture plates (final plasma concentrations were 2.5, 5, and 10%). Plasma samples were then covered with 1 ml of 0.3% agar in McCoy's 5a culture medium supplemented with 15% FCS that contained 1×10^5 nucleated tibial bone marrow cells harvested from nonirradiated B6D2F1/J mice. Cultures were incubated in 6% CO_2 at 37°C for 7 days and colonies were counted with a dissecting microscope. CSF activity, expressed as U/ml, was calculated as the product of the reciprocal of the sample dilution and the mean number of colonies per plate.

RT-PCR

RNase-free plastic ware, water, and surgical gloves were used throughout the procedure.

Isolation and purification of RNA. Total RNA was isolated using modifications of a one-step phenol guanidium isothiocyanate chloroform extraction technique (33). After 2-propanol precipitation and UV spectrophotometric quantitation for total cellular RNA, 5 μg of RNA was electrophoresed in a 2% formaldehyde agarose gel that contained ethidium bromide to ascertain whether the RNA was undegraded and accurately quantitated. With this technique, the final preparation was free of DNA and protein, with a 260:280-nm ratio >1.8.

RT reaction. RT of RNA was performed in a final volume of 25 μl using the technique described by Svetic et al. (24), which is a modification of that described by Diamond et al. (34). The final mixture was heated to 70°C for 5 min to denature the RNA and cooled on ice. Then, 1.2 μl of RT (200 U/ml) was added to the mixture, centrifuged to bring down any condensation, and incubated at 37°C for 60 min. The reaction was then heated at 90°C for 5 min then quickly chilled on ice.

PCR. Sense and antisense primers, specific for the desired cytokine, were added to the RT reaction product, along with PCR buffer, deoxynucleotide mixtures, and Taq polymerase (24). For each cytokine, the optimum number of cycles was determined by achieving a detectable concentration that was well below saturating conditions, as previously described (24). To further ensure that equal amounts of RNA were added to each PCR reaction, primers for a housekeeping gene, HPRT, were used to amplify the cDNA that was reverse transcribed from total RNA and probed in the same manner as the cytokines. Amplified product was identified by Southern blot analysis (35) and quantitated by densitometry with a PhosphorImager (Molecular Dynamics, Sunnyvale, CA), as previously described (24). The probes were specifically selected to hybridize to a portion of the amplified segment that was between the nucleotide sequences complementary to the primers to ensure identification of the amplified segment. Sequences for primers and probes for IL-6 and HPRT were as previously described (24). Sequences for HPRT, G-CSF, M-CSF, IL-3, TNF-α, IL-6, IL-1β, and the c-*kit* ligand, SCF, appear in Table I.

Bacteria

K. pneumoniae AFRRI 7 was prepared as previously described (36). Bacteria were injected s.c. into mice that were lightly anesthetized with methoxyflurane.

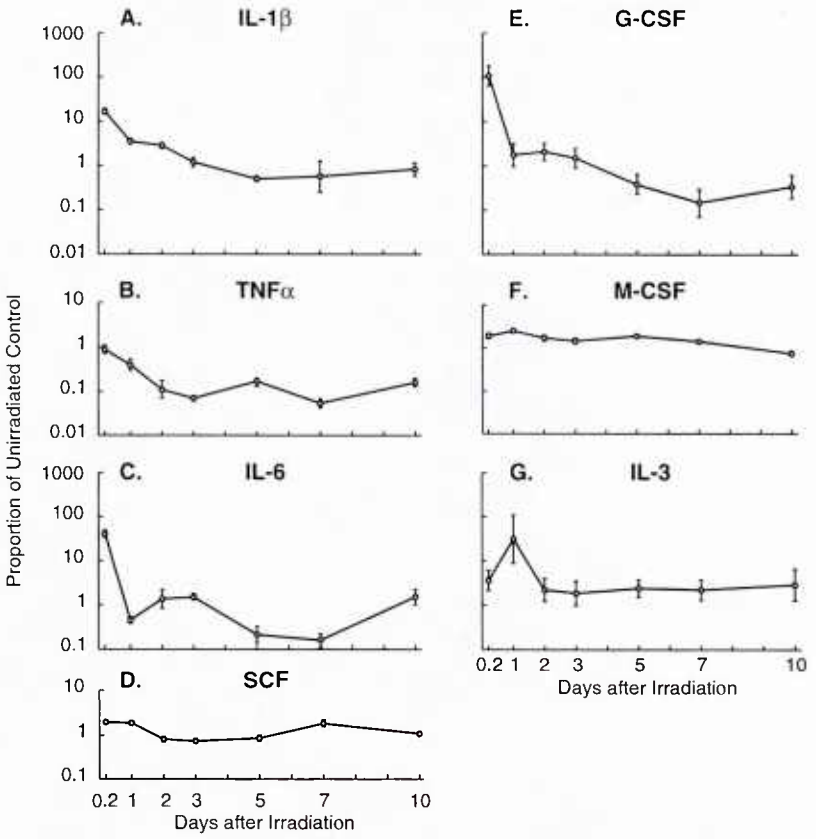

FIGURE 1. Effect of sublethal gamma-irradiation on kinetics of splenic cytokine gene expression determined by RT-PCR. One hour after gamma irradiation (7.0 Gy) groups of five mice received a single i.p. injection of TS and were killed at the times indicated. Splenic cytokine mRNA levels of IL-1β, IL-3, IL-6, TNF-α, G-CSF, M-CSF, and SCF are expressed as a proportional change relative to the respective cytokine mRNA levels in untreated, nonirradiated controls.

Survival measurement and statistical evaluation

Thirty-day survival among the various experimental groups of irradiated mice were compared with the generalized Savage (Mantel-Cox) procedure (Program 1L, BMD Statistical Software, Inc., Los Angeles, CA). When analyzing cytokine gene expression by RT-PCR, a log transform was made of the ratio of the corrected densities for cytokine mRNA measurements to the corrected densities for the housekeeping gene, HPRT. For each time period and treatment group (e.g., LPS, MPL, S-TDCM, Sm-BRM, and TS), the mean of these values was calculated and the mean of the log transformed ratio for untreated values was subtracted from these means. The antilog values of these differences were then plotted along with their standard error. A proportion of the nonirradiated control of "1" indicates that the value for a treated group equals the value for the untreated, unirradiated control group. In addition, a one-way analysis of variance was performed on the log transformed ratios at each time period to compare treatments. If the one-way analysis of variance was significant, then a Newman-Keul's test was conducted to determine where statistically significant differences among treatment groups existed. Unless stated otherwise, data are calculated as the mean ± SEM, and statistical significance is assumed for $p \leq 0.05$.

Results

Effects of irradiation on cytokine gene expression

Irradiation (i.e., irradiated mice injected with TS) was sufficient to induce an early (4 h after TS or 5 h after irradiation) increase in cytokine gene expression for IL-1β, IL-3, IL-6, and G-CSF but TNF-α, M-CSF, and SCF mRNA levels were unaltered compared with untreated, unirradiated control mice (Fig. 1). At 24 h after radiation, mRNA levels for all cytokines, except IL-3, had returned to baseline. Exposure to sublethal irradiation alone thus induces a transient expression of mRNA for IL-1β, IL-6, and G-CSF and a slightly more prolonged expression of mRNA encoding IL-3.

Effects of BRMs on cytokine gene expression after irradiation

The kinetics of cytokine gene expression of IL-1β, IL-3, IL-6, TNF-α, G-CSF, M-CSF, and SCF were monitored for 10 days beginning 4 h after a single i.p. injection of either 25 μg LPS, 200 μg MPL, 200 μg S-TDCM, 100 μg Sm-BRM, or 0.5 ml TS. Because the biologic responses were equivalent at the dosages of LPS and MPL used in this study, only data from LPS-injected mice are presented for cytokine gene expression after injection of these two BRMs. Initially, injection of BRMs tended to enhance and/or prolong cytokine gene expression but over time gene expression returned toward levels observed in irradiated mice injected with TS. For example, IL-1β mRNA levels 4 h after injection (i.e., 5 h after irradiation) were not increased by BRMs above the initial ≈15-fold increase seen in TS-injected, irradiated controls (Fig. 2*A*), but injection of S-TDCM or Sm-BRM maintained IL-1β gene expression above levels seen in TS-injected mice at day 2. Only an Sm-BRM injection prolonged IL-1β gene expression beyond day 2.

TNF-α gene expression was modestly enhanced (≈5-fold increase over irradiated controls) at 4 h after injection

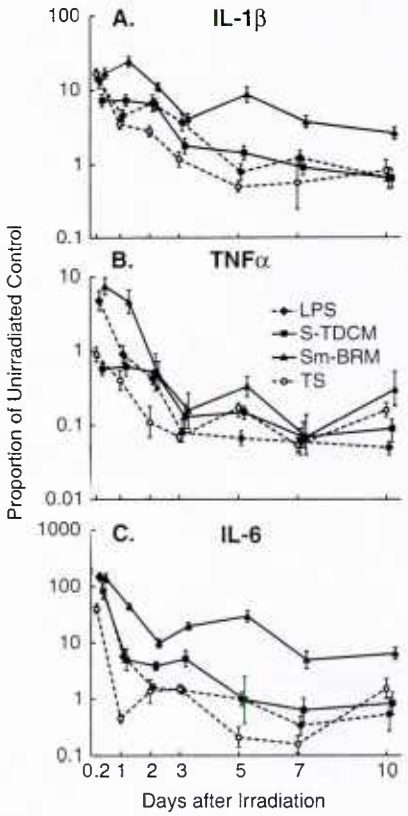

FIGURE 2. Comparative effects of a single i.p. injection of BRMs on gene expression for IL-1β, TNF-α, and IL-6 after sublethal gamma irradiation. One hour after irradiation, LPS, MPL, S-TDCM, Sm-BRM, or TS was injected into groups of five mice and splenic mRNA levels quantitated serially by RT-PCR for IL-1β (*A*), TNF-α (*B*), and IL-6 (*C*). Data are expressed as a proportional change relative to the respective cytokine mRNA levels in untreated, unirradiated controls. Cytokine gene expression for LPS and MPL are comparable and only data for LPS-injected mice are shown.

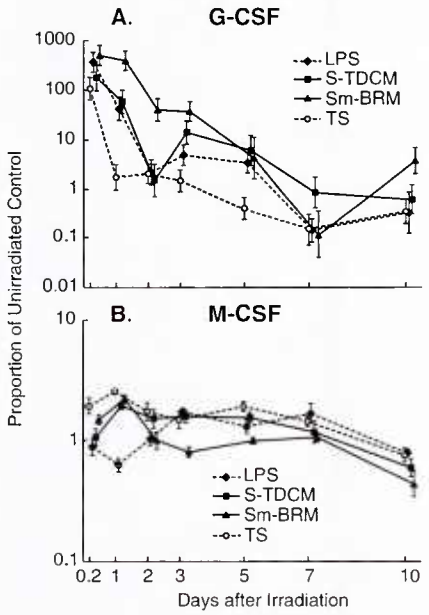

FIGURE 3. Comparative effects of a single i.p. injection of BRMs on gene expression for G-CSF and M-CSF after sublethal gamma irradiation. One hour after irradiation, LPS, MPL, S-TDCM, Sm-BRM, or TS was injected into groups of five mice and splenic mRNA levels quantitated serially by RT-PCR for G-CSF (*A*) and M-CSF (*B*). Data are expressed as a proportional change relative to the respective cytokine mRNA levels in untreated, unirradiated controls. Cytokine gene expression for LPS and MPL were comparable and only data for LPS-injected mice are shown.

of LPS and at both 4 and 24 h after injection of Sm-BRM (Fig. 2*B*). S-TDCM administration failed to induce expression of TNF-α mRNA at any time point after injection. Although irradiation resulted in an ≈40-fold increase in levels of IL-6 mRNA, injection of BRMs further enhanced IL-6 gene expression at 4 and 24 h after injection (Fig. 2*C*). Subsequently, only Sm-BRM or S-TDCM maintained levels of IL-6 gene expression above levels found in TS-injected, irradiated controls, and beyond day 3, only irradiated mice that received Sm-BRM continued to express high levels of IL-6 mRNA.

Levels of G-CSF mRNA were increased ≈100-fold 4 h after injection of TS but subsequent determinations found G-CSF mRNA levels equal to or below those observed in unirradiated controls (Fig. 3*A*). Administration of LPS or Sm-BRM amplified gene expression threefold and fourfold, respectively, above levels seen in TS-treated mice at 4 h but S-TDCM injection did not enhance G-CSF gene expression. However, injection of LPS, S-TDCM, or Sm-BRM was associated with enhanced levels of G-CSF mRNA at days 1, 3, and 5 after irradiation, although not to the levels observed in the Sm-BRM treatment group. In contrast, BRM administration failed to alter splenic gene expression of M-CSF at any time point after irradiation (Fig. 3*B*).

IL-3 and SCF genes were also expressed differentially in response to administration of BRMs (Fig. 4). IL-3 gene expression was markedly enhanced at 4 h and at days 1, 2, and 5 after injection of Sm-BRM compared with irradiated mice injected with TS (Fig. 4*A*). LPS, MPL, and S-TDCM did not augment IL-3 gene expression, and, similar to the pattern of gene expression observed for M-CSF, splenic mRNA levels of SCF were not enhanced at any time after irradiation by any of the BRMs evaluated in this study (Fig. 4*B*).

Effects of BRMs on plasma CSF activity

Irradiated mice that were given saline exhibited a minimal increase in plasma CSF activity (110 ± 30 U/ml) 5 h after irradiation but all subsequent plasma determinations for CSF activity were comparable to plasma CSF levels in unirradiated, untreated controls (i.e., ≤40 U/ml) (Fig. 5). Administration of BRMs resulted in an enhanced but transient plasma CSF response 4 h after injection. The CSF

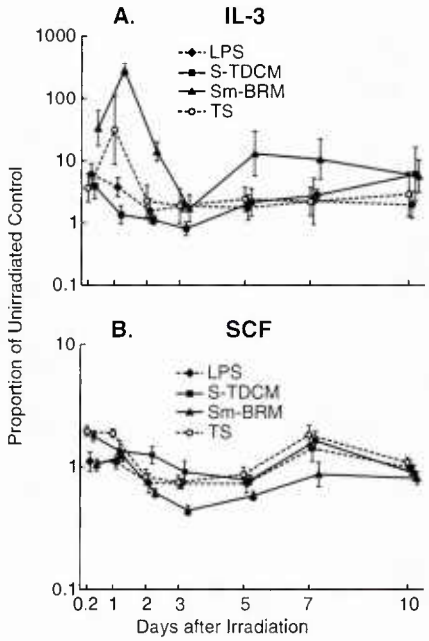

FIGURE 4. Comparative effects of a single i.p. injection of BRMs on gene expression of IL-3 and SCF after sublethal gamma irradiation. One hour after irradiation, LPS, MPL, S-TDCM, Sm-BRM, or TS was injected into groups of five mice and splenic mRNA levels quantitated serially by RT-PCR for IL-3 (*A*) and SCF (*B*). Data are expressed as a proportional change relative to the respective cytokine mRNA levels in untreated, unirradiated controls. Cytokine gene expression for LPS and MPL were comparable and only data for LPS-injected mice are shown.

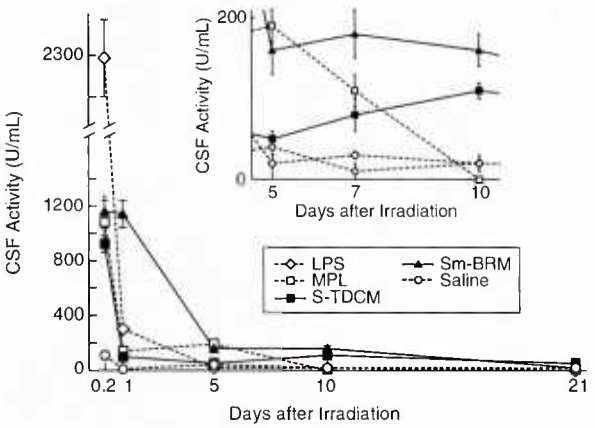

FIGURE 5. Comparative effects of BRMs on the plasma CSF response after sublethal gamma irradiation. One hour after irradiation, LPS, MPL, S-TDCM, Sm-BRM, or saline was injected into groups of three mice and plasma was collected at 4 h and on days 1, 2, 3, 5, 7, 10, 14 and 21 after irradiation. Serial dilutions of pooled plasma (three mice/pool) were assayed in triplicate for CSF activity, as outlined in the *Materials and Methods* section. Data represent one of two identical experiments with comparable results.

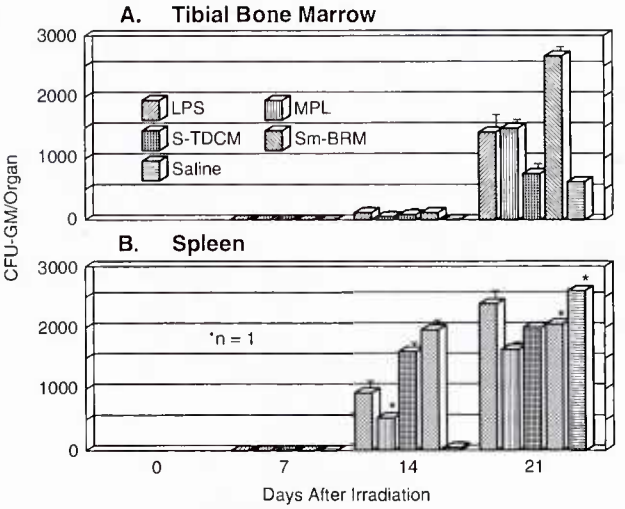

FIGURE 6. Comparative effects of BRMs on recovery of myeloid progenitors (CFU-GM) in bone marrow and spleen after sublethal gamma irradiation. One hour after irradiation, LPS, MPL, S-TDCM, Sm-BRM or saline was injected into groups of three mice and animals were killed at the times indicated. Pooled tibial bone marrows and spleens (three mice/pool) were assayed in triplicate to quantitate CFU-GM, as outlined in the *Materials and Methods* section.

response to LPS was approximately twice that observed after injection of MPL, S-TDCM, or Sm-BRM and ≈15-fold above levels found in irradiated mice injected with TS. However, plasma CSF levels in LPS-treated mice declined to levels seen in irradiated controls 5 days after irradiation. Plasma CSF levels in irradiated mice injected with MPL or S-TDCM also fell rapidly but remained higher than CSF levels seen in mice injected with LPS or TS. In contrast, irradiated mice injected with Sm-BRM experienced a rise in plasma levels of CSF activity that was sustained for 24 h before declining. Measureable plasma CSF activity beyond day 7 was observed only in irradiated mice treated with Sm-BRM and S-TDCM. This late advantage in the plasma CSF response to Sm-BRM and S-TDCM is depicted in the insert in Figure 5.

Effects of BRMs on myeloid progenitors after radiation

Late myeloid progenitors (CFU-GM) in bone marrow and spleen were undetectable in all treatment groups at day 7 after irradiation (Fig. 6). However, CFU-GM appeared in both the bone marrow and spleen in all BRM treatment groups but not irradiated controls by day 14 after irradiation. CFU-GMs were not detected in bone marrow or spleen of TS-treated, irradiated mice until day 21. At day 14, splenic CFU-GM were ≈2-fold greater in mice treated with S-TDCM and Sm-BRM compared with LPS and MPL treatment groups. Compared with all other treatment groups, bone marrow CFU-GM were ≈1.5-fold higher in Sm-BRM-treated mice at day 21.

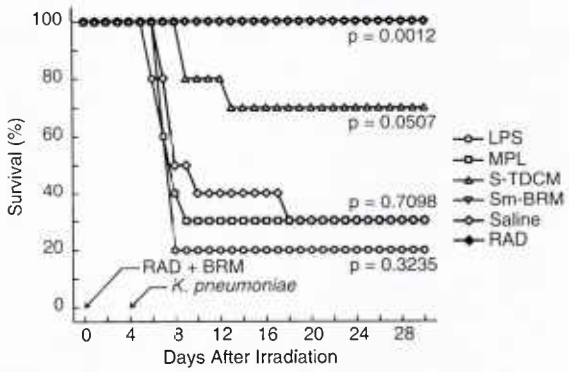

FIGURE 7. Comparative effects of BRMs on 30-day survival in sublethally gamma irradiated mice inoculated with *K. pneumoniae*. One hour after irradiation, LPS, MPL, S-TDCM, Sm-BRM, or saline was injected into groups of 10 mice and 4 days later mice were given a subcutaneous inoculation of 6.1×10^2 CFU (2 $LD_{50/30}$). Survival in each experimental group was noted daily for 30 days after irradiation.

Effects of BRMs on survival in irradiated mice challenged with K. pneumoniae

To determine whether the differences that were observed in cytokine gene expression, plasma CSF levels, or mycloid progenitor recovery among experimental groups altered survival in response to sepsis, BRMs were used in an experimental infection model in irradiated mice. One hour after irradiation, groups of 10 mice received a single i.p. injection of a BRM or TS. Four days later, mice received a s.c. inoculation of either saline or 6.1×10^2 CFU (2 $LD_{50/30}$) of a washed suspension of *K. pneumoniae*. Survival was assessed for 30 days and *K. pneumoniae* was isolated from heart blood of dead mice to confirm the cause of infection. The resulting survival curves, depicted in Figure 7, revealed that all mice treated with Sm-BRM survived. Mice that were treated with S-TDCM suffered no mortality until the 5th day after bacterial challenge, and the 30-day survival was 70%. In contrast, ≤30% of irradiated mice that were injected with saline, LPS, or MPL survived infection. The majority of mortalities in these experimental groups occurred within 7 days of bacterial challenge.

Discussion

Our data demonstrated a rapid, transient increase in endogenous splenic gene expression of IL-1β, IL-3, IL-6, and G-CSF in response to sublethal irradiation. The cytokine gene response observed in splenic tissue in our in vivo model appeared to be specific because gene expression of TNF-α, SCF, and M-CSF was not amplified after irradiation. The data also indicated that expression of cytokine genes could be differentially enhanced and prolonged, depending on the BRM used. Although LPS and MPL elicited abbreviated splenic cytokine gene responses and transient increases in plasma CSF activity, both S-TDCM and Sm-BRM elicited more prolonged gene responses and an early and late increase in plasma CSF activity. In addition, prolonged expression of multiple cytokine genes, such as that seen after a single injection of S-TDCM or Sm-BRM, was associated with superior protection against experimental infection.

No previous in vivo studies to our knowledge have provided direct evidence of endogenous cytokine gene expression after irradiation but several in vivo studies have provided indirect evidence that reconstitution of medullary and extramedullary hematopoiesis after sublethal irradiation is mediated by hematoregulatory cytokines (3, 4, 6, 8, 36, 37). Neta and Oppenheim (6) reported that a single i.p. injection of IL-1 1 to 3 h after lethal irradiation improved survival in a dose-dependent fashion in mice, presumably due to known myelopoietic effects of IL-1 (38–40). Administration of IL-3, IL-6, G-CSF, and GM-CSF has also hastened myelorestoration after irradiation by enhancing proliferation of myeloid progenitors (6, 41–45).

Irradiation did not induce increased expression of TNF-α, SCF, and M-CSF genes. The absence of splenic expression of these cytokines may be a reflection of the specificity of the cytokine gene response to sublethal irradiation. Alternatively, an apparent lack of expression of these genes may have resulted from tight gene regulation and by waiting 5 h after irradiation to sample spleens transient early gene expression may have been missed. Evidence for this possiblity has been found in cell culture studies in which ionizing radiation induced transient gene expression of TNF-α and IL-1 that returned to baseline within 6 h (46, 47). Several in vivo studies have provided indirect evidence that endogenous expression of TNF-α, SCF, and M-CSF is induced after irradiation and is important for survival. Therapeutic administration of TNF-α improved survival in lethally irradiated mice and injection of an Ab that is specific for TNF-α before irradiation decreased survival (6, 12). Chronic administration of recombinant canine SCF restored bone marrow hematopoiesis and enhanced recovery of circulating neutrophils in lethally irradiated dogs (10) and injection of an Ab specific for SCF before radiation decreased survival in mice (14). Similar studies with Abs specific for M-CSF have not been reported, but administration of M-CSF accelerated hematopoietic regeneration after bone marrow ablation in mice (48). Therefore, it is possible that expression of genes for TNF-α, SCF, and M-CSF occurred after irradiation in our murine model but probably took place in extrasplenic tissues, such as endothelium, bone marrow stroma, or skin (16, 49–51).

The mechanisms responsible for prolonged cytokine gene expression in sublethally irradiated mice injected with S-TDCM or Sm-BRM are unknown but the manner in which macrophages ingest and subsequently degrade S-TDCM and Sm-BRM may explain the protracted cytokine gene response (31, 52, 53). The superior ability of

Sm-BRM to protect septic mice may represent synergistic effects of LPS and non-LPS-related components of Sm-BRM. Ribi et al. (54) showed that a combination of MPL and S-TDCM was superior to either BRM alone in improving survival to *Salmonella enteritidis* infection. It is possible that Sm-BRM, by providing both LPS and non-LPS components of the bacterial cell wall, ensured a similar synergistic advantage in our study.

The ranked order of the ability of BRMs to induce and sustain cytokine gene expression (Sm-BRM > S-TDCM > LPS ≈ MPL ≈ TS) paralleled the ability of each group to survive infection. This relationship was most pronounced for IL-6 gene expression. IL-6 has been shown to improve survival after a septic challenge by decreasing overexpression of IL-1 and TNF-α, increasing a protective hepatic acute phase protein response, and augmenting adrenocortical responsiveness (13, 49–51). In addition, all BRMs induced an early plasma CSF response and an accelerated appearance of CFU-GM in bone marrow and spleen. Enhanced gene expression of IL-3 was observed in Sm-BRM-treated, irradiated mice and may have been partly responsible for the late increase in plasma CSF levels and improved survival to infection. IL-3 synergizes with M-CSF in vitro to enhance myeloproliferation and prevents apoptosis by reducing the rate of DNA cleavage during a G_2 arrest point, which occurs in the first few hours after radiation (55, 56).

Although BRMs may have been present in plasma samples that were assayed for CSF activity, it is unlikely that a carryover of BRMs was responsible for the measured CSF activity. In our hands, spiking plasma samples with BRMs before bioassay does not increase colony formation (i.e., CSF activity). Comparable plasma CSF responses have been noted by other investigators in normal and irradiated mice injected with LPS (16, 31, 57, 58). The importance of this prolonged, endogenous expression of CSFs in mice injected with S-TDCM and Sm-BRM in this study is suggested by earlier studies that reported that chronic administration of hematoregulatory cytokines accelerated bone marrow recovery and improved survival after myeloablative therapy (8, 9, 43, 59–61).

Bone marrow and splenic proliferation of CFU-GM were absent in all treatment groups at day 7 after irradiation, and no correlation between the absolute number of CFU-GM and postinfection survival at day 7 was evident. Other studies have documented the absence of myeloid progenitors and circulating neutrophils 7 days after irradiation, even after therapy with hematopoietic cytokines (8, 9, 43). The lack of correlation between the number of myeloid progenitors found in the bone marrow and host survival after irradiation has been noted by others (17, 55, 58, 62).

On balance it appears that sublethal irradiation induces limited splenic cytokine gene expression that can be expanded, amplified, and prolonged by a single i.p. injection of BRM 1 h after irradiation. Kinetics of the BRM-associated cytokine gene response to radiation depends on the particular BRM used. LPS and MPL elicit an abbreviated cytokine gene expression and initiate prompt but transient increases in plasma CSF activity. S-TDCM and Sm-BRM elicit similar early responses but the responses tend to be more prolonged. The ability of irradiated mice to withstand a septic challenge appears to depend on the amplitude and duration of cytokine gene expression and the genes that are expressed. Induction of a broad-based cytokine response after sublethal irradiation, such as that seen after a single injection of S-TDCM or Sm-BRM, is associated with the best protection against septic mortality. Additional studies need to be performed to determine whether these BRMs are efficacious in the setting of lethal gamma irradiation, with and without superimposed infection.

Acknowledgments

We are grateful for the excellent technical assistance provided by Patricia L. Henderson and Christine H. Rundus.

References

1. Gale, R. P. 1987. Immediate medical consequences of nuclear accidents. *JAMA 258:625.*
2. Bodey, G. P., M. Buckley, Y. S. Sathe, and E. J. Freireich. 1965. Quantitative relationship between circulating leukocytes and infections in patients with acute leukemia. *Ann. Intern. Med. 64:328.*
3. Metcalf, D. 1991. Control of granulocytes and macrophages: molecular, cellular, and clinical aspects. *Science 254:529.*
4. Moore, M. A. S. 1991. Clinical implications of positive and negative hematopoietic stem cell regulators. *Blood 78:1.*
5. Neta, R., J. J. Oppenheim, and S. D. Douches. 1988. Interdependence of the radioprotective effects of human recombinant interleukin-1α, tumor necrosis factor-α, granulocyte colony-stimulating factor, and murine recombinant granulocyte-macrophage colony-stimulating factor. *J. Immunol. 140:108.*
6. Neta, R., and J. J. Oppenheim. 1988. Cytokines in therapy of radiation injury. *Blood 72:1093.*
7. Talmadge, J. E., H. Tribble, R. Pennington, O. Bowersox, M. A. Schneider, P. Castelli, P. L. Black, and F. Abe. 1989. Protective, restorative, and therapeutic properties of recombinant colony-stimulating factors. *Blood 73:2093.*
8. Patchen, M. L., T. J. MacVittie, B. D. Solberg, and L. M. Souza. 1990. Survival enhancement and hemopoietic regeneration following radiation exposure: therapeutic approach using glucan and granulocyte colony-stimulating factor. *Exp. Hematol. 18:1042.*
9. Patchen, M. L., R. Fischer, and T. J. MacVittie. 1993. Effects of combined administration of interleukin-6 and granulocyte colony-stimulating factor on recovery from radiation-induced hemopoietic aplasia. *Exp. Hematol. 21:338.*
10. Schuening, F. G., F. R. Appelbaum, H. J. Deeg, M. Sullivan-Pepe, T. C. Graham, R. Hackman, K. M. Zsebo, and R. Storb. 1993. Effects of recombinant canine stem cell factor, a c-*kit* ligand, and recombinant granulocyte colony-stimulating factor on hematopoietic recovery after otherwise lethal total body irradiation. *Blood 81:20.*
11. Neta, R., S. N. Vogel, J. M. Plocinski, N. S. Tare, W. Benjamin, R. Chizzonite, and M. Pilcher. 1990. In vivo modulation with anti-interleukin-1 (IL-1) receptor (p80) antibody 35F5 of the response to IL-1: the relationship of radioprotection, colony-stimulating factor, and IL-6. *Blood 76:57.*
12. Neta, R., J. J. Oppenheim, R. D. Schreiber, R. Chizzonite, G. D. Ledney, and T. J. MacVittie. 1991. Role of cytokines (interleukin 1, tumor necrosis factor, and transforming growth factor b) in natural

and lipopolysaccaride-enhanced radioresistance. *J. Exp. Med. 173: 1177.*

13. Neta R., R. Perlstein, S. N. Vogel, G. D. Ledney, and J. Abrams. 1992. Role of IL 6 in protection from lethal irradiation and in endocrine responses to IL 1 and TNF. *J. Exp. Med. 175:689.*
14. Neta, R., D. Williams, F. Selzer, and J. Abrams. 1993. Inhibition of c-*kit* ligand/steel factor by antibodies reduces survival of lethally irradiated mice. *Blood 81:324.*
15. Broxmeyer, H. E. 1992. Combination cytokine therapy or a compound that may indirectly mimic such effects by stimulating production of multiple cytokines? *Exp. Hematol. 20:149.*
16. Vogel, S. N., and M. M. Hogan. 1990. Role of cytokines in endotoxin-mediated host responses. In *Immunophysiology: The Role of Cells and Cytokines in Immunity and Inflammation.* J. J. Oppenheim and E. M. Shevach, eds. Oxford University Press, New York, pp. 238–258.
17. Ainsworth, E. J. 1988. From endotoxins to newer immunomodulators: survival-promoting effects of microbial polysaccharide complexes in irradiated animals. *Pharmacol. Ther. 39:223.*
18. Smith, W. W., I. M. Alderman, and R. E. Gillespie. 1957. Increased survival in irradiated animals treated with bacterial endotoxins. *Am. J. Physiol. 191:124.*
19. Richardson, R. P., C. D. Rhyne, Y. Fong, D. G. Hesse, K. J. Tracey, M. A. Marano, S. F. Lowrey, A. C. Antonacci, and S. E. Calvano. 1989. Peripheral blood leukocyte kinetics following in vivo lipopolysaccharide (LPS) administration to normal human subjects: influence of elicited hormones and cytokines. *Ann. Surg. 210:239.*
20. Hesse, D. G., K. J. Tracey, Y. Fong, K. R. Manogue, M. A. Palladino, A. Cerami, G. T. Shires, and S. F. Lowry. 1988. Cytokine appearance in human endotoxemia and primate bacteremia. *Surg. Gynecol. Obstet. 166:147.*
21. Ribi, E. 1984. Beneficial modification of the endotoxin molecule. *J. Biol. Response Mod. 3:1.*
22. Henricson, B., W. R. Benjamin, and S. N. Vogel. 1990. Differential cytokine induction by doses of lipopolysaccharide and monophosphoryl lipid A that result in equivalent early endotoxin tolerance. *Infect. Immun. 58:2429.*
23. Madonna, G. S., G. D. Ledney, D. C. Funckes, and E. E. Ribi. 1988. Monophosphoryl lipid A and trehalose dimycolate therapy enhances survival in sublethally irradiated mice challenged with *Klebsiella pneumoniae.* In *Immunomodulators and Nonspecific Host Defense Mechanisms Against Microbial Infections.* K. Masihi and W. Lange, eds. Pergamon Press, Oxford, UK, p. 351–356.
24. Svetić, A., F. D. Finkelman, C. W. Dieffenbach, D. E. Scott, A. D. Steinberg, and W. C. Gause. 1991. Cytokine gene expression after in vivo primary immunization with goat antibody to mouse IgD antibody. *J. Immunol. 147:2391.*
25. Rappolee, D. A., A. Wang, D. Mark, and Z. Werb. 1989. Novel method for studying mRNA phenotypes in single or small numbers of cells. *J. Cell. Biochem. 39:1.*
26. Stewart, D. A., G. D. Ledney, W. H. Baker, E. G. Daxon, and P. A. Sheehy. 1982. Bone marrow transplantation of mice exposed to a modified fission neutron (N/G-30:1) field. *Radiat. Res. 92:268.*
27. Task Group 21, Radiation Therapy Committee, American Association of Physicists in Medicine, AAPM Task Group 21. 1983. A protocol for the determination of absorbed dose from high-energy photon and electron beams. *Med. Phys. 10:741.*
28. Vosika, G. J., and G. R. Gray. 1983. Phase 1 study of IV mycobacteria cell wall skeleton and cell wall skeleton combined with trehalose dimycolate. *Cancer Treatment Rep. 67:785.*
29. Madonna, G. S., G. D. Ledney, M. M. Moore, T. B. Elliott, and I. Brook. 1991. Treatment of mice with sepsis following irradiation and trauma with antibiotics and synthetic trehalose dicorynomycolate (S-TDCM). *J. Trauma 31:316.*
30. Kierszenbaum, F., A. Zenian, and J. J. Wirth. 1984. Macrophage activation by cord factor (trehalose 6, 6-dimycolate): enhanced association with and intracellular killing of *Trypanosoma cruzi. Infect. Immun. 43:531.*
31. Peterson, V. M., C. H. Rundus, P. J. Reinoehl, S. R. Schroeter, C. A. McCall, and E. J. Bartle. 1992. The myelopoietic effects of a *Serratia marcescens*-derived biologic response modifier in a mouse model of thermal injury. *Surgery 111:447.*
32. Madonna, G. S., J. E. Peterson, E. E. Ribi, and S. N. Vogel. 1986. Early-phase endotoxin tolerance: induction by a detoxified lipid A derivative, monophosphoryl lipid A. *Infect. Immun. 52:6.*
33. Chomczynski, P., and N. Sacchi. 1987. Single-step method of RNA isolation by acid guanidium thiocyanate-phenol-chloroform extractions. *Anal. Biochem. 162:156.*
34. Diamond, S. L., J. B. Sharefkin, C. Dieffenbach, K. Frasier-Scott, L. V. McIntire and S. G. Eskin. 1990. Tissue plasminogen activator mRNA levels increase in cultured human endothelial cells exposed to laminar sheer stress. *J. Cell. Physiol. 143:364.*
35. Sambrook, J., E. F. Fritsch, and T. Maniatis. 1989. *Molecular Cloning: A Laboratory Manual*, Cold Spring Harbor Laboratory Press, Cold Spring Harbor, NY.
36. Madonna, G. S., G. D. Ledney, T. B. Elliott, I. Brook, J. T. Ulrich, K. R. Myers, M. L. Patchen, and R. I. Walker. 1989. Trehalose dimycolate enhances resistance to infection in neutropenic animals. *Infect. Immun. 57:2495.*
37. Elliott, T. B., I. Brook, and S. M. Stiefel. 1990. Quantitative study of wound infection in irradiated mice. *Int. J. Radiat. Biol. 58:341.*
38. Neta, R., M. B. Stein, J. J. Oppenheim, S. Gillis, and S. D. Douches. 1987. The in vivo effects of interleukin-1. I. Bone marrow cells are induced to cycle after administration of interleukin 1. *J. Immunol. 139:1861.*
39. Dinarello, C. A. 1991. Interleukin-1 and interleukin-1 antagonism. *Blood 77:1627.*
40. Hestdal, K., S. E. W. Jacobsen, F. W. Ruscetti, C. M. Dubois, D. L. Longo, R. Chizzonite, J. J. Oppenheim, and J. R. Keller. 1992. In vivo effect of interleukin-1α on hematopoiesis: role of colony-stimulating factor receptor modulation. *Blood 80:2486.*
41. Okano, A., C. Suzuki, F. Takatsuki, Y. Akiyama, K. Koike, K. Ozawa, T. Hirano, T. Kishimoto, T. Nakahata, and S. Asano. 1989. In vitro expansion of the murine pluripotent hematopoietic stem cell population in response to interleukin 3 and interleukin 6: application to bone marrow transplantation. *Transplantation 48:495.*
42. Okano, A., C. Suzuki, F. Takatsuki, Y. Akiyama, K. Koike, T. Nakahata, T. Hirano, T. Kishimoto, K. Ozawa, and S. Asano. 1989. Effects of interleukin-6 on hematopoiesis in bone marrow-transplanted mice. *Transplantation 47:738.*
43. Patchen, M. L., T. J. MacVittie, J. L. Williams, G. N. Schwartz, and L. M. Souza. 1991. Administration of interleukin-6 stimulates multilineage hematopoiesis and accelerates recovery from radiation-induced hematopoietic depression. *Blood 77:472.*
44. Tanikawa, S., I. Nakao, K. Tsuncoka, and N. Nara. 1989. Effects of recombinant granulocyte colony-stimulating factor (rG-CSF) and recombinant granulocyte-macrophage colony-stimulating factor (rGM-CSF) on acute radiation hemopoietic injury in mice. *Exp. Hematol. 17:883.*
45. Patchen, M. L., T. J. MacVittie, B. D. Solberg, and L. M. Souza. 1990. Therapeutic administration of recombinant human granulocyte colony-stimulating factor accelerates hematopoietic regeneration and enhances survival in a murine model of radiation-induced myelosuppression. *Int. J. Cell. Cloning 8:107.*
46. Hallahan, D. E., D. R. Spriggs, M. A. Beckett, D. W. Kufeand, and R. R. Weickselbaum. 1989. Increased tumor necrosis factor α mRNA after cellular exposure to ionizing radiation. *Proc. Natl. Acad. Sci. USA 86:10102.*
47. Woloschak, G. E., C. M. Chang-Liu, P. S. Jones, and C. A. Jones. 1990. Modulation of gene expression in Syrian hamster embryo cells following ionizing radiation. *Cancer Res. 50:339.*
48. Broxmeyer, H. E., D. E. Williams, S. Cooper, A. Waheed, and R. K. Shadduck. 1987. The influence of in vivo murine colony-stimulating factor-1 in myeloid progenitor cells in mice recovering from sublethal doses of cyclophosphamide. *Blood 69:913.*
49. Oppenheim, J. J., F. W. Ruscetti, and C. Faltynek. 1991. Cytokines. In *Basic and Clinical Immunology*, 7th Ed. D. P. Stites and A. I. Terr, eds. Appelton and Lange, East Norwalk, CT, pp. 78–100.
50. Bass, B., and S. Beckner. 1991. Role of lymphokines and cytokines in bone marrow stem cell differentiation. *Focus 12:90.*

51. Arai, K., F. Lee, A. Miyajima, S. Miyatake, N. Arai, and T. Yokota. 1990. Cytokines: coordinators of immune and inflammatory responses. *Annu. Rev. Biochem. 59:783.*

52. Allen, P. M. 1987. Antigen processing at the moleeular level. *Immunol. Today 8:270.*

53. Yarkoni, E., L. Wang, and A. Bekierkunst. 1977. Stimulation of macrophages by cord faetor and by heat-killed and living BCG. *Infect. Immun. 16:1.*

54. Ribi, E., J. T. Ulrich, and K. N. Masihi. 1987. Immunopotentiating activities of monophosphoryl lipid A. In *Immunopharmacology of Infectious Diseases: Vaccine Adjuvants and Modulators of Nonspecific Resistance.* J. Majde, ed. Alan R. Liss, Inc., New York. pp. 101–112.

55. Williams, D. E., G. Hangoc, S. Cooper, H. S. Boswell, R. K. Shadduek, S. Gillis, A. Waheed, D. Urdal, and H. E. Broxmeyer. 1987. The effeets of purified reeombinant murine interleukin-3 and/or purified natural murine CSF-1 in vivo on the proliferation of murine high- and low-proliferative potential eolony-forming eells: demonstration of in vivo synergism. *Blood 70:401.*

56. Collins, M. K. L., J. Marvel, P. Malde, and A. Lopez-Rivas. 1992. Interleukin 3 protects murine bone marrow eells from apoptosis indueed by DNA damaging agents. *J. Exp. Med. 176:1043.*

57. Quesenberry, P. J., A. Morley, F. Stohlman, Jr., K. Riekard, D. Howard and M. Smith. 1972. Effect of endotoxin on granulopoiesis and eolony-stimulating faetor. *N. Engl. J. Med. 286:227.*

58. Shadduek, R. K. 1974. CSF response to endotoxin in normal and leukopenic recipients. *Exp. Hematol. 2:147.*

59. Neta, R., J. J. Oppenheim, S. D. Douehes, P. C. Giclas, R. J. Imbro, and M. Karin. 1986. Radioprotection with IL-1. Comparison with other eytokines. *Prog. Immunol. 5:900.*

60. Kindler V., B. Thorens, S. De Kossodo, B. Allet, J. F. Eliason, D. Thaeher, N. Farber, and P. Vassalli. 1986. Stimulation of hematopoiesis in vivo by reeombinant baeterial murine interleukin 3. *Proc. Natl. Acad. Sci. USA 83:1001.*

61. Monroy, R. I., R. R. Skelly, T. J. MaeVittie, T. A. Davis, J. J. Sauber, S. C. Clark, and R. E. Donahue. 1987. The effeet of reeombinant GM-CSF on the reeovery of monkeys transplanted with autologous bone marrow. *Blood 70:1696.*

62. Sehwartz, G. N., M. L. Patehen, R. Neta and T. J. MaeVittie. 1989. Radioproteetion of mice with interleukin-1: relationship to the number of spleen colony-forming units. *Rad. Res. 119:101.*

63. Tsuehiya, M., S. Asano, Y. Kaziro, and S. Nagata. 1986. Isolation and eharacterization of the eDNA for murine granuloeyte colony-stimulating faetor. *Proc. Natl. Acad. Sci. USA 83:7633.*

64. Ladner, M. B., G. A. Martin, J. A. Noble, V. P. Wittman, M. K. Warren, M. MeGrogan, and E. R. Stanley. 1988. eDNA eloning and expression of murine maerophage colony stimulating faetor from L929 eells. *Proc. Natl. Acad. Sci. USA 85:6706.*

65. Morris, S. C., K. B. Madden, J. J. Adamoviez, W. C. Gause, B. R. Hubbard, M. K. Gately, and F. D. Finkelman. 1994. Effeets of IL-12 on in vivo eytokine gene expression and Ig isotype selection. *J. Immunol. 152:1047.*

66. Gray, P. D., D. Glaister, E. Chen, D. V. Goeddel, and D. Penniea. 1986. Two interleukin 1 genes in the mouse: eloning and expression of the eDNA for murine interleukin 1β. *J. Immunol. 137:3644.*

67. Zsebo, K. M., D. A. Williams, E. N. Geisser, V. C. Broudy, F. H. Martin, H. L. Atkins, R. Y. Hsu, N. C. Burkitt, K. H. Okino, D. C. Murdoek, F. W. Jaeobsen, K. E. Langley, K. A. Smith, T. Takeishi, B. M. Cattanaeh, S. J. Galli, and S. V. Suggs. 1990. Stem eell faetor is eneoded at the Sl loeus of the mouse and is the ligand for the e-*kit* tyrosine kinase reeeptor. *Cell 63:213.*

CLINICAL AND DIAGNOSTIC LABORATORY IMMUNOLOGY, Sept. 1994, p. 493–499 Vol. 1, No. 5
1071-412X/94/$04.00+0

Identification of Antigens of Pathogenic Free-Living Amoebae by Protein Immunoblotting with Rabbit Immune and Human Sera

ERIC L. POWELL,[1] ANTHONY L. NEWSOME,[1]† STEPHEN D. ALLEN,[1]*
AND GREGORY B. KNUDSON[2]

Department of Pathology, Indiana University School of Medicine, Indianapolis, Indiana 46202,[1] and Armed Forces Radiobiology Institute, Bethesda, Maryland 20889[2]

Received 21 December 1993/Returned for modification 9 February 1994/Accepted 11 May 1994

Prominent antigens of pathogenic and nonpathogenic free-living amoebae were identified by using polyclonal rabbit immune sera in immunoblot assays. The intent was to determine if prominent epitopes identified with rabbit immune sera could also be recognized by human sera. With rabbit sera, the development of immunoreactive bands was restricted to molecular masses of greater than 18.5 kDa for *Naegleria*, *Hartmannella*, and *Vahlkampfia* antigens. Two or more broad bands of less than 18.5 kDa were prominent features in three different *Acanthamoeba* species. Few cross-reactive antibodies could be detected between representative species of the three different subgroups of *Acanthamoeba*. *Naegleria* antigen was likewise serologically distinct, as were *Hartmannella* and *Vahlkampfia* antigens. The relative lack of cross-reacting antibodies between the pathogenic amoebae suggested that it would be desirable to use a panel of amoebic antigens to represent the range of serologically distinct antigens for assessing reactive antibodies in human sera. In pooled human serum (10 serum specimens per pool), the appearance of minimally reactive bands ranging from 32.5 to 106 kDa was a common feature of all six antigens. A prominent band of less than 18.5 kDa was identified in the *Acanthamoeba culbertsoni* antigen lane in 2 of the 10 human serum specimen pools. When the sera from each of the two groups were tested individually by immunoblotting, the reaction with the *A. culbertsoni* antigen could be associated with one individual. By using a panel of amoebic antigens, this method could prove useful in recognizing undiagnosed amoebic infections by revealing specific reactive antibodies.

The genera *Acanthamoeba* and *Naegleria* include species of free-living soil and water amoebae that are widespread in the environment and that have the potential to produce life-threatening illness. To date, the pathogenic potentials of certain species within these genera have been adeptly demonstrated in laboratory animals and have occasionally been observed in humans (6, 12, 13, 27). In humans, *Naegleria fowleri* amoebic meningoencephalitis is associated with intranasal instillation of amoebae during swimming. The amoebae subsequently penetrate the central nervous system via the olfactory nerves. *Acanthamoeba* species may also produce meningoencephalitis, but the illness in humans may be more chronic, with resulting granuloma formation. Although the A-1 strain of *Acanthamoeba culbertsoni* invades the central nervous systems of experimental animals by first penetrating the nasal mucosa and then spreading to the brain via the olfactory nerves, *Acanthamoeba* species may also spread to the lower respiratory tract and other sites hematogenously. *Acanthamoeba* species can also infect the cornea (*Acanthamoeba* keratitis), and this disease is often associated with contact lens wear (12, 15). Studies with immune sera from laboratory rabbits demonstrated that the species of *Acanthamoeba* share some common antigens, but they can be subdivided into distinct serogroups (5, 16, 24). In addition, species of the genus *Naegleria* share common antigens but also have distinct epitopes, as demonstrated by using the Western blot (immunoblot) methodology (14). *Naegleria* immune serum does not cross-react with *Acanthamoeba* antigen (12).

The purpose of the investigation described here was to identify prominent epitopes of certain pathogenic and nonpathogenic free-living amoebae by using rabbit immune sera and the Western blot methodology. Subsequently, human sera from patients and apparently healthy individuals were screened by immunoblotting for antibodies reactive with amoebic antigens. The majority of the human serum specimens screened were obtained from Army recruits who suffered from acute respiratory disease (ARD). Viral agents such as adenovirus or influenza virus as well as *Mycoplasma pneumoniae* have previously been identified as occasional causative agents of ARD in Army recruits (8, 26). Despite attempts at isolation and serological surveillance programs, the etiologic agent in many cases of ARD has remained unidentified. A logical extension of these studies would be attempts to associate with ARD other potentially infectious agents such as amoebae.

Amoebae have repeatedly been cultivated from the upper respiratory tracts of humans in different surveys. The incidence of amoebae in upper respiratory tract samples has ranged from less than 1% to as high as 24% (1, 4, 11, 25). It has not been clearly determined whether the occurrence of amoebae represents the outgrowth of transient cysts that were inadvertently trapped in the respiratory tract or if the amoebae were in the active motile trophozoite form in vivo. Amoebae have been observed in the lung tissues of laboratory animals which have been experimentally infected intranasally. The possibility exists that amoebae also could cause lower respiratory tract disease in humans.

It was the intention of our study to determine if the

* Corresponding author. Mailing address: Department of Pathology, Indiana University School of Medicine, 4587 University Hospital, 550 North University Blvd., Indianapolis, IN 46202-5113. Phone: (317) 274-2557.

† Present address: Department of Biology, Middle Tennessee State University, Murfreesboro, TN 37132.

prominent amoebic epitopes identified by using rabbit immune sera could be identified in human sera by using different amoebic antigens of four different genera. *A. culbertsoni*, *Acanthamoeba polyphaga*, and *Acanthamoeba astronyxis* were each used as sources of antigen. Each species is a representative of a different subgroup of *Acanthamoeba* on the basis of morphology, isoenzyme analysis, and serology (23). Three other genera were represented by using antigens of *N. fowleri* and the nonpathogenic free-living amoebae *Hartmannella vermiformis* and *Vahlkampfia avara*. On the basis of the taxonomic scheme of Page (17), the genus *Hartmannella* and particularly the genus *Vahlkampfia* are considered to be closely related to the genus *Naegleria* (17). The serologic features and antigenic characteristics of these two genera are less well known than are those of the genera *Naegleria* and *Acanthamoeba*.

This report extends the available information regarding the serologic relationships and prominent epitopes associated with the pathogenic free-living amoebae. Certain epitopes representing different amoeba species are occasionally recognized by adult human serum. This documentation of electrophoretically separated antigens and reactive human sera supports the concept that humans are exposed to antibody-inducing levels of antigen from both pathogenic and nonpathogenic amoebae. With additional studies, immunoblots with human sera and amoebic antigens could be useful in recognizing this exposure, the associated pathologic manifestations, and both clinical and subclinical infections with the pathogenic free-living amoebae.

MATERIALS AND METHODS

Amoeba cultivation. Amoebae were cultivated axenically in 75-cm^2 tissue culture flasks containing medium that promoted the optimum growth for each species. *A. culbertsoni* ATCC 30171 and *A. polyphaga* ATCC 30461 were grown in Trypticase soy broth. Plate count broth (Difco, Detroit, Mich.) was used for cultivating *A. astronyxis* ATCC 30137. Medium H4 was used for cultivating *V. avara*, *H. vermiformis*, and *N. fowleri* (2). Cells were incubated at 25°C (except for *N. fowleri* cells, which were incubated at 35°C) and were harvested after a monolayer was formed in approximately 72 h. *H. vermiformis* was kindly provided by Barry Fields from the Centers for Disease Control and Prevention, Atlanta, Ga.; *N. fowleri* Lee was kindly provided by Francine Marciano-Cabral of Virginia Commonwealth University, Richmond.

Antigen and immune serum preparation. Amoebae were harvested by placing the culture flasks on ice to dislodge adherent cells. The amoebae were pelleted by centrifugation ($400 \times g$) and were washed three times in sterile phosphate-buffered saline (PBS; pH 7.6). Immunizing antigen was prepared by adjusting the concentration to 2×10^5 cells per ml in PBS and then freezing-thawing four times with liquid nitrogen. New Zealand White rabbits (weight, 2 kg) were immunized once weekly with 2 ml of the antigen preparation for 4 consecutive weeks. Antigen was delivered via the marginal ear vein. One week after the final immunization, the rabbits were bled by cardiac puncture. Washed cells for electrophoresis were prepared for Pierce BCA protein determination (Pierce, Rockford, Ill.) by solubilizing amoeba pellets in 100 μl of 1% sodium dodecyl sulfate (SDS). The soluble protein was boiled for 5 min in a 0.1 M dithiothreitol reducing buffer prior to electrophoresis.

Human sera. The human serum samples used in immunoblots consisted of five banked infant and seven adult serum samples stored at the Indiana University Medical Center. One hundred additional human serum samples drawn from Army recruits diagnosed with ARD were provided by Letterman Army Medical Center, San Francisco, Calif. To facilitate the number tested, serum samples from Army recruits were pooled into 10 groups of 10 sera, with each serum present in its respective pool at a dilution of 1:200. Serum pools were subsequently tested for their reactions with the electrophoresed amoebic antigens.

Electrophoresis and immunoblotting. SDS-polyacrylamide gel electrophoresis (PAGE) was performed by using a Mini-Protein II Dual Slab Cell apparatus (Bio-Rad, Hercules, Calif.). Five micrograms of amoebic protein was loaded into each lane of a 1.5-mm 15% acrylamide gel with a 4% stacking gel (preweighed acrylamide-bisacrylamide [37.5:1] mixture; Bio-Rad). Complete electrophoresis occurred in approximately 35 min at 200 V with the voltage held constant. Gels to be stained for protein were stained with Coomassie blue. Proteins were transferred onto 0.45-μm-pore-size nitrocellulose Trans-Blot Transfer Medium (Bio-Rad) by using a Mini Trans-Blot Electrophoretic Transfer Cell with a Bio-Ice unit (Bio-Rad). Complete transfer occurred at 130 V, while the current ranged from 250 to 350 mA over 60 min.

Following transfer, blots were washed in PBS for 10 min in glass staining dishes on a clinical rotator (Fisher, Pittsburgh, Pa.) at slow speed. They were then blocked for 30 min at room temperature with 1% bovine serum albumin diluted in PBS with 0.05% Tween 20 (pH 7.4; PBS-Tween). After washing the blots twice in PBS-Tween for 5 min each time, they were incubated in the diluted serum at room temperature for 60 min. Preliminary studies comparing the intensities of staining of immunoblots by using a range of dilutions yielded optimum dilutions for rabbit and human sera. From 1:2 serial dilutions of hyperimmune rabbit sera ranging from 1:100 to 1:10,000, a dilution of 1:1,000 was selected. From 1:2 serial dilutions of human sera ranging from 1:10 to 1:1,000, a dilution of 1:200 was selected. Blots were then washed twice in PBS-Tween for 5 min each time before the conjugate was added. The alkaline phosphatase conjugate (Sigma, St. Louis, Mo.) of anti-rabbit immunoglobulin G (IgG; whole molecule) was diluted 1:20,000 in PBS-Tween, or the alkaline phosphatase conjugate (Sigma) of anti-human IgG (gamma chain specific) was diluted 1:2,500 in PBS-Tween. Immunoblots were incubated in the diluted conjugates at room temperature for 30 min. Before adding the substrate, the immunoblots were washed twice for 5 min in PBS-Tween and then once for 5 min in PBS. Immunoblots were then developed in 5-bromo-4-chloro-3-indolylphosphate toludinium–Nitro Blue Tetrazolium Color Development Solution (Bio-Rad) for 10 min at room temperature.

Absorption. For absorption studies, 5×10^5 amoebae (formalin fixed and washed in PBS) were incubated in a 1-ml volume containing 40 μl of human serum and 960 μl of PBS, and the incubation mixture was rocked at 35°C for 1 h. This preparation was then centrifuged ($400 \times g$), and the serum supernatant was subsequently diluted to 1:200 before immunoblotting.

Immunofluorescence. For immunofluorescence testing, an indirect fluorescent-antibody procedure described by Sheets et al. (22) was used. The procedure uses formalin-fixed amoebae and incorporates a primary antibody of either hyperimmune rabbit serum or human serum. The secondary antibody is affinity-purified goat anti-rabbit or anti-human fluorescein-conjugated IgG (Sigma).

RESULTS

Whole amoeba lysates subjected to SDS-PAGE were stained with Coomassie blue (Fig. 1A). Multiple protein bands were apparent in each species. Most bands were greater than 18.5

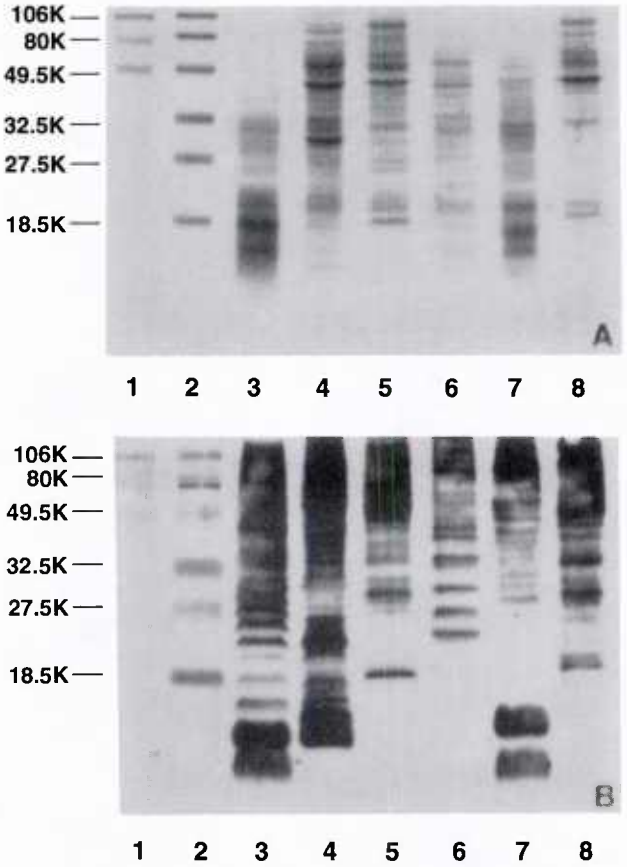

FIG. 1. (A) SDS-PAGE of different amoeba species stained with Coomassie blue. The low- and high-molecular-weight markers (lanes 1 and 2) are shown on the left (in thousands). Lanes: 3, *A. culbertsoni*; 4, *A. astronyxis*; 5, *H. vermiformis*; 6, *N. fowleri*; 7, *A. polyphaga*; 8, *V. avara*. (B) Immunoblot panel representing the total number of immunoreactive protein bands of amoeba antigens treated with pooled rabbit immune sera composed of immune serum from each of the six amoeba species (1:1,000 final dilution each). Molecular weight markers (lanes 1 and 2) are shown on the left (in thousands). Lanes: 3, *A. culbertsoni*; 4, *A. astronyxis*; 5, *H. vermiformis*; 6, *N. fowleri*; 7, *A. polyphaga*; 8, *V. avara*.

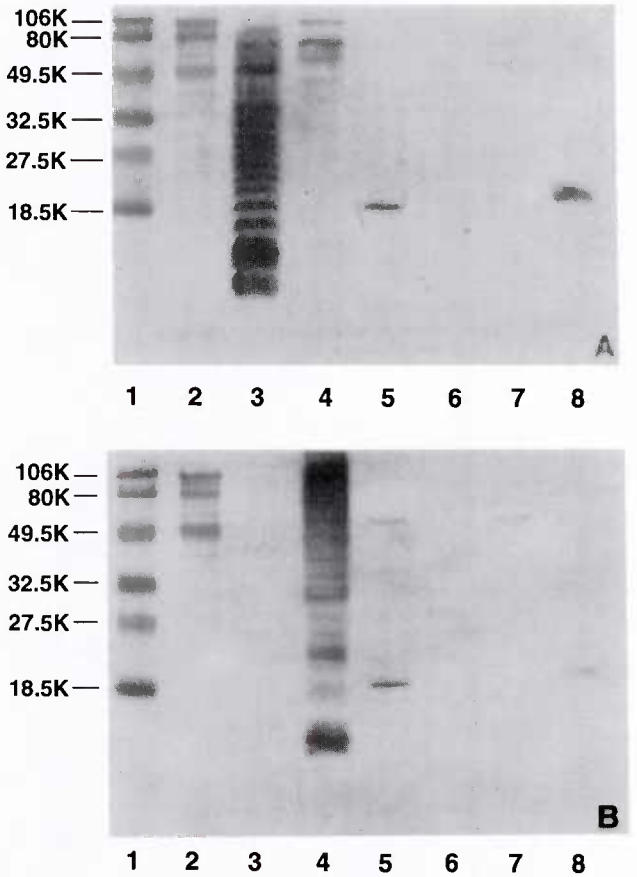

FIG. 2. (A) Immunoblot panel of amoeba antigens treated with only *A. culbertsoni* rabbit immune serum (1:1,000 dilution). Molecular weight markers (lanes 1 and 2) are shown on the left (in thousands). Lanes: 3, *A. culbertsoni*; 4, *A. astronyxis*; 5, *H. vermiformis*; 6, *N. fowleri*; 7, *A. polyphaga*; 8, *V. avara*. (B) Immunoblot panel of amoeba antigens treated with only *A. astronyxis* rabbit immune serum (1:1,000 dilution). Molecular weight markers (lanes 1 and 2) are shown on the left (in thousands). Lanes: 3, *A. culbertsoni*; 4, *A. astronyxis*; 5, *H. vermiformis*; 6, *N. fowleri*; 7, *A. polyphaga*; 8, *V. avara*.

kDa, with the exception of a broad diffuse area with heavy bands in both *A. polyphaga* and *A. culbertsoni* of less than 18.5 kDa. Each of the three *Acanthamoeba* species had a different banding profile. In *A. astronyxis*, the deeply staining band between 27.5 and 32.5 kDa was unique, and the most numerous and densely staining bands were greater than 27.5 kDa. *A. culbertsoni* showed its most intensely staining bands at less than 27.5 kDa. *A. polyphaga* had prominent bands that ranged from less than 18.5 to 49.5 kDa. *V. avara* and *H. vermiformis* shared a number of minor and major protein bands, with the primary differences related to the intensity of band staining rather than to the presence of different proteins. *N. fowleri* was distinct from the other genera, but its protein profile was likewise composed of many bands which were most numerous at greater than 27.5 kDa.

The total number of immunoreactive protein bands resolved by immunoblotting with the six pooled hyperimmune rabbit serum samples is illustrated in Fig. 1B. The bands represent the epitope reactions of each amoeba species with both homologous and heterologous immune sera. Immunoreactive bands for *Naegleria*, *Hartmannella*, and *Valulkampfia* antigens developed at molecular masses of greater than 18.5 kDa. In each *Acanthamoeba* species, two or more broad bands of less than 18.5 kDa were prominent features. By Coomassie blue staining, there were relatively low numbers of protein bands in areas above 32.5 kDa in the *A. culbertsoni* lysate, below 18.5 kDa in *A. astronyxis*, and above 49.5 kDa in *A. polyphaga*; however, the Western blot showed several major bands in these areas, indicating that these proteins were highly immunogenic. The presence of multiple bands by Western immunoblotting was a common feature of each species.

The occurrence of cross-reacting antibodies was assessed by allowing the panel of transferred amoebic antigens to react with individual rabbit immune serum (Fig. 2 to 4). Numerous well-defined bands were observed only with the homologous antigen at a rabbit immune serum dilution of 1:1,000 with 5 μg of amoebic antigen per lane. Few cross-reacting antibodies were detected between the three *Acanthamoeba* species chosen to represent different subgroups of the genus (Fig. 2 and 3A). *N. fowleri* was similarly serologically distinct (Fig. 3B). Despite the similarities in polyacrylamide gels stained with Coomassie blue, the immunoblots of *H. vermiformis* and *V. avara* were relatively distinct. *H. vermiformis* antiserum re-

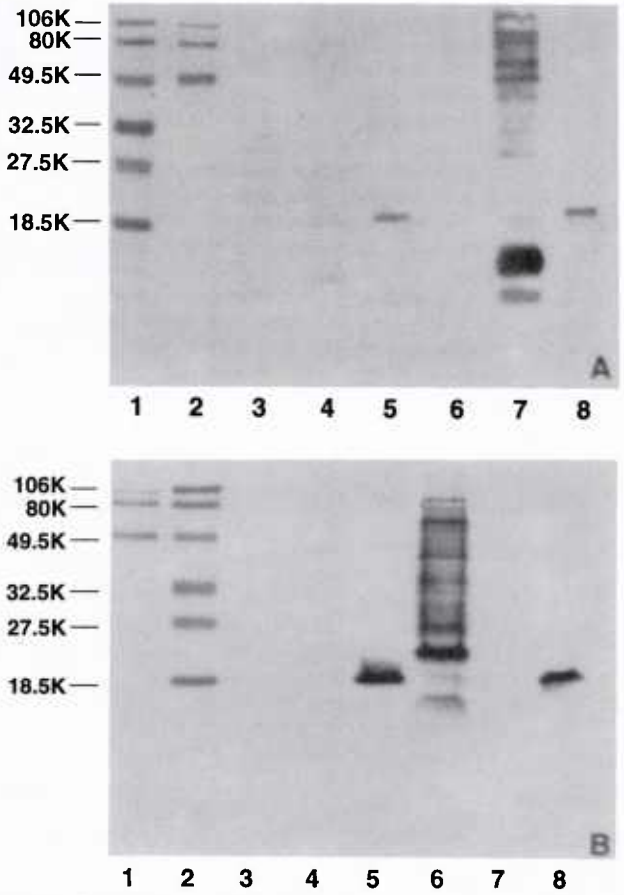

FIG. 3. (A) Immunoblot panel of amoeba antigens treated with only *A. polyphaga* rabbit immune serum (1:1,000 dilution). Molecular weight markers (lanes 1 and 2) are shown on the left (in thousands). Lanes: 3, *A. culbertsoni*; 4, *A. astronyxis*; 5, *H. vermiformis*; 6, *N. fowleri*; 7, *A. polyphaga*; 8, *V. avara*. (B) Immunoblot panel of amoeba antigens treated with only *N. fowleri* rabbit immune serum (1:1,000 dilution). Molecular weight markers (lanes 1 and 2) are shown on the left (in thousands). Lanes: 3, *A. culbertsoni*; 4, *A. astronyxis*; 5, *H. vermiformis*; 6, *N. fowleri*; 7, *A. polyphaga*; 8, *V. avara.*

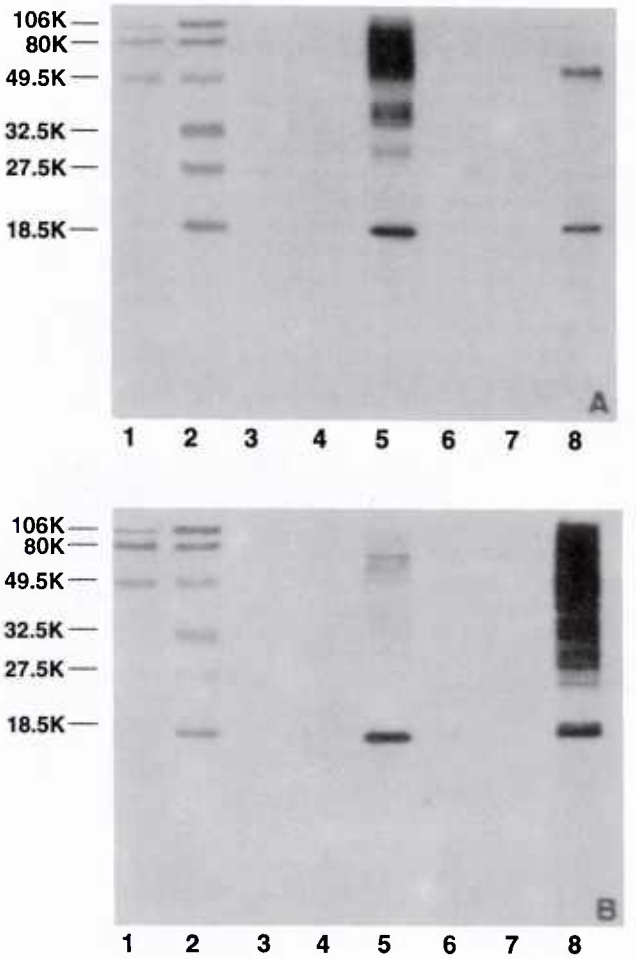

FIG. 4. (A) Immunoblot panel of amoeba antigens treated with only *H. vermiformis* rabbit immune serum (1:1,000 dilution). Molecular weight markers (lanes 1 and 2) are shown on the left (in thousands). Lanes: 3, *A. culbertsoni*; 4, *A. astronyxis*; 5, *H. vermiformis*; 6, *N. fowleri*; 7, *A. polyphaga*; 8, *V. avara*. (B) Immunoblot panel of amoeba antigens treated with only *V. avara* rabbit immune serum (1:1,000 dilution). Molecular weight markers (lanes 1 and 2) are shown on the left (in thousands). Lanes: 3, *A. culbertsoni*; 4, *A. astronyxis*; 5, *H. vermiformis*; 6, *N. fowleri*; 7, *A. polyphaga*; 8, *V. avara.*

vealed shared bands between 49.5 and 80 kDa (Fig. 4A), and *V. avara* antiserum revealed several shared bands between 32.5 and 106 kDa (Fig. 4B). A prominent band between 14 and 21 kDa was always seen in the *Hartmannella* and the *Valulkampfia* lanes. This band was also observed in control blots consisting of only the affinity-purified immunoglobulin conjugate of goat anti-human IgG or goat anti-rabbit IgG (no rabbit immune or human serum was used) and appeared to be attributable to the affinity of each conjugate to an unidentified amoebic protein.

Because of the lack of prominent cross-reactive amoebic antigens, a panel of amoebic antigens representing serologically distinct epitopes was used to screen human serum samples for amoeba-reactive antibodies. In 2 of the 10 pools of serum from Army recruits, a prominent band of less than 18.5 kDa was located in the *A. culbertsoni* antigen lane (Fig. 5A). When the sera from each group were tested individually by immunoblotting, the reaction with the *A. culbertsoni* antigen could be associated with one individual from each group. Lightly reactive bands of greater than 32.5 kDa were seen in all 10 serum pools tested (Fig. 5A). Little reactivity was observed in immunoblots of serum from seven laboratory personnel; however, a prominent band of approximately 18.5 kDa was present in the *A. culbertsoni* antigen lane of one individual (Fig. 5B). This band was comparable to the one observed in two of the serum samples from the Army recruit group.

The specificity of human antibodies reactive to *A. culbertsoni* antigen was assessed by absorption with fixed whole cells. A comparison of absorbed and unabsorbed sera showed that the *A. culbertsoni*-reactive antibody was removed by the absorption with homologous antigen (data not shown). Banked infant sera from infants less than 6 months old were also tested by immunoblotting against the panel of amoebic antigens. No evidence of amoeba-reactive antibodies was present in any of the five infant serum samples.

Immunofluorescence testing showed that human serum reactive to *A. culbertsoni* antigen via immunoblotting also caused formalin-fixed *A. culbertsoni* to fluoresce under UV light. Negative controls made with human serum that was unreactive to *A. culbertsoni* antigen did not result in the fluorescence of the formalin-fixed amoebae.

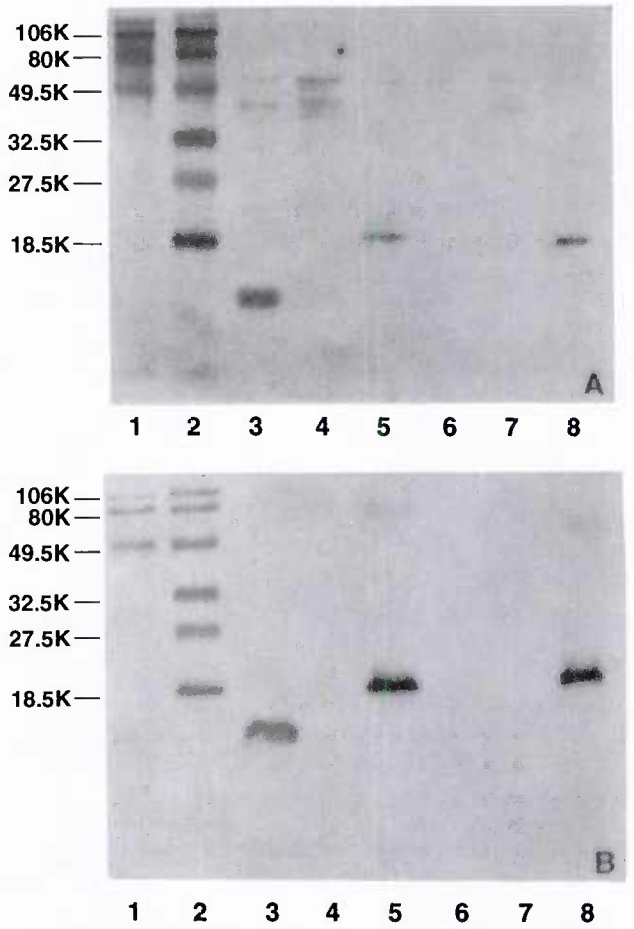

FIG. 5. (A) Immunoblot panel of amoeba antigens treated with 10 pooled serum samples from Army recruits with ARD (1:200 final dilution). Molecular weight markers (lanes 1 and 2) are shown on the left (in thousands). Lanes: 3, *A. culbertsoni*; 4, *A. astronyxis*; 5, *H. vermiformis*; 6, *N. fowleri*; 7, *A. polyphaga*; 8, *V. avara*. (B) Immunoblot panel of amoeba antigens treated with the serum of a laboratory worker (1:200 dilution). Molecular weight markers (lanes 1 and 2) are shown on the left (in thousands). Lanes: 3, *A. culbertsoni*; 4, *A. astronyxis*; 5, *H. vermiformis*; 6, *N. fowleri*; 7, *A. polyphaga*; 8, *V. avara*.

DISCUSSION

Several species of *Acanthamoeba* and one species of *Naegleria* are capable of producing disease in humans (12, 15). The route of infection, the course of the disease, and preventive measures have been defined for certain amoebic diseases such as amoebic meningoencephalitis caused by *Naegleria* species and keratitis caused by *Acanthamoeba* species (9, 12, 13). The factors involved in the spread of pathogenesis of other forms of *Acanthamoeba*-associated human illness are less clear. Although *Acanthamoeba* meningoencephalitis has been most frequently encountered in immunocompromised individuals, the majority of the population undoubtedly has been exposed to these amoebae in the environment. *Legionella pneumophila* can use *Naegleria* and *Acanthamoeba* organisms as host cells for intracellular replication, and Rowbotham (20, 21) hypothesized that amoebae could also serve as vectors for the delivery of *Legionella* bacteria to humans.

To better understand the environmental transmission of amoebae to humans and the epidemiology of disease involving free-living amoebae, various serologic methods have been used to assess the presence of amoeba-reactive antibody in humans. The serologic methods used previously have included the indirect fluorescent-antibody assay, complement fixation, agglutination, indirect hemagglutination, and Western blot analysis (3, 7, 10, 14, 19). Results of those studies suggest that humans have naturally occurring amoeba-reactive antibodies represented by IgG and IgM. At the present time, it is not known if these antibodies are a reflection of environmental exposure to amoebic antigen, the consequence of subclinical infection, or the result of cross-reacting antibodies from some other source.

The number and character of *Naegleria* epitopes identified by using human serum have been examined by Marciano-Cabral et al. (14) by Western blot analysis. Their results suggested that human IgG reacts primarily with internal amoebic antigens, and these antigens show extensive cross-reactivity among species. Conversely, the amoeba-agglutinating activity of normal human serum is a function of IgM reactivity with surface antigens. These antibodies are species specific. Antibodies from human serum react to both pathogenic and nonpathogenic *Naegleria* species, and individuals appear to have been exposed to different amoebic antigens. In a study by Dubray et al. (7), immunoblot analysis of selected human serum against *N. fowleri* or *Naegleria lovaniensis* antigen demonstrated four bands of reactivity. The results suggested that human antibodies recognized identical antigenic sites in both of these species.

Most recently, Moura et al. (16) compared the antigenic characteristics of 13 *Acanthamoeba* strains by immunoblot analysis by using homologous and heterologous rabbit immune sera. Most bands were observed between 20 and 116.5 kDa, and the staining intensity was often so great that it was difficult to distinguish individual bands. In some instances, antibodies cross-reacted extensively among the 13 strains. Certain antigens were more extensively shared within each of three *Acanthamoeba* morphologic groupings on the basis of immunoblot profiles. It was also apparent that certain subgroups of *Acanthamoeba* were more closely related serologically.

Results from the present study demonstrate the complex protein profiles associated with the free-living amoebae following SDS-PAGE. It is apparent that the majority of these proteins are highly immunogenic in laboratory rabbits. A notable observation is the relative lack of cross-reacting antibodies among the selected amoebae by immunoblotting. Even within the genus *Acanthamoeba*, the selected type species from each subgroup were serologically distinct. These differences are consistent with the division of *Acanthamoeba* species into distinct subgroups, in part on the basis of serology. A prominent feature of our study with *Acanthamoeba* species was the observation of distinct broadly immunoreactive proteins of less than 18.5 kDa. These bands were observed only in immunoblots of the three *Acanthamoeba* species with homologous rabbit immune serum and in the *A. culbertsoni* antigen lanes of approximately 3% (3 of 112) of the immunoblots developed with human serum. Immunofluorescence testing confirmed the reactivity of one of these three human serum samples. The supply of the other two serum samples was exhausted during immunoblotting and absorption assays.

No distinction has been made between the two reactive serum samples from Army recruits and normal adult serum taken at Indiana University. It is likely that additional studies representing other groups of humans will be needed to define the range of naturally occurring amoeba-reactive antibodies in humans. Previously, investigators have demonstrated by immunoblotting that certain individuals have naturally occurring antibodies that react with protozoa such as *Toxoplasma gondii*

(18). The source of the antigenic stimulation was unknown. Studies have suggested antigenic similarities between *T. gondii* and other organisms that are not considered to be pathogens and that rarely occur in humans (18). The specificity of amoeba-reactive antibodies detected with our assay was confirmed by absorption studies with *A. culbertsoni* antigen. However, the exact events associated with antigen exposure or antibody induction in our investigation cannot be determined. Our observations support the concept that previous exposure to *A. culbertsoni* may be responsible for the occurrence of reactive antibodies in this small group of individuals. The ability of the immunoblot to detect human antibodies that specifically react with *A. culbertsoni* epitopes suggests a likelihood of detecting patient seroconversions to this amoeba and other serologically distinct species of *Acanthamoeba* as well.

Human antibodies reactive with *N. fowleri* antigen were detected in pooled serum from Army recruits. In one blot, a sharp doublet was observed at 49.5 kDa (data not shown). Other antibodies reactive with *N. fowleri* were detected by the presence of three to four bands between 32.5 and 106 kDa. The appearance of these bands did not differ from the appearance of similar bands of the same molecular size in the lanes of the other five amoebic antigens. These bands were not as prominent or deeply staining as those reported by other investigators who used immunoblotting to assess the reactivity of human serum with *N. fowleri* antigen (7, 14). This could be, in part, a reflection of the test parameters such as antigen concentration, serum concentration, or other variables. Other investigators used a 1:50 human serum dilution, whereas a 1:200 serum dilution was used in the present study. In our study, we did not note major differences in blot results when the serum dilution was reduced from 1:200 to 1:50. This lower dilution resulted mainly in increased background staining. Our investigation also represents a study population different from that of other investigators, and as suggested previously, differences in results with the *Naegleria* antigen used in immunoblotting may represent geographical variation in amoebic antigen exposure (14).

The similarity between *H. vermiformis* and *V. avara* in the Coomassie blue-stained gel was pronounced. These two genera are closely related morphologically, and the similarities in protein bands would serve to underscore this similarity. Additional gel electrophoresis of these two strains was performed on replicate cultures from the American Type Culture Collection, and the nearly identical Coomassie blue staining patterns were again apparent. To our knowledge, these two strains of amoebae have not previously been compared by SDS-PAGE. The results of this initial comparison indicate that additional studies are needed to determine the significance of this similarity and if this is a consistent feature of other strains and species in these two genera. These results demonstrate that these two species from different genera are remarkably similar by SDS-PAGE, yet they can be distinguished by immunoblotting. The consistent appearance of nearly identical bands between 14 and 21 kDa in only the *Hartmannella* and *Vahlkampfia* antigen lanes also merits additional study. The visualization of these bands in the absence of rabbit immune or human serum suggests that the electrophoresed proteins directly bind some component of the alkaline phosphatase-immunoglobulin conjugate. The ability of certain components of microorganisms to bind immunoglobulins in a nonimmune fashion, as observed with protein A, has been well established. This has not been observed previously in the pathogenic free-living amoebae.

This report documented the major antibody-reactive antigens in six species of free-living amoeba. Reactions with rabbit immune sera demonstrated that each amoeba was serologically distinct, and there was little cross-reacting antibody. This insight has important implications for future attempts to diagnose human amoebic infections serologically. Apparently, it will be necessary to use a battery of amoebic antigens representing the serologically distinct species and genera in order to recognize the presence of amoeba-reactive antibodies. This study provides baseline information on the presence of antibodies reactive with free-living amoebae in human serum and suggests the feasibility of using immunoblotting to detect seroconversions in individuals infected with the pathogenic free-living amoebae.

ACKNOWLEDGMENTS

We thank Kay Pinkston for the care and typing in preparation of the manuscript and Richard Gregory for helpful direction and advice.

REFERENCES

1. **Badenoch, P. R., T. R. Grimmond, J. Cadwgan, S. E. Deayton, M. S. Essery, and B. D. Hill.** 1988. Nasal carriage of free-living amoebae. Microb. Ecol. Health Dis. **110:**749–751.
2. **Band, R. N., and W. Balamuth.** 1974. Hemin replaces serum as a growth requirement for *Naegleria*. Appl. Microbiol. **28:**64–65.
3. **Cerva, L.** 1989. *Acanthamoeba culbertsoni* and *Naegleria fowleri*: occurrence of antibodies in man. J. Hyg. Epidemiol. Microbiol. Immunol. **33:**99–103.
4. **Cerva, L., C. Serbus, and V. Skocil.** 1973. Isolation of limax amoebae from the mucosa of man. Folia Parasitol. (Praha) **20:** 97–103.
5. **Culbertson, C. G.** 1981. Amebic meningoencephalitis. Antibiot. Chemother. **30:**28–53.
6. **Culbertson, C. G., J. W. Smith, H. K. Cohen, and J. R. Minner.** 1959. Experimental infection of mice and monkeys by *Acanthamoeba*. Am. J. Pathol. **35:**185–197.
7. **Dubray, B. L., W. E. Wilhelm, and B. R. Jennings.** 1987. Serology of *Naegleria fowleri* and *Naegleria lovaniensis* in a hospital survey. J. Protozool. **34:**322–327.
8. **Dudding, B. A., F. H. Top, Jr., P. E. Winter, E. L. Buescher, T. H. Lamson, and A. Leibovitz.** 1972. Acute respiratory disease in military trainees. Am. J. Epidemiol. **97:**187–198.
9. **Ferrante, A.** 1991. Free-living amoebae: pathogenicity and immunity. Parasite Immunol. **13:**31–47.
10. **Kenney, M.** 1971. The Micro-Kolmer complement fixation test in routine screening for soil ameba infection. Health Lab. Sci. **8:**5–10.
11. **Lawande, R. V., S. N. Abraham, I. John, and L. J. Egler.** 1979. Recovery of soil amoebas from the nasal passages of children during the dusty Harmattan period in Zaria. Am. J. Clin. Pathol. **71:**201–203.
12. **Ma, P., G. S. Visvesvara, A. J. Martinez, F. H. Theodore, P. M. Daggett, and T. K. Sawyer.** 1990. *Naegleria* and *Acanthamoeba* infections: review. Rev. Infect. Dis. **12:**490–513.
13. **Marciano-Cabral, F.** 1988. Biology of *Naegleria* spp. Microbiol. Rev. **52:**114–133.
14. **Marciano-Cabral, F., M. L. Cline, and S. G. Bradley.** 1987. Specificity of antibodies from human sera for *Naegleria* species. J. Clin. Microbiol. **25:**692–697.
15. **Martinez, A. J., and G. S. Visvesvara.** 1991. Laboratory diagnosis of pathogenic free-living amoebas: *Naegleria*, *Acanthamoeba*, and *Leptomyxid*. Clin. Lab. Med. **11:**861–872.
16. **Moura, H., S. Wallace, and G. S. Visvesvara.** 1992. *Acanthamoeba healyi* N. Sp. and the isoenzyme and immunoblot profiles of *Acanthamoeba* spp., groups 1 and 3. J. Protozool. **39:**573–583.
17. **Page, F. C.** 1988. Potential pathogens, p. 7. *In* A new key to freshwater and soil gymnamoebae. Freshwater Biological Association, The Ferry House, Cumbria, England.
18. **Potasman, I., F. G. Araujo, and J. S. Remington.** 1986. Toxoplasma antigens recognized by naturally occurring human antibodies. J. Clin. Microbiol. **24:**1050–1054.
19. **Reilly, M., F. Marciano-Cabral, D. W. Bradley, and S. G. Bradley.**

1983. Agglutination of *Naegleria fowleri* and *Naegleria gruberi* by antibodies in human serum. J. Clin. Microbiol. **17**:576–581.
20. **Rowbotham, T. J.** 1980. Preliminary report on the pathogenicity of *Legionella pneumophila* for freshwater and soil amoebae. J. Clin. Pathol. **33**:1179–1183.
21. **Rowbotham, T. J.** 1986. Current views on the relationships between amoebae, legionellae and man. Isr. J. Med. Sci. **22**:678–689.
22. **Sheets, P. B., A. L. Newsome, and S. D. Allen.** 1992. Detection of human serum antibodies reactive with *Acanthamoeba polyphaga* by use of an indirect fluorescent antibody (IFA) test, part D, subsection 8, D-8.1–D-8.6. *In* J. J. Lee and A. T. Soldo (ed.), Protocols in protozoology. Allen Press, Inc., Lawrence, Kans.
23. **Visvesvara, G. S.** 1991. Classification of *Acanthamoeba*. Rev. Infect. Dis. **13**(Suppl. 5):S369–S372.
24. **Visvesvara, G. S., and W. Balamuth.** 1975. Comparative studies on related free-living and pathogenic amebae with special reference to *Acanthamoeba*. J. Protozool. **22**:245–256.
25. **Wang, S. S., and H. A. Feldman.** 1967. Isolation of *Hartmannella* species from human throats. N. Engl. J. Med. **277**:1174–1179.
26. **Wenzel, R. P., D. P. McCormick, E. P. Smith, and W. E. Beam, Jr.** 1971. Acute respiratory disease: clinical and epidemiologic observations of military trainees. Mil. Med. **136**:873–880.
27. **Wong, M. M., S. L. Karr, and W. B. Balamuth.** 1975. Experimental infections with pathogenic free-living amebae in laboratory primate hosts. I. (B) A study on susceptibility to *Acanthamoeba culbertsoni*. J. Parasitol. **61**:682–690.

0022-3565/94/2701-0142$00.00/0
THE JOURNAL OF PHARMACOLOGY AND EXPERIMENTAL THERAPEUTICS

Vol. 270, No. 1
Printed in U.S.A.

Effects of Chlordiazepoxide, 8-OH-DPAT and Ondansetron on Radiation-Induced Decreases in Food Intake in Rats[1]

PETER J. WINSAUER, JAMES F. VERREES, KEVIN P. O'HALLORAN, MICHAEL A. BIXLER and PAUL C. MELE
Behavioral Sciences Department, Armed Forces Radiobiology Research Institute, Bethesda, Maryland
Accepted for publication March 11, 1994

ABSTRACT

Studies of radiation effects on performance are often complicated by concurrent radiation-induced decreases in feeding behavior (*i.e.*, "anorexia"). To evaluate the pharmacological specificity of these decreases in food intake, the interactions of radiation with three prototypical drugs were studied. Single daily i.p. administration of a dose of chlordiazepoxide, ondansetron or 8-hydroxy-2-(di-*n*-propylamino)tetralin (8-OH-DPAT) was given to groups of rats for 5 days after either a single nonlethal 4.5-Gy dose of ionizing radiation (bremsstrahlung or *gamma* rays) or a sham exposure. The food intake for each group was measured 60 min and 24 hr after food presentation. Radiation alone significantly decreased food intake during the 60-min test on each treatment day and for the 5-day period when data were averaged. Chlordiazepoxide (1.8–18 mg/kg) and 8-OH-DPAT (0.1–1 mg/kg) produced significant dose-dependent increases in food intake during the 60-min test in both irradiated and sham-irradiated groups, whereas ondansetron (0.1–1 mg/kg) did not alter food intake at any dose tested. The dose effects at 60 min were significant on each treatment day for chlordiazepoxide, on 4 of 5 days for 8-OH-DPAT and for both drugs when data for all 5 days were combined. In no case, however, was a significant interaction obtained for radiation and any dose of the three drugs. After 24 hr, decreases in intake were obtained in a few subjects in 3 of 12 total radiation groups. These results suggest that radiation-induced decreases in food intake do not result from damage to the mechanisms by which chlordiazepoxide and 8-OH-DPAT increase food intake and that hyperphagic agents from these two different classes may have therapeutic value for attenuating radiation-induced anorexia.

Radiation-induced decreases in food intake occur in a variety of species, including humans, shortly after exposure and they may persist for several days, depending on the dose (Anno *et al.*, 1989; Davis, 1965; Mickley *et al.*, 1989). Although the mechanisms responsible for these decreases in food intake are poorly understood, this prominent behavioral effect has not been studied extensively and continues to be a problem in therapeutic and experimental situations. For example, in patients receiving radiotherapy for cancer, both conditioned (*e.g.*, food aversions) and unconditioned (*e.g.*, general decreases in food intake or appetite) effects compromise treatment regimens by decreasing compliance and by increasing anxiety in regard to treatment (King and Makale, 1991; Mattes *et al.*, 1991; Smith *et al.*, 1984). In experiments using rats and monkeys as subjects, exposure to various types of radiation produced changes in food preference, decreases in food intake and loss of body weight (Davis, 1965; Johnson *et al.*, 1946; Mickley *et al.*, 1989; Ruch *et al.*, 1962; Smith and Tyree, 1954; Smith *et al.*, 1952a). Moreover, these changes have complicated the study of other behavioral effects of radiation, such as changes in volitional activity (Jones *et al.*, 1954), changes in motivated or operant responding (Jarrard, 1963; Mele *et al.*, 1990) and assessment of learning deficits postexposure (Arnold, 1952; Furchtgott, 1951).

Most carefully controlled studies on radiation and feeding behavior have been conducted with rats. Jarrard (1963), for example, reported that 0.9, 2.9 and 4.8 Gy of x-ray irradiation (250 kV) in rats produced dose-dependent decreases in food intake during a 2-hr test period. (For ease of comparison with previous research, all the radiation doses cited, either roentgen or rad, have been converted to gray. The conversion factor for roentgen to rad is 0.966 to account for the difference between air and muscle. Rad can be converted to gray by multiplying the dose by 1/100.) He also reported that decreases in food consumption in rats lasted for 1 to 5 days, depending on the dose administered. In another study involving rats, Smith and Tyree (1954) reported that anorexia and a resulting loss in body weight occurred within the first 24 hr after exposure and lasted for several days when doses of approximately 2.5 Gy or

Received for publication July 21, 1993.
[1] This work was supported by the AFRRI, Defense Nuclear Agency. Research was conducted according to the principles enunciated in the "Guide for the Care and Use of Laboratory Animals" prepared by the Institute of Laboratory Animal Resources, National Research Council, National Institutes of Health publication number (NIH) 86-23, revised 1985. AFRRI is fully accredited by the American Association for Accreditation of Laboratory Animal Care.

ABBREVIATIONS: 5-HT, serotonin; 8-OH-DPAT, 8-hydroxy-2-(di-*n*-propylamino)tetralin; AFRRI, Armed Forces Radiobiology Research Institute; ANOVA, analysis of variance; Gy, gray.

higher of x-ray irradiation (200 kV) were tested. Furthermore, these investigators obtained effects on feeding behavior at doses as low as 0.25 to 0.5 Gy and determined that these changes reflected early and sensitive signs of whole-body radiation exposure.

Despite obvious changes in food intake after radiation exposure, few studies have systematically examined these changes with pharmacological and behavioral methods comparable to those used when studying various drugs known to affect feeding behavior. The extensive study of the benzodiazepines and 5-HT_{1A} agonists, in particular, has been important in understanding the pharmacological specificity of the mechanisms involved in feeding behavior. A recent review by Cooper (1991) states that benzodiazepine receptors probably exert bidirectional control over feeding responses and the effects of drugs acting at benzodiazepine receptors can span the full range, *i.e.*, from marked hyperphagia at one extreme to anorexia at the other, depending on whether agonists or inverse agonists are present, respectively. More recently, hyperphagic properties have been attributed to agonists with actions at 5-HT_{1A} receptors (Cooper, 1991). Similar to some prototypical benzodiazepine receptor agonists, 5-HT_{1A} receptor agonists have been shown to increase food intake reliably in both monkeys (Pomerantz, 1990) and rats (Dourish *et al.*, 1985; Fletcher and Davies, 1990; Hutson *et al.*, 1988; Montgomery *et al.*, 1989). Although differences between the behavioral effects of these two classes of compounds have been reported in rats (Fletcher and Davies, 1990), experiments with both classes of drug have helped to identify specific neurotransmitters and receptors involved with feeding behavior.

In an attempt to examine and attenuate radiation-induced decreases in food intake potentially, drugs from three different pharmacological classes were given in combination with radiation. Briefly, chlordiazepoxide (a prototypical benzodiazepine agonist), 8-OH-DPAT (a prototypical 5-HT_{1A} agonist) or ondansetron (a 5-HT_3 antagonist) were given to schedule-fed rats for 5 consecutive days after either a single nonlethal dose of ionizing radiation or a sham irradiation. Food intake was measured on each treatment day 60 min after food presentation and this food-intake measure was collected for 5 days postexposure. In addition, each subject's cage was examined for remaining food 23 hr later, immediately before the next food presentation. Chlordiazepoxide and 8-OH-DPAT were selected specifically for their ability to increase food intake over comparable test periods (Cooper, 1980, 1991). Ondansetron was given as a comparison because of data, which indicated that it can also increase feeding under certain conditions (Shepherd and Rodgers, 1990). The effects of ondansetron on radiation-induced decreases in food intake were of special interest because this drug has been found to be highly efficacious and potent in controlling radiation-induced emesis in several animal species (Andrews *et al.*, 1988; King and Makale, 1991) and nausea and emesis in patients with cancer (Priestman, 1991). Finally, like chlordiazepoxide and 8-OH-DPAT (Engel *et al.*, 1984; Randall *et al.*, 1960), ondansetron has been shown to possess anxiolytic properties in experiments involving rats (Jones *et al.*, 1988).

Methods

Subjects. The subjects were 191 male Sprague-Dawley rats (Charles River Breeding Laboratories, Kingston, NY) approximately 8 to 12 weeks of age. On arrival, all subjects were quarantined for 10 days and screened for evidence of disease. During this time, commercial rodent chow and acidified water (pH 2.5–3) were provided *ad libitum*. Acidified water was used routinely throughout the experiment to minimize the possibility of opportunistic bacterial infections. Before testing began, all subjects were housed individually in plastic Micro-Isolator (Allentown Caging Equipment Co., Inc., Allentown, NJ) cages, which contained sterilized hardwood-chip bedding. All housing rooms were maintained at 21 ± 1°C with 50 ± 10% relative humidity on a 12-hr light/dark cycle, which began with lights on at 6:00 A.M. each day.

Procedure. The subjects used to test each of three drugs were allowed to adapt to single housing and were provided with continuous access to food and water for approximately 2 weeks. At this time, all food was removed from the cages and each subject was weighed. This weight was considered the nondeprived body weight for each subject, which then was maintained throughout the study with the daily presentation of a measured amount of chow in the home cage. The mean body weights for the chlordiazepoxide-, ondansetron- and 8-OH-DPAT-treated groups were 372 g (range, 302–437 g), 465 g (range, 394–553 g), and 386 g (range, 343–427 g), respectively. Specifically, each subject received an amount of food (measured in grams) necessary to maintain its nondeprived body weight for a single 24-hr period. In general, the amount of chow presented on a given day was considered appropriate if the entire ration was consumed over that period and the daily body weight remained stable. Mean daily food intakes in grams for the chlordiazepoxide-, ondansetron- and 8-OH-DPAT-treated groups were 23 g (range, 17–32 g), 20 g (range, 16–24 g), and 22 g (range, 18–27 g), respectively. Food was always presented immediately after the daily weighing, which generally occurred between 2:00 P.M. and 3:00 P.M.. An electronic top-loading balance (Sartorius, type 1401, Mc Gaw Park, IL) with a recording accuracy to 0.1 mg was used to weigh both the subjects and the amounts of food.

Under base-line conditions, the daily food intake for each group was measured 60 min after food was presented. Any food remaining in the cage at the end of this time was collected and weighed. This amount, which reflected the uneaten balance of each subject's total daily ration, was always returned to the home cage after weighing. The base line was considered stable when all the subjects reliably ate during this 60-min period after food presentation and individual consumption patterns showed no increasing or decreasing trends. After the base line had stabilized (6–13 days), the subjects that would receive each drug were subdivided into eight groups ($n = 8$ per group), except for one group of controls in the experiment using chlordiazepoxide ($n = 7$). The subjects were allocated within each group, such that all groups were balanced for mean food consumption during the 60-min test period.

For each drug tested, the treatment regimen for the eight groups remained the same and food intake for all groups was measured over 5 consecutive days. Three groups received a single 4.5-Gy dose of radiation on day 1 of the experiment followed by 5 days of drug injections. Three other groups received a sham exposure on day 1 followed by 5 days of drug injections. The remaining two groups, which served as controls, received 5 days of saline injections after either a 4.5-Gy dose of radiation or a sham exposure. The 4.5-Gy dose of radiation was selected on the basis of preliminary dose-effect data with other rats.

Radiation. Both sham and radiation exposures were conducted 4 hr before the first test period on day 1. At this time, the subjects were placed in well ventilated plastic restraining tubes and either a single unilateral whole-body dose of bremsstrahlung (before testing chlordiazepoxide) or a single bilateral whole-body dose of ^{60}Co *gamma* radiation (before testing ondansetron and 8-OH-DPAT) was administered. Bremsstrahlung (3 MeV average energy) was generated by the AFRRI high-energy electron linear accelerator by using 18.1-MeV electrons (a 3.8-μsec pulse at 30 pulses/sec) and administered at a nominal dose rate of 2 Gy/min. *Gamma* radiation from the AFRRI ^{60}Co facility was administered bilaterally at a nominal dose rate of 2.5 Gy/min. The lower dose rate for bremsstrahlung exposures was due to technical difficulties on the irradiation day. The subjects were generally exposed four at a time by using a clear plastic stand that held the restraining

tubes horizontally one above the other. One subject from each of the four radiation treatment groups was included in each exposure such that these groups were counterbalanced for variability in administered dose over the multiple exposures (*e.g.*, a maximum variability of ± 0.19 Gy was estimated for the linear accelerator). Before the actual animal irradiations, the desired midline tissue dose rates were established by using an acrylic rat phantom with a tissue equivalent ionization chamber (calibration traceable to National Institute of Standards and Technology). Dosimetric measurements were made according to the American Association of Physicists in Medicine protocol for the determination of absorbed dose from high-energy photon and electron beams (Task Group 21, 1983). The tissue-to-air ratio for the dose was determined for the ^{60}Co *gamma* irradiations and found to be 0.93 (for midline tissue dose at abdomen level). Each irradiation was conducted on a Monday and required approximately 20 min. This time included the actual exposure and the time necessary for transporting the rats to and from the exposure area. Sham exposures for the groups not receiving radiation consisted of placing the subjects in restraining tubes for a comparable amount of time and transporting them to and from the exposure area.

Drugs. The drugs used were chlordiazepoxide hydrochloride (Sigma, St. Louis, MO), ondansetron hydrochloride dihydrate (Glaxo Group Research, Middlesex, UK) and 8-OH-DPAT (Research Biochemicals, Natick, MA). Doses of each drug were dissolved in sterile saline (0.9%). The injection volume for both saline and drug was 0.1 ml/100 g body weight. Each drug was given i.p.. Chlordiazepoxide was administered 30 min before each of the five 60-min test periods; ondansetron and 8-OH-DPAT were given 20 min before the 60-min test periods. The doses of chlordiazepoxide (1.8, 5.6 and 18 mg/kg), ondansetron (0.1, 0.3 and 1 mg/kg), and 8-OH-DPAT (0.1, 0.3 and 1 mg/kg) were selected from the literature (Cooper and Moores, 1985; Dourish *et al.*, 1985; Shepherd and Rodgers, 1990). To ensure familiarity with both injection procedures and radiation procedures, all subjects were injected with saline (20 or 30 min before feeding) and placed in the restraining tubes (4 hr before feeding) on three separate occasions during the pretreatment base-line phase.

Data analysis. The food intake was calculated in grams for each rat on each day of the 5-day treatment period; the mean food intake for each rat over the 5-day treatment period was also calculated. Group data on food intake for individual treatment days and for the 5-day average were analyzed statistically using a two-way ANOVA. After the two-way ANOVAs, Dunnett's tests were used to make pairwise comparisons. All pairwise comparisons were two-tailed with an *alpha* level set at less than .05.

Results

The effects of chlordiazepoxide on the mean food intake in both irradiated and sham-irradiated groups are shown in table 1. As indicated by the data in the table, food intake during the daily 60-min test was stable across all 5 days of treatment in the control group that received sham irradiation followed by 5 days of saline injections. However, a 4.5-Gy dose of bremsstrahlung photon radiation significantly decreased food intake on each treatment day in the group that received saline and the groups that received chlordiazepoxide (ANOVA, main effect of radiation, $P < .01$ on each day). This main effect of radiation was particularly evident in the group that received radiation followed by 5 days of saline injections. In this group, food intake on postirradiation days 2, 3 and 4 was reduced 40% to 56% relative to the control group. In irradiated chlordiazepoxide groups on treatment day 2, for example, radiation-induced decreases in food intake were most evident in the groups that received dose of 1.8 and 18 mg/kg.

Chlordiazepoxide dose-dependently increased the mean food intake in both irradiated and sham-irradiated subjects. This finding was confirmed by a significant main effect for the chlordiazepoxide dose when individual treatment days were analyzed ($P < .05$ for each of the 5 days). The interaction of radiation and chlordiazepoxide dose, however, was not significant for any individual treatment day ($P > .1$ for each of the 5 days), which indicated that chlordiazepoxide did not selectively increase food intake in irradiated or sham-irradiated groups. The increases in mean food intake produced by chlordiazepoxide were clearly evident in the data obtained with the 5.6-mg/kg dose. In sham-irradiated subjects, this dose increased food intake above 13 g on 4 of 5 treatment days and, in irradiated subjects, this dose increased the mean intake to levels that approximated those of the control group.

TABLE 1

Effects of chlordiazepoxide (CDZP) on food intake in grams during a daily 60-min test period in both irradiated and sham-irradiated rats

Group	Days of Treatment				
	1	2	3	4	5
Sham + Saline	10.1[a]	9.4	10.7	9.4	10.6
	0.6	1.1	1.2	0.9	0.8
Radiation[b] + Saline	8.3	4.4	4.7	5.6	7.6
	1.4	0.9	0.8	0.9	0.7
Sham + CDZP 1.8 mg/kg	11.7	9.7	12.2	13.1	14.7
	1.2	1.1	1.1	1.0	0.9
Radiation + CDZP 1.8 mg/kg	9.5	4.8	6.2	6.9	9.8
	1.0	0.7	0.7	0.8	1.2
Sham + CDZP 5.6 mg/kg	14.8	10.4	13.2	13.5	16.4
	0.9	0.9	1.0	0.8	0.7
Radiation + CDZP 5.6 mg/kg	11.1	7.5	9.0	8.7	12.4
	0.9	0.9	0.8	0.7	1.2
Sham + CDZP 18 mg/kg	10.5	11.4	11.7	10.9	12.3
	1.4	0.9	1.0	1.2	1.0
Radiation + CDZP 18 mg/kg	8.9	6.9	6.5	6.6	9.5
	1.1	1.1	1.0	0.9	1.1

[a] Mean intake and one S.E.M. (below) for eight subjects (seven for sham irradiation and saline).
[b] 4.5 Gy of bremsstrahlung administered at a nominal rate of 2 Gy/min.

Figure 1 shows the overall changes in the mean food intake produced by both radiation and chlordiazepoxide when the data for all 5 days were averaged. As shown, chlordiazepoxide produced a comparable dose-dependent increase in food intake in both sham-irradiated and irradiated subjects. Inferential statistics conducted on these data confirmed that the 4.5-Gy dose of radiation significantly decreased food intake ($F(1,55) = 54.75$, $P < .001$), whereas chlordiazepoxide significantly increased food intake ($F(3,55) = 7.38$, $P < .001$). Similar to the analysis for individual treatment days, the analysis of the combined data indicated that the interaction of the radiation and chlordiazepoxide dose was not significant ($F(3,55) = .25$, $P > .1$). Subsequent pairwise comparisons done with sham-irradiated and irradiated groups collapsed for each dose, which indicated that both the 1.8- and 5.6-mg/kg doses of chlordiazepoxide increased food intake significantly ($P < .05$, by Dunnett's test) *versus* saline treatment for the entire 5-day treatment period.

The effects of ondansetron alone and ondansetron in combination with *gamma* photon radiation on food intake are shown in table 2. Although the mean intake for the control group was relatively high on the initial day of treatment (16.6 g), food intake was stable over the subsequent 4 days. In

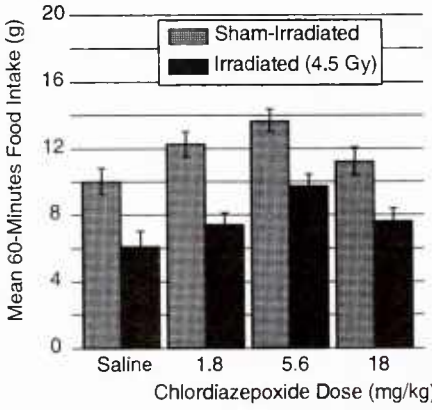

Fig. 1. Effects of chlordiazepoxide on mean food intake for 5 days during a 60-min test period in both sham-irradiated and irradiated (■) groups. Each group contained eight rats, with the exception of the group that received saline and sham irradiation, which had seven rats. Both sham irradiation and irradiation with 4.5 Gy occurred 4 hr before the first 60-min test period on day 1. Chlordiazepoxide was given i.p. 30 min before each of the five 60-min test periods. The vertical lines above each bar represent the S.E.M. for each group. Two-way ANOVA showed significant main effects of radiation and chlordiazepoxide dose ($P < .05$) and a nonsignificant radiation × chlordiazepoxide dose interaction. Dunnett's tests done with sham-irradiated and irradiated groups combined indicated the 1.8- and 5.6-mg/kg doses were significantly different from saline controls ($P < .05$). For other details, see text.

TABLE 2

Effects of ondansetron (OND) on food intake in grams during a daily 60-min test period in both irradiated and sham-irradiated rats

Group	Days of Treatment				
	1	2	3	4	5
Sham + Saline	16.6[a] 1.3	12.1 1.3	13.4 1.1	14.3 1.5	14.6 1.7
Radiation[b] + Saline	10.4 1.5	4.6 1.1	6.0 1.1	6.6 1.5	9.9 1.7
Sham + OND 0.1 mg/kg	14.9 1.6	12.2 1.8	12.4 2.1	11.7 1.9	13.0 1.7
Radiation + OND 0.1 mg/kg	11.6 1.3	6.1 0.3	5.4 0.6	8.1 0.6	9.2 1.2
Sham + OND 0.3 mg/kg	16.2 1.7	11.9 2.3	11.1 1.7	11.8 1.5	12.8 2.2
Radiation + OND 0.3 mg/kg	11.5 1.5	5.3 0.7	6.1 1.2	5.3 0.8	7.0 1.2
Sham + OND 1 mg/kg	13.4 1.1	10.8 1.0	12.3 0.8	9.4 0.9	12.1 1.1
Radiation + OND 1 mg/kg	11.3 1.3	6.1 1.1	6.3 0.8	7.8 1.3	9.5 1.4

[a] Mean intake and one S.E.M. (below) for eight subjects.
[b] 4.5 Gy of *gamma* rays (^{60}Co) administered at a nominal rate of 2.5 Gy/min.

contrast, a 4.5-Gy dose of *gamma* radiation sharply decreased the daily food intake during the 60-min test period in all radiation-treated groups. This main effect of *gamma* radiation was highly significant when individual treatment days were analyzed ($P < .001$ for each of the 5 days). Radiation-induced decreases in the mean food intake can easily be seen in the data for all irradiated groups on treatment days 2 and 3. On these days, the food intake for irradiated subjects receiving either saline or ondansetron was approximately one-half that for subjects in the control group.

Although analyses of daily treatment data produced a main effect of radiation, both the ondansetron dose and the interaction of ondansetron dose and radiation were not significant ($P > .1$ on each of the 5 treatment days in both). In general, the fact that ondansetron dose had no effect on food intake was reflected in data obtained from both sham-irradiated and irradiated groups. For example, the intake for the sham-irradiated drug groups across all 5 treatment days remained stable, whereas the intake for the irradiated drug groups on consecutive treatment days was comparable to that of the group receiving radiation and saline. These same effects were also evident in the 5-day averages depicted in figure 2. As shown, radiation significantly ($F(1,56) = 34.45$, $P < .001$) reduced the mean food intake, regardless of postirradiation treatment (*i.e.*, saline or one of the three doses of ondansetron), whereas ondansetron in combination with either sham irradiation or radiation had no significant effect ($F(3,56) = 0.29$, $P > .1$; $F(3,56) = 0.64$, $P > .1$, respectively) compared with the respective control groups that received saline.

Table 3 shows the effects of 8-OH-DPAT in both sham-irradiated and irradiated subjects. As found previously, food intake was stable after sham irradiation and 5 consecutive days of saline injections. Although these control subjects consumed somewhat less food during the 60-min test period than control subjects for chlordiazepoxide and ondansetron treatments, the mean intake was stable on each treatment day. In subjects that received a 4.5-Gy dose of *gamma* rays and daily injections of either saline or drug, the mean food intake was significantly decreased on each treatment day (ANOVA, main effect of radiation, $P < .001$). Note that the intake for the irradiated group receiving saline was consistently below 3 g on all 5 days of treatment; the intake for control subjects was consistently two- or threefold greater on each of the 5 days. The effect of radiation in all dose groups, although somewhat less evident, can be seen on several of the treatment days. On treatment days 2 and 3, for example, food intake in the 0.1- and 0.3-mg/kg dose groups exposed to radiation was substantially lower than that for the control subjects or subjects that received the same dose of 8-OH-DPAT after sham irradiation.

The effects of 8-OH-DPAT were most similar to those for chlordiazepoxide in that drug alone significantly increased the

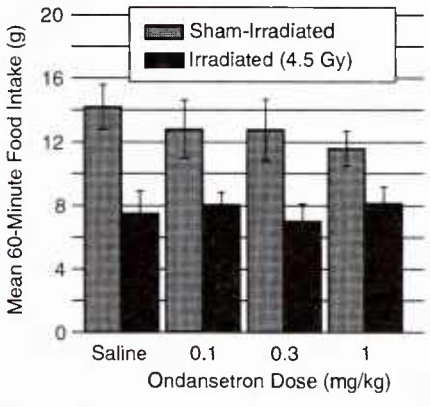

Fig. 2. Effects of ondansetron on mean food intake for 5 days during a 60-min test period in both sham-irradiated and irradiated (4.5 Gy) groups. Each group contained eight rats and doses of ondansetron were given i.p. 20 min before each of the five 60-min test periods. The vertical lines above each bar represent the S.E.M. for each group. Two-way ANOVA showed a significant main effect of radiation ($P < .05$) and nonsignificant effects for ondansetron dose or the radiation × ondansetron dose interaction. For other details, see text.

TABLE 3

Effects of 8-OH-DPAT (8-OH) on food intake in grams during a daily 60-min test period in both irradiated and sham-irradiated rats

Group	Days of Treatment				
	1	2	3	4	5
Sham + Saline	6.8[a] 1.3	5.5 0.9	7.5 1.1	6.7 0.7	5.9 0.9
Radiation[b] + Saline	2.1 0.8	2.5 1.0	2.9 1.1	2.3 0.9	2.3 0.9
Sham + 8-OH 0.1 mg/kg	8.0 1.0	7.3 1.0	7.9 1.3	13.0 1.1	6.0 0.9
Radiation + 8-OH 0.1 mg/kg	6.5 0.8	2.3 0.4	2.5 0.6	8.8 1.1	4.7 0.4
Sham + 8-OH 0.3 mg/kg	8.3 1.2	7.7 0.7	6.4 0.9	9.9 1.1	8.2 0.5
Radiation + 8-OH 0.3 mg/kg	5.2 0.6	3.3 0.8	3.0 0.7	5.2 1.1	3.8 0.6
Sham + 8-OH 1 mg/kg	7.4 1.0	9.6 1.1	9.9 1.0	11.0 1.1	9.0 0.8
Radiation + 8-OH 1 mg/kg	4.8 1.0	3.9 0.7	4.8 0.8	4.3 0.9	4.4 1.3

[a] Mean intake and one S.E.M. (below) for eight subjects.
[b] 4.5 Gy of *gamma* rays (^{60}Co) administered at a nominal rate of 2.5 Gy/min.

mean food intake on individual treatment days (ANOVA, main effect of 8-OH-DPAT, $P < .05$) but the interaction between radiation and drug dose was not significant ($P > .1$). One exception was that the effects of all three doses of 8-OH-DPAT were not significant on treatment day 3 ($F(3,56) = 2.17$, $P > .1$). Despite the absence of a significant effect on this day, the effects of 8-OH-DPAT on the mean food intake can be seen over multiple days in several dose groups. When 1 mg/kg of 8-OH-DPAT was given on successive days after sham irradiation, for example, the mean food intake was greater than 9 g on 3 of 5 treatment days. Moreover, irradiated subjects that received this dose consistently ate more, on average, than subjects that received radiation and saline.

The overall effects represented by the 5-day averages are shown in figure 3. In general, mean food intake was decreased in all irradiated subjects compared with that in the sham-irradiated subjects and 8-OH-DPAT tended to increase the intake similarly in both irradiated and sham-irradiated groups. These effects were confirmed by a highly significant effect of radiation ($F(1,56) = 76.99$, $P < .001$) and a significant effect of 8-OH-DPAT dose ($F(3,56) = 5.52$, $P < .05$). In addition, analyses of these data supported the analyses of daily treatment data in that the interaction between radiation and drug dose was not significant ($F(3,56) = 0.24$, $P > .1$). Pairwise comparisons conducted on the collapsed data indicated a significant effect ($P < .05$, by Dunnett's test) for all three doses of 8-OH-DPAT.

The effects on food intake were occasionally apparent 24 hr after radiation and the administration of all three drugs. More specifically, 24-hr decreases in food intake occurred in 3 of 12 total radiation groups and these 3 groups were part of 8 groups of subjects designated for testing 8-OH-DPAT. Even in these three groups, however, the decreases in 24-hr consumption were limited to only one-half of the subjects in each group. Unfortunately, 24-hr increases in food intake were not detectable using this feeding procedure in which only a measured amount of food was presented on each treatment day.

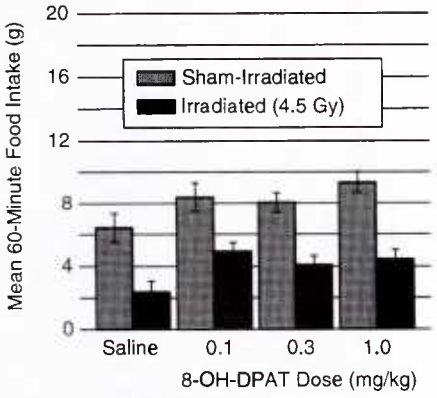

Fig. 3. Effects of 8-OH-DPAT on mean food intake for 5 days during a 60-min test period in both sham-irradiated and irradiated (4.5 Gy) groups. Each group contained eight rats and doses of 8-OH-DPAT were given i.p. 20 min before each of the five 60-min test periods. The vertical lines above each bar represent the S.E.M. for each group. Two-way ANOVA showed significant main effects of radiation and 8-OH-DPAT dose ($P < .05$) and a nonsignificant radiation × 8-OH-DPAT dose interaction. Dunnett's tests done with sham-irradiated and irradiated groups combined indicated all three doses of 8-OH-DPAT were significantly different from saline controls ($P < .05$). For other details, see text.

Discussion

Although the results on mean food intake with ionizing radiation, chlordiazepoxide and 8-OH-DPAT alone might have been predicted from previous research, no study to our knowledge has examined food intake in rats after the administration of both radiation and drugs that directly affect food intake. It is well established, for example, that ionizing radiation alone can decrease food intake for a period of 1 to 5 days, which depends on the total dose administered (Jarrard, 1963; Morse and Mickley, 1988; Newsom and Kimeldorf, 1954; Smith and Tyree, 1954; Smith *et al.*, 1952a). By using a 2-hr test period, Jarrard (1963) found that rats that received 0.9 Gy of x-ray irradiation ate less than did nonirradiated control animals 1 day after exposure, whereas those that received 2.9 and 4.8 Gy ate less for 5 days.

In the present study, 4.5 Gy of both bremmsstrahlung from a linear accelerator and *gamma* rays from a ^{60}Co source (delivered at 2 Gy/min and 2.5 Gy/min, respectively) produced comparable deficits that lasted 4 to 5 days. The fact that different dose rates did not produce a change in effect was not surprising, given the small difference in the rate and the reports of several investigators, which showed that the total dose, not the dose rate, was primarily responsible for the observed behavioral effects on feeding (Morse and Mickley, 1988; Smith and Tyree, 1954). Morse and Mickley (1988), in one of the few rodent feeding studies that involved ^{60}Co *gamma* radiation, found that 3 or 8 Gy decreased eating behaviors relatively independently of a 0.4 to 10 Gy/min change in the exposure rate.

Unlike radiation, both chlordiazepoxide and 8-OH-DPAT have been tested extensively in feeding paradigms similar to the one in the present study (Cooper, 1991). In general, these drugs consistently increased food intake in rats during test periods ranging from 5 min to 4 hr. In the present study with rats, administering three doses of each drug for 5 consecutive days before a 60-min test period resulted in significant increases in food intake compared with that in saline-treated controls. As mentioned, these effects were similar to the effects in many

studies that specifically examined the hyperphagic properties of chlordiazepoxide (Cole, 1983; Cooper and Moores, 1985; Fletcher *et al.*, 1980; Sanger, 1984; Witkin and Leander, 1982) and 8-OH-DPAT (Aulakh *et al.*, 1988; Dourish *et al.*, 1985; Dourish *et al.*, 1986; Hutson *et al.*, 1988; Montgomery *et al.*, 1989). For example, Cooper and Moores (1985) found that 1.25 to 20 mg/kg of chlordiazepoxide in nondeprived rats increased food intake during a 30-min test by as much as 10 g at higher doses. Similarly, Dourish *et al.* (1986) reported that 0.25 to 4 mg/kg of 8-OH-DPAT in nondeprived rats increased food intake approximately 2 to 4 g during a 2-hr period. In the only feeding study that gave chlordiazepoxide and saline over a 5-day period and directly compared chlordiazepoxide with 8-OH-DPAT, Fletcher and Davies (1990) found that both drugs prolonged the total time spent eating during a 10-min test. However, they also found that chlordiazepoxide, unlike 8-OH-DPAT, reduced the latency to begin eating and increased the consumption of novel food items (*i.e.*, abolished food neophobia) during an initial 10-min test period. Although these types of differences were not examined in this study, specific differences in hyperphagic effects (Fletcher and Davies, 1990) and mechanism of action (Fletcher *et al.*, 1980; Hutson *et al.*, 1988; Kennett *et al.*, 1987) have been reported for these drugs. One notable difference between the present 8-OH-DPAT data and the results from a previous study with 8-OH-DPAT involved repeated administrations. In the present study, repeated administrations of 8-OH-DPAT did not attenuate the hyperphagic effect, whereas Kennett *et al.* (1987) found that a 1-mg/kg injection of 8-OH-DPAT on the initial test day attenuated the subsequent day's drug effect on feeding. This was clearly not the case with either 8-OH-DPAT or chlordiazepoxide in the present study. In fact, analyses indicated a significant dose effect on 4 of 5 treatment days for 8-OH-DPAT and all 5 treatment days for chlordiazepoxide.

In contrast to chlordiazepoxide and 8-OH-DPAT, all three doses of ondansetron did not produce any significant effects on food intake. This finding with ondansetron was similar to that in a study by Mele *et al.* (1992), which showed that 0.1 to 10 mg/kg of ondansetron did not attenuate a cisplatin-induced conditioned taste aversion. As Cooper (1991) points out in a review of $5HT_3$ antagonists on ingestional responses, the behavioral effects with these compounds have been extremely limited in scope and lack consistency. In one study, for example, van der Hoek and Cooper (1990) reported that comparatively low doses of ondansetron in rats (3–30 μg/kg i.p.) decreased food intake during a 60-min test period. In another study, Shepherd and Rodgers (1990) reported that ondansetron in mice (1 and 2 mg/kg s.c.) increased feeding during a 5-min control test. Finally, a third study found that low doses of the $5HT_3$ antagonist ICS 205–930 (tropesition) decreased food intake in rats, whereas higher doses were ineffective (Fletcher and Davies, 1990). Because these few studies reported equivocal effects on food intake with either ondansetron or other $5HT_3$ antagonists, it is difficult to interpret the role $5HT_3$ receptors might play in feeding.

The present results and previous research with $5HT_3$ antagonists indicate the need for further research on the involvement of $5HT_3$ receptors in feeding. At the least, existing studies with these drugs point to the need for examining a broad range of doses. The present results show that ondansetron doses of 0.1 to 1 mg/kg do not affect food intake, even though comparable doses have been shown to affect rats' social interactions (Jones *et al.*, 1988), gastric emptying (Buchheit *et al.*, 1989; Forster and Dockray, 1990), cisplatin-induced pica (Takeda *et al.*, 1993) and anorexia related to benzodiazepine withdrawal (Goudie and Leathley, 1990). As Goudie and Leathley (1990) suggest, $5HT_3$ antagonists may have an inverted U-shaped dose-effect curve for behaviors other than those associated with food intake. In any case, the present results with ondansetron at two periods (60 min and 24 hr) extend their work at a single time period (24 hr) and show that repeated administration with comparable doses does not affect food intake.

Of particular note in the present study was the somewhat surprising finding that no significant interactions were obtained between radiation and the three types of drugs tested. Although there were instances in which doses of both chlordiazepoxide and 8-OH-DPAT increased the food intake in irradiated subjects, these increases were independent of the decreases in food intake produced by a 4.5-Gy dose of radiation. In the cases of chlordiazepoxide and 8-OH-DPAT, specifically, these findings indicate that radiation probably did not affect the mechanisms by which each drug is thought to stimulate food intake. Chlordiazepoxide, for example, exerts hyperphagic effects through direct action on benzodiazepine receptors on the GABA complex (Fletcher *et al.*, 1980; Cooper, 1980; Cooper and Moores, 1985). The drug 8-OH-DPAT and other $5HT_{1A}$ agonists are thought to exert hyperphagic effects by stimulating serotonin autoreceptors that, in turn, decrease the release of serotonin (Dourish *et al.*, 1985; Dourish *et al.*, 1986), a neurotransmitter known to inhibit food intake in rats (Luo and Li, 1991). Thus, radiation does not seem to affect these proposed mechanisms and it would appear that the anorectic effect of radiation in the present study was not due to damage or disruption of these mechanisms because they functioned in an expected manner at the doses tested when pharmacologically challenged.

There are some interesting points concerning the observations made 24 hr after food presentation. One important observation was the fact that 4.5 Gy of radiation tended to decrease consumption more over a 60-min test period than over a 24-hr period between food presentations. In other words, acute periods of consumption or meal patterns were more disrupted in rats than was the overall consumption for a 24-hr period. The groups that did show 24-hr decreases tended to have 60-min food intake levels that were lower than those that occurred for the other 16 groups used to test radiation and the two other drugs. Therefore, lower base-line levels of consumption for the daily 60-min test period may have contributed to the 24-hr decreases obtained in these radiation groups. A second possibility for the few 24-hr decreases obtained was compensatory hypophagia. Although such an effect was not apparent in this study with chlordiazepoxide, such effects have been reported after acute increases in food intake after chronic administration of some benzodiazepines (Seyrig *et al.*, 1986). It is also difficult to attribute the 24-hr decreases to differences in radiation exposure (*e.g.*, dose rate, bremmsstrahlung *versus gamma* radiation or unilateral *versus* bilateral exposure) because the overall behavioral effect of radiation at 60 min was no greater in these subjects compared with that in control groups across all three drugs. In addition, 24-hr decreases in food intake were not found in any of the eight ondansetron-treated groups, which had similar exposure conditions to those in the 8-OH-DPAT groups.

Far more research with radiation and drugs that affect feed-

ing is needed to begin addressing the problems associated with radiation-induced decreases in food intake. Certainly, several factors alone or a combination of factors may contribute to the anorectic effect commonly found in many species after radiation exposure. Irritation of the alimentary tract (Smith *et al.*, 1952ab), decreases in gastric emptying (Goodman *et al.*, 1952; Hulse, 1966; Hulse and Patrick, 1977; Smith and Tyree, 1954) or even decreases in activity (Johnson *et al.*, 1946; Jones *et al.*, 1954), all occur in rats after radiation exposure at the dose tested and each can lead to a decrease in food intake. One reason to suspect a combination of factors stems from the fact that none of these factors alone adequately explains the present results or other existing data. For example, if decreases in gastric emptying alone were responsible, we might have expected ondansetron to have either increased or decreased food intake because ondansetron and other $5HT_3$ antagonists have been shown in rats to increase (Buchheit *et al.*, 1989) or decrease (Forster and Dockray, 1990) basal levels of gastric emptying, respectively. Likewise, if irritation of the alimentary tract were the predominant factor, the two drugs that increased 60-min food intake should have decreased food intake over a 24-hr period and subsequent days by producing added irritation. Smith *et al.* (1952b) found that large amounts of fluid and gas accumulated in the alimentary tract in rats fed by stomach tubes during the first few days after irradiation with 7.2 Gy. They concluded that feeding subjects even predigested diets was distinctly harmful to the alimentary tract when given to irradiated rats on days 1 to 3 postexposure.

It is especially interesting that ondansetron, a $5HT_3$ receptor antagonist that was generally proved to be extremely efficacious and potent for controlling radiation-induced emesis and nausea in ferrets and humans (Andrews *et al.*, 1988; Gralla, 1991; Priestman, 1991), was ineffective in attenuating radiation-induced decreases in food intake in rats. Although rats are devoid of an emetic reflex (and little can be determined about antiemetic properties from this study), the same doses of ondansetron used here were shown to be effective in attenuating benzodiazepine withdrawal-induced anorexia in rats (Goudie and Leathley, 1990). These results with ondansetron highlight the need for examining the effects of all three classes of drugs used here on more than one type of behavior (Cole, 1983) and in more than one experimental species (*e.g.*, rats, ferrets, cats, dogs, monkeys and humans). Furthermore, the present study with rats clearly indicates that postirradiation treatment with chlordiazepoxide and 8-OH-DPAT was far more effective in directly increasing food intake than was ondansetron. In general, these findings may be relevant for therapeutic situations in which treatment for radiation-induced anorexia remains a clinical problem (Mattes *et al.*, 1992; Smith *et al.*, 1984).

References

Andrews, P. L. R., Bailey, H. E., Hawthorn, J., Stables, R. and Tyers, M. B.: GR38032F, a novel $5\text{-}HT_3$ antagonist, can abolish emesis induced by cyclophosphamide or radiation in the ferret. Br. J. Pharmacol. **91:** 417P, 1988.

Anno, G. H., Baum, S. J., Withers, H. R. and Young, R. W.: Symptomatology of acute radiation effects in humans after exposure to doses of 0.5–30 Gy. Health Phys. **56:** 821–838, 1989.

Arnold, W. J.: Maze learning and retention after x radiation of the head. J. Comp. Physiol. Psychol. **45:** 358–361, 1952.

Aulakh, C. S., Hill, J. L. and Murphy, D. L.: A comparison of feeding and locomotion responses to serotonin agonists in three rat strains. Pharmacol. Biochem. Behav. **31:** 567–571, 1988.

Buchheit, K. H., Gamse, R., Bertholet, A. and Buscher, H. H.: Antagonists at serotoninergic $5\text{-}HT_3$-receptors increase gastric emptying of solids and liquids in the rat. Gastroenterology **96:** A63, 1989.

Cole, S. O.: Combined effects of chlordiazepoxide treatment and food deprivation on concurrent measures of feeding and activity. Pharmacol. Biochem. Behav. **18:** 369–372, 1983.

Cooper, S. J.: Benzodiazepines as appetite-enhancing compounds. Appetite **1:** 7–19, 1980.

Cooper, S. J.: Ingestional responses following benzodiazepine receptor ligands, selective $5\text{-}HT_{1A}$ agonists and selective $5\text{-}HT_3$ receptor antagonists. *In* $5\text{-}HT_{1A}$ Agonists, $5\text{-}HT_3$ Antagonists and Benzodiazepines: Their Comparative Behavioural Pharmacology, ed. by R. J. Rodgers and S. J. Cooper, pp. 233–265, John Wiley & Sons, Inc., New York, 1991.

Cooper, S. J. and Moores, W. R.: Benzodiazepine-induced hyperphagia in the nondeprived rat: Comparisons with CL 218,872, zopiclone, tracazolate and phenobarbital. Pharmacol. Biochem. Behav. **23:** 169–172, 1985.

Davis, R. T.: The radiation syndrome. *In* Behavior of Nonhuman Primates, ed. by A. M. Schrier, H. F. Harlow and F. Stollnitz, pp. 495–524, Academic Press, New York, 1965.

Dourish, C. T., Hutson, P. H. and Curzon, G.: Low doses of the putative serotonin agonist 8-hydroxy-2-(di-*n*-propylamino)tetralin (8-OH-DPAT) elicit feeding in the rat. Psychopharmacology **86:** 197–204, 1985.

Dourish, C. T., Hutson, P. H. and Curzon, G.: Parachlorophenyl-alanine prevents feeding induced by the serotonin agonist 8-hydroxy-2-(di-*n*-propylamino) tetralin (8-OH-DPAT). Psychopharmacology **89:** 467–471, 1986.

Engel, J. A., Hjorth, S., Svensson, K., Carlsson, A. and Liljequist, S.: Anticonflict effect of the putative serotonin receptor agonist 8-hydroxy-2-(di-*n*-propylamino) tetralin (8-OH-DPAT). Eur. J. Pharmacol. **105:** 365–368, 1984.

Fletcher, A., Green, S. E. and Hodges, H. M.: Evidence for a role for GABA in benzodiazepine effects on feeding in rats. Br. J. Pharmacol. **69:** 274–275, 1980.

Fletcher, P. J. and Davies, M.: Effects of 8-OH-DPAT, buspirone, and ICS 205–930 on feeding in a novel environment: Comparisons with chlordiazepoxide and FG 7142. Psychopharmacology **102:** 301–308, 1990.

Forster, E. R. and Dockray, G. J.: The effect of ondansetron on gastric emptying in the conscious rat. Eur. J. Pharmacol. **191:** 235–238, 1990.

Furchtgott, E.: Effects of total body x-irradiation on learning: An exploratory study. J. Comp. Physiol. Psychol. **44:** 197–203, 1951.

Goodman, R. D., Lewis, A. E. and Schuck, E. A.: Effects of x-irradiation on gastrointestinal transit and absorption availability. Am. J. Physiol. **169:** 242–247, 1952.

Goudie, A. J. and Leathley, M. J.: Effects of the $5\text{-}HT_3$ antagonist GR38032F (ondansetron) on benzodiazepine withdrawal in rats. Eur. J. Pharmacol. **185:** 179–186, 1990.

Gralla, R. J.: An outline of anti-emetic treatment. Eur. J. Clin. Oncol. **25:** suppl., S7-S11, 1991.

Hulse, E. V.: Gastric emptying in rats after part-body irradiation. Int. J. Radiat. Biol. **10:** 521–532, 1966.

Hulse, E. V. and Patrick, G.: A model for treating post-irradiation nausea and vomiting in man: The action of insulin in abolishing radiation-induced delay in gastric emptying in the rat. Br. J. Radiol. **50:** 645–651, 1977.

Hutson, P. H., Dourish, C. T. and Curzon, G.: Evidence that the hyperphagic response to 8-OH-DPAT is mediated by $5\text{-}HT_{1A}$ receptors. Eur. J. Pharmacol. **150:** 361–366, 1988.

Jarrard, L. E.: Effects of x irradiation on operant behavior in the rat. J. Comp. Physiol. Psychol. **56:** 608–611, 1963.

Johnson, C. G., Vilter, C. F. and Spies, T. D.: Irradiation sickness in rats. Am. J. Roentgenol. **56:** 631–639, 1946.

Jones, B. J., Costall, B., Domeney, A. M., Kelly, M. E., Naylor, R. J., Oakley, N. R. and Tyers, M. B.: The potential anxiolytic activity of GR38032F, a $5\text{-}HT_3$-receptor antagonist. Br. J. Pharmacol. **93:** 985–993, 1988.

Jones, D. C., Kimeldorf, D. J., Rubadeau, D. O., Osborn, G. K. and Castanera, T. J.: Effect of x-irradiation on performance of volitional activity by the adult male rat. Am. J. Physiol. **177:** 243–250, 1954.

Kennett, G. A., Marcou, M., Dourish, C. T. and Curzon, G.: Single administration of $5\text{-}HT_{1A}$ agonists decreases $5\text{-}HT_{1A}$ presynaptic, but not postsynaptic receptor-mediated responses: Relationship to antidepressant-like action. Eur. J. Pharmacol. **138:** 53–60, 1987.

King, G. L. and Makale, M. T.: Postirradiation emesis. *In* Nausea and Vomiting: Recent Research and Clinical Advances, ed. by J. Kucharczyk, D. J. Stewart and A. D. Miller, pp. 103–142, CRC Press, Boston, 1991.

Luo, S. and Li, E. T. S.: Effects of repeated administration of serotonergic agonists on diet selection and body weight in rats. Pharmacol. Biochem. Behav. **38:** 495–500, 1991.

Mattes, R. D., Curran, W. J., Alavi, J., Powlis, W. and Whittington, R.: Clinical implications of learned food aversions in patients with cancer treated with chemotherapy or radiation therapy. Cancer **70:** 192–200, 1992.

Mattes, R. D., Curran, W. J., Powlis, W. and Whittington R.: A descriptive study of learned food aversions in radiotherapy patients. Physiol. Behav. **50:** 1103–1109, 1991.

Mele, P. C., Franz, C. G. and Harrison, J. R.: Effects of ionizing radiation on fixed-ratio escape performance in rats. Neurotoxicol. Teratol. **12:** 367–373, 1990.

Mele, P. C., McDonough, J. H., McLean, D. B. and O'Halloran, K. P.: Cisplatin-induced conditioned taste aversion: Attenuation by dexamethasone but not zacopride or GR38032F. Eur. J. Pharmacol. **218:** 229–236, 1992.

Mickley, G. A., Bogo, V. and West, B. R.: Behavioral and neurophysiological changes with exposure to ionizing radiation. *In* Textbook of Military Medicine.

Medical Consequences of Nuclear Warfare, ed. by R. Zajtchuk, R. F. Bellamy and V. M. Ingram, pp. 105–151, TMM Publications, Falls Church, VA, 1989.

MONTGOMERY, A. M. J., WILLNER, P. AND MUSCAT, R.: 8-OH-DPAT reliably increases ingestion of solid but not liquid diets. *In* Behavioural Pharmacology of 5-HT, ed. by P. Bevan, A. R. Cools and T. Archer, pp. 291–294, Lawrence Erlbaum Associates, Hillsdale, NJ, 1989.

MORSE, D. E. AND MICKLEY, G. A.: Dose-rate and sex effects on the suppression of appetitive behavior following exposure to gamma-spectrum radiation. *In* Abstracts of 36th Annual Meeting of Radiation Research Society, p. 163, Philadelphia, 1988.

NEWSOM, B. D. AND KIMELDORF, D. J.: Food consumption of irradiated animals exposed to a low ambient temperature. Fed. Proc. **13:** 391, 1954.

POMERANTZ, S. M.: The 5-HT1A agonist, 8-OH-DPAT, stimulates food intake of rhesus monkeys. Soc. Neurosci. Abstr. **16:** 1323, 1990.

PRIESTMAN, T. J.: Clinical studies with ondansetron in the control of radiation-induced emesis. Eur. J. Cancer **25:** suppl., S29-S33, 1991.

RANDALL, L. O., SCHALLEK, W., HEISE, G. A., KEITH, E. F. AND BAGDON, R. E.: The psychosedative properties of methaminodiazepoxide. J. Pharmacol. Exp. Ther. **129:** 163–171, 1960.

RUCH, T. C., ISAAC, W. AND LEARY, R. W.: Behavioral and correlated hematologic effects of sublethal whole body irradiation. *In* Response of the Nervous System to Ionizing Radiation, ed. by T. J. Haley and R. S. Snider, pp. 691–703, Academic Press, New York, 1962.

SANGER, D. J.: Chlordiazepoxide-induced hyperphagia in rats: Lack of effect of GABA agonists and antagonists. Psychopharmacology **84:** 388–392, 1984.

SEYRIG, J. A., FALCOU, R., BETOULLE, D. AND APFELBAUM, M.: Effects of a chronic administration of two benzodiazepines on food intake in rats given a highly palatable diet. Pharmacol. Biochem. Behav. **25:** 913–918, 1986.

SHEPHERD, J. K. AND RODGERS, R. J.: 8-OH-DPAT specifically enhances feeding behaviour in mice: Evidence from behavioural competition. Psychopharmacology **101:** 408–413, 1990.

SMITH, D. E. AND TYREE, E. B.: Influence of x-irradiation upon body weight and food consumption of the rat. Am. J. Physiol. **177:** 251–260, 1954.

SMITH, D. E., TYREE, E. B., PATT, H. M. AND BINK, N.: Effect of x-irradiation upon food and water intake and body weight. Fed. Proc. **11:** 149, 1952a.

SMITH, J. C., BLUMSACK, J. T., BILEK, F. S., SPECTOR, A. C., HOLLANDER, G. R. AND BAKER, D. L.: Radiation-induced taste aversion as a factor in cancer therapy. Cancer Treat. Rep. **68:** 1219–1227, 1984.

SMITH, W. W., ACKERMANN, I. B. AND SMITH, F.: Body weight, fasting and forced feeding after whole body x-irradiation. Am. J. Physiol. **168:** 382–390, 1952b.

TAKEDA, N., HASEGAWA, S., MORITA, M. AND MATSUNAGA, T.: Pica in rats is analogous to emesis: An animal model in emesis research. Pharmacol. Biochem. Behav. **45:** 817–821, 1993.

TASK GROUP 21, RADIATION THERAPY COMMITTEE A. A. P. M.: A protocol for the determination of absorbed dose from high energy photon and electron beams. Med. Phys. **10:** 741, 1983.

VAN DER HOEK, G. A. AND COOPER, S. J.: Microstructural analysis of the effects of the selective 5-HT_3 antagonist, ondansetron, on feeding and other behavioural responses. Br. J. Pharmacol. **99:** 238P, 1990.

WITKIN, J. M. AND LEANDER, J. D.: Effects of the appetite stimulant chlordimeform on food and water consumption of rats: Comparison with chlordiazepoxide. J. Pharmacol. Exp. Ther. **223:** 130–134, 1982.

Send reprint requests to: Dr. Peter J. Winsauer, Behavioral Sciences Department, AFRRI, 8901 Wisconsin Ave, Bethesda, MD 20889–5603.

DISTRIBUTION LIST

DEPARTMENT OF DEFENSE

ARMED FORCES INSTITUTE OF PATHOLOGY
ATTN: RADIOLOGIC PATHOLOGY DEPARTMENT

ARMED FORCES RADIOBIOLOGY RESEARCH INSTITUTE
ATTN: PUBLICATIONS DIVISION
ATTN: LIBRARY

ARMY/AIR FORCE JOINT MEDICAL LIBRARY
ATTN: DASG-AAFJML

ASSISTANT TO SECRETARY OF DEFENSE
ATTN: AE
ATTN: HA(IA)

DEFENSE NUCLEAR AGENCY
ATTN: TITL
ATTN: DDIR
ATTN: RAEM
ATTN: MID

DEFENSE TECHNICAL INFORMATION CENTER
ATTN: DTIC-DDAC
ATTN: DTIC-FDAC

FIELD COMMAND DEFENSE NUCLEAR AGENCY
ATTN: FCFS

INTERSERVICE NUCLEAR WEAPONS SCHOOL
ATTN: TCHTS/RH

LAWRENCE LIVERMORE NATIONAL LABORATORY
ATTN: LIBRARY

UNDER SECRETARY OF DEFENSE (ACQUISITION)
ATTN: OUSD(A)/R&AT

UNIFORMED SERVICES UNIVERSITY OF THE HEALTH SCIENCES
ATTN: LIBRARY

DEPARTMENT OF THE ARMY

AMEDD CENTER AND SCHOOL
ATTN: HSMC-FCM

HARRY DIAMOND LABORATORIES
ATTN: SLCHD-NW
ATTN: SLCSM-SE

SURGEON GENERAL OF THE ARMY
ATTN: MEDDH-N

U.S. ARMY AEROMEDICAL RESEARCH LABORATORY
ATTN: SCIENTIFIC INFORMATION CENTER

U.S. ARMY CHEMICAL RESEARCH, DEVELOPMENT, AND ENGINEERING CENTER
ATTN: SMCCR-RST

U.S. ARMY INSTITUTE OF SURGICAL RESEARCH
ATTN: DIRECTOR OF RESEARCH

U.S. ARMY MEDICAL RESEARCH INSTITUTE OF CHEMICAL DEFENSE
ATTN: SGRD-UV-R

U.S. ARMY NUCLEAR AND CHEMICAL AGENCY
ATTN: MONA-NU

U.S. ARMY RESEARCH INSTITUTE OF ENVIRONMENTAL MEDICINE
ATTN: SGRD-UE-RPP

U.S. ARMY RESEARCH OFFICE
ATTN: BIOLOGICAL SCIENCES PROGRAM

WALTER REED ARMY INSTITUTE OF RESEARCH
ATTN: DIVISION OF EXPERIMENTAL THERAPEUTICS

DEPARTMENT OF THE NAVY

NAVAL AEROSPACE MEDICAL RESEARCH LABORATORY
ATTN: COMMANDING OFFICER

NAVAL MEDICAL COMMAND
ATTN: MEDCOM-21

NAVAL MEDICAL RESEARCH AND DEVELOPMENT COMMAND
ATTN: CODE 40C

NAVAL MEDICAL RESEARCH INSTITUTE
ATTN: LIBRARY

NAVAL RESEARCH LABORATORY
ATTN: LIBRARY

OFFICE OF NAVAL RESEARCH
ATTN: BIOLOGICAL SCIENCES DIVISION

DEPARTMENT OF THE AIR FORCE

BOLLING AIR FORCE BASE
ATTN: AFOSR

BROOKS AIR FORCE BASE
ATTN: AL/OEBSC
ATTN: USAFSAM/RZ
ATTN: OEHL/RZ

OFFICE OF AEROSPACE STUDIES
ATTN: OAS/XRS

SURGEON GENERAL OF THE AIR FORCE
ATTN: HO USAF/SGPT
ATTN: HO USAF/SGES

U.S. AIR FORCE ACADEMY
ATTN: HO USAFA/DFBL

OTHER FEDERAL GOVERNMENT

ARGONNE NATIONAL LABORATORY
ATTN: ACQUISITIONS

BROOKHAVEN NATIONAL LABORATORY
ATTN: RESEARCH LIBRARY, REPORTS SECTION

CENTER FOR DEVICES AND RADIOLOGICAL HEALTH
ATTN: HFZ-110

GOVERNMENT PRINTING OFFICE
ATTN: DEPOSITORY RECEIVING SECTION
ATTN: CONSIGNED BRANCH

LIBRARY OF CONGRESS
ATTN: UNIT X

LOS ALAMOS NATIONAL LABORATORY
ATTN: REPORT LIBRARY/P364

NATIONAL AERONAUTICS AND SPACE ADMINISTRATION
ATTN: RADLAB

NATIONAL AERONAUTICS AND SPACE ADMINISTRATION
GODDARD SPACE FLIGHT CENTER
ATTN: LIBRARY

NATIONAL CANCER INSTITUTE
ATTN: RADIATION RESEARCH PROGRAM

NATIONAL DEFENSE UNIVERSITY
ATTN: LIBRARY

U.S. DEPARTMENT OF ENERGY
ATTN: LIBRARY

U.S. FOOD AND DRUG ADMINISTRATION
ATTN: WINCHESTER ENGINEERING AND ANALYTICAL CENTER

U.S. NUCLEAR REGULATORY COMMISSION
ATTN: LIBRARY

RESEARCH AND OTHER ORGANIZATIONS

AUSTRALIAN DEFENCE FORCE
ATTN: SURGEON GENERAL

BRITISH LIBRARY (SERIAL ACQUISITIONS)
ATTN: DOCUMENT SUPPLY CENTRE

CENTRE DE RECHERCHES DU SERVICE DE SANTE DES ARMEES
ATTN: DIRECTOR

INHALATION TOXICOLOGY RESEARCH INSTITUTE
ATTN: LIBRARY

INSTITUTE OF RADIOBIOLOGY
ARMED FORCES MEDICAL ACADEMY
ATTN: DIRECTOR

KAMAN SCIENCES CORPORATION
ATTN: DASIAC

NBC DEFENSE RESEARCH AND DEVELOPMENT CENTER OF THE FEDERAL ARMED FORCES
ATTN: WWDBW ABC-SCHUTZ

NCTR-ASSOCIATED UNIVERSITIES
ATTN: EXECUTIVE DIRECTOR

RUTGERS UNIVERSITY
ATTN: LIBRARY OF SCIENCE AND MEDICINE

UNIVERSITY OF CALIFORNIA
ATTN: LABORATORY FOR ENERGY-RELATED HEALTH RESEARCH
ATTN: LAWRENCE BERKELEY LABORATORY

UNIVERSITY OF CINCINNATI
ATTN: UNIVERSITY HOSPITAL, RADIOISOTOPE LABORATORY

XAVIER UNIVERSITY OF LOUISIANA
ATTN: COLLEGE OF PHARMACY